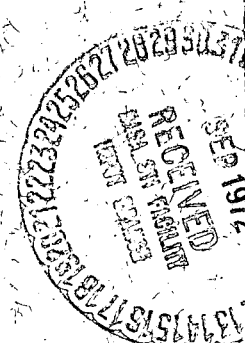NASA TM-X- *65988*

SSS-A ATTITUDE CONTROL PRELAUNCH ANALYSIS AND OPERATIONS PLAN

R. D. WERKING
J. BECK
D. GARDNER
P. MOYER
M. PLETT

OCTOBER 1971

GSFC —— GODDARD SPACE FLIGHT CENTER
GREENBELT, MARYLAND

SSS-A ATTITUDE CONTROL PRELAUNCH
ANALYSIS AND OPERATIONS PLAN

R. D. Werking

J. Beck

D. Gardner

P. Moyer

M. Plett

ABSTRACT

This document has been prepared by the Attitude Determination Office and contractors (Computer Sciences Corporation) in order to provide Mr. Gerald Longanecker, SSS Project Manager, with a description of the attitude control support being supplied by the Mission and Data Operations Directorate. Included within are descriptions of the computer programs being used to support the mission for attitude determination, prediction, control and definitive attitude processing. In addition, descriptions of the operating procedures which will be used to accomplish mission objectives are provided.

TABLE OF CONTENTS

TABLE OF CONTENTS (Cont'd)

TABLE OF CONTENTS (Cont'd)

LIST OF ILLUSTRATIONS

LIST OF ILLUSTRATIONS (Cont'd)

SECTION 1

INTRODUCTION

1.1   PURPOSE AND SUMMARY

The purpose of this report is to document the attitude analysis that has been performed in support of the Small Scientific Satellite (SSS)-A and to give a brief description of the attitude software systems that have been developed by the Attitude Determination Office in support of this mission. Some of the analysis efforts performed for SSS-A were:

- A study of the optimum mounting angle for the optical telescope
- The SSS-A attitude disturbance study
- The SSS-A launch window study

An attitude support system has been developed to meet the various SSS-A mission attitude requirements. This system consists of five programs written to operate on the IBM S/360-95 or the IBM S/360-75 computer at Goddard Space Flight Center (GSFC). A description of the SSS Attitude Support System (SSSASS) is presented later in this document. The main components of SSSASS are an optical aspect and star sensor prediction program; the SSS Attitude Determination Program made up of a telemetry processor subroutine, an optical aspect subroutine, and a Control Data Corporation (CDC) star subroutine; the CDC Star Program as a stand-alone program; the Multi-Satellite Attitude Prediction Program for SSS-A (MSAP/SSS); and a merge program to be used for definitive attitude processing only.

1.2   MISSION OBJECTIVES

The primary objective of the SSS-A mission is to study dynamic processes in the inner magnetosphere near the magnetic equator. Specific objectives include:

- Investigating the activities of low-energy particles in the ring current, as well as the development of the main phase magnetic storm

- Investigating the relationship between auroral phenomena, magnetic storms, and the acceleration of charged particles within the inner magnetosphere

- Measuring the directional intensities of 0.5 to 100 kev protons and electrons with an energy resolution of about a factor of 2

- Measuring the vector magnetic field from 0 to 10 Hz in a field strength of up to 3000 gammas

- Measuring the magnetic fluctuations greater than 0.0001 gamma over the range 1 to 3000 Hz

- Measuring the complete spectrum of electric fields from DC to 200 kHz

The SSS-A mission requires a low-inclination (3°), elliptical orbit with an apogee of approximately 6 earth radii geocentric. A minimum orbital lifetime of 12 months is required. The spacecraft will be spin stabilized at 4 rpm. The spacecraft will be launched by a Scout vehicle from the San Marco platform located three miles east of Kenya in the Indian Ocean. To perform its functions the satellite will be tracked and commanded from the Space Tracking and Data Acquisition Network (STADAN). Data to be used for attitude determination will be transmitted to GSFC, where it will be processed on the XDS 930 in the Multi Satellite Operations Control Center (MSOCC). Attitude data is stripped from the telemetry stream by this computer and sent to the IBM S/360-95 via a data link.

1.3   SPACECRAFT CONFIGURATION

The SSS-A spacecraft is an octagonal structure with external appendages (booms), a center tube, and body-mounted solar panels (see Figure 1-1). Excluding the antennas, there are five appendages: the flux-gate boom extends from the forward section of the spacecraft, two single-hinged booms support search-coil magnetometers, and two double-hinged booms contain electric field detectors. The booms are released after the yo-yo despins the spacecraft.

The data processing system (DPS) provides all data handling operations for the spacecraft, interfacing between the detectors and the transmitter (there will be no tape recorder). The DPS accomplishes its tasks by:

- Using stored programs to perform data acquisition from detector outputs

- Formatting data into a standard skeleton telemetry format

- Outputting the formatted data to the transmitter

- Producing control signals for the detectors

- Providing an input/output module (IOM) to interface between the various detector signals and the standard data form required for launching the data internal to the DPS

By in-flight changes of the stored programs, experimenters may optimize their data collection for a specific investigation. Not only can the data rate from a given output be varied, but also the number of detector outputs sampled at a given time can be changed. The system thus permits unexpected observations to be investigated in greater detail and allows the reallocation of data from detectors that have failed or that are producing insignificant results.
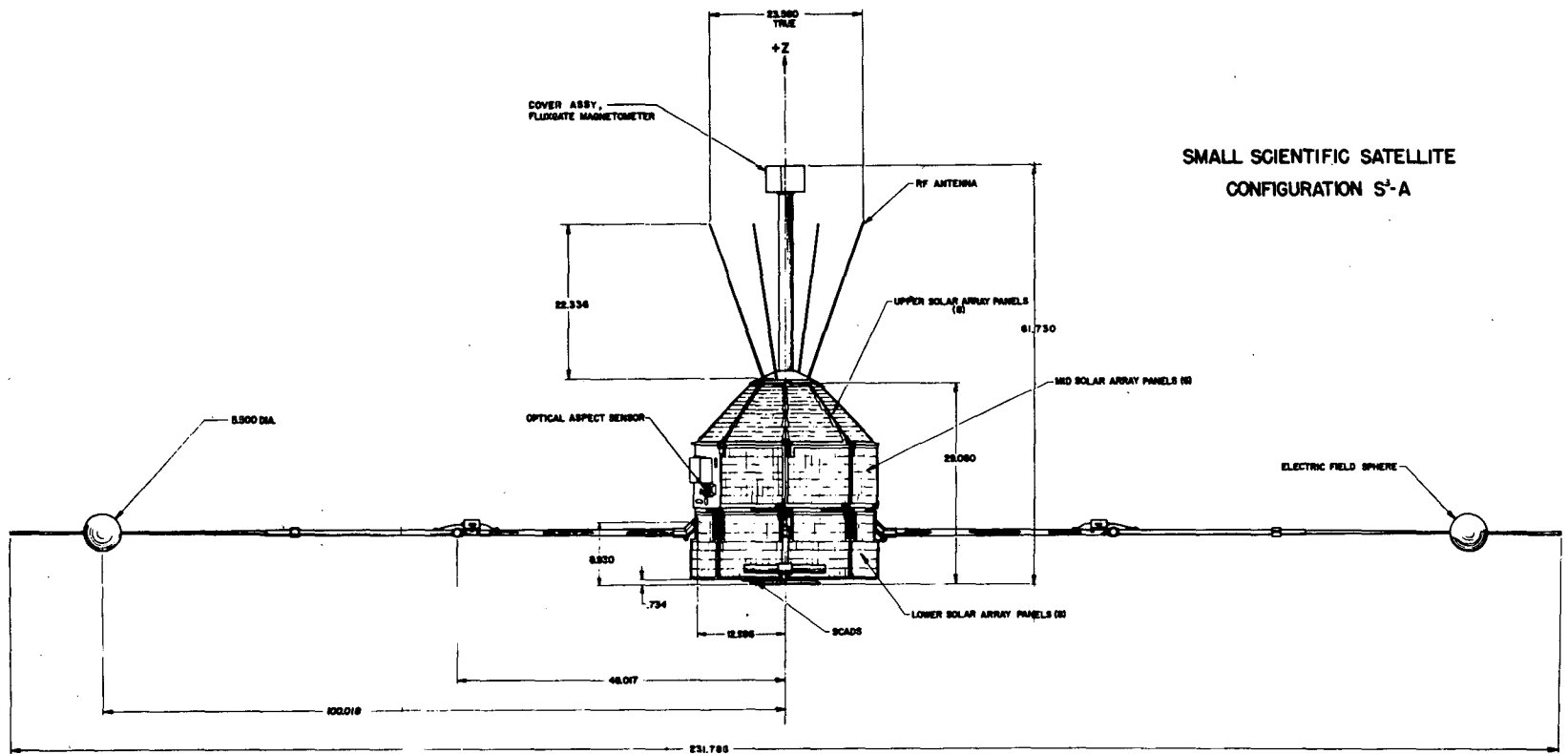
Figure 1-1. SSS–A Spacecraft Geometry

The thermal and power profiles of the SSS-A spacecraft are such that the sun angle must be kept between 30 and 70 degrees. This, as well as other mission constraints, will be provided for by using the attitude and spin control system (ASCS) described in the next section.

1.4 ATTITUDE SENSORS AND ATTITUDE CONTROL SYSTEM

The SSS-A spacecraft will be equipped with both attitude sensing and attitude control subsystems. When these subsystems are combined, through ground processing, the spacecraft attitude can be determined and controlled to satisfy mission requirements.

1.4.1 Digital Solar Sensor

A schematic representation of a digital solar sensor is given in Figure 1-2. Incident sunlight, passing through a slit on the top of a quartz block, falls on a gray-coded pattern on the bottom of the block and, depending on the angle of incidence, illuminates or fails to illuminate each of the photocell detectors in the pattern. The solar sensor also includes a command slit mounted perpendicular to the gray-coded reticle.

Assuming the detector is mounted such that the command slit is parallel to the Z axis and the Z axis is coincident with the satellite spin axis, the time of illumination of the command slit provides a measurement of the azimuth angle of the sun and the gray-coded reticle provides a digital representation of the elevation angle of the sun with respect to the spin axis. The times of successive solar crossings of the command slit yield the spin rate in the straightforward manner.

SPIN AXIS

COMMAND
SLIT FIELD
OF VIEW

SPACECRAFT

SPIN AXIS

COMMAND SLIT

RETICLE

PHOTOCELLS

AMPLIFIER

GATE

| 1 | 1 | 0 | 0 | 1 | 0 | 0 | STORAGE
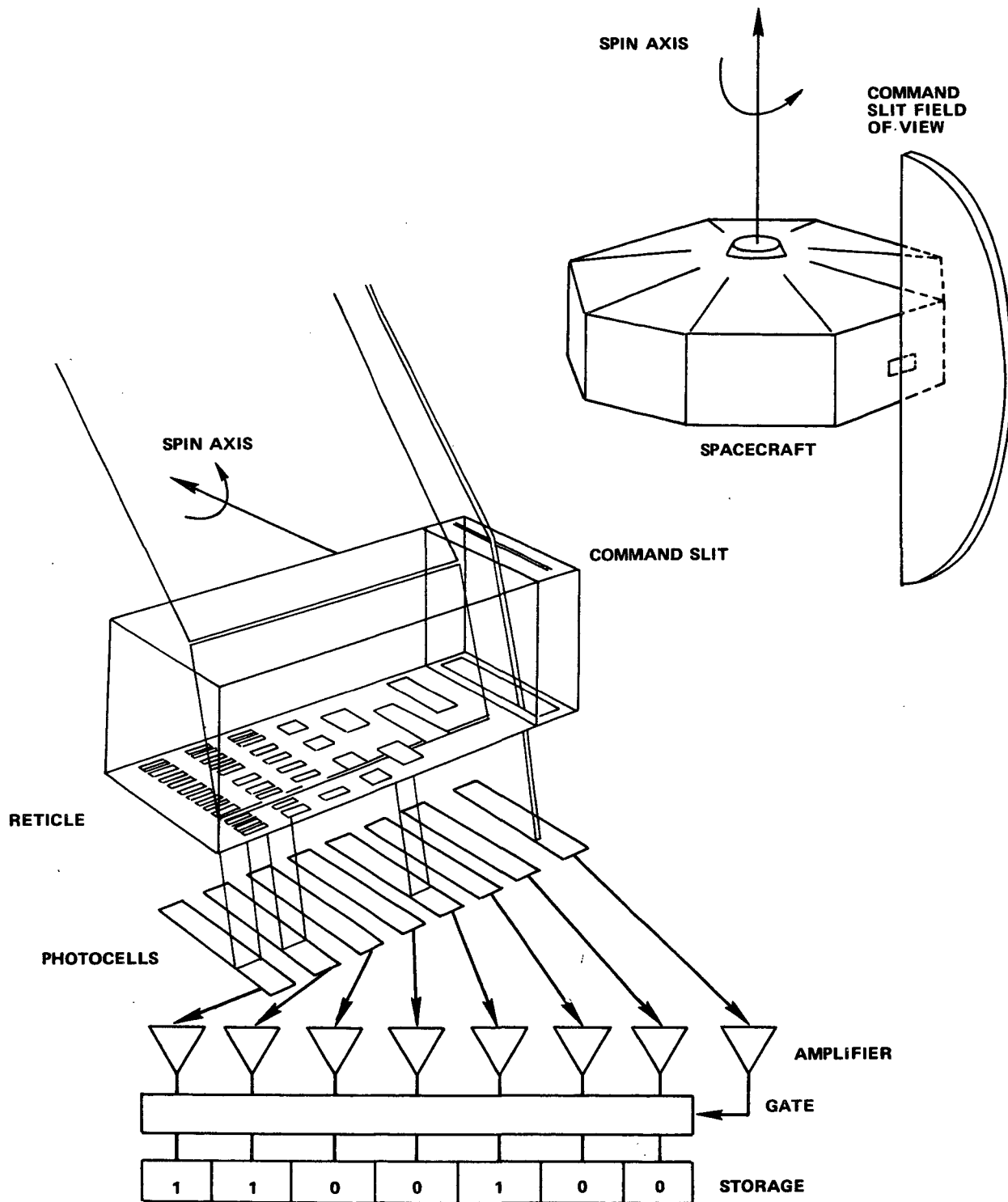
Figure 1-2. Schematic Representation of a Digital Solar Sensor

1.4.2   Horizon Detector

The horizon detector consists of a telescope and lens system focused onto a photodiode. The field-of-view of the lens is approximately 2.3 degrees in diameter and is mounted at a 135-degree angle from the spacecraft Z axis or presumed spin axis. A positive output pulse is produced when the field-of-view of the sensor sweeps across the discontinuity caused by the sunlit earth against the background of interplanetary space. The time of this earth-in pulse provides the azimuthal distance of the earth horizon from the sun. An output pulse is also produced when the sensor sweeps across the discontinuity from the sunlit earth to the background of interplanetary space. This earth-out pulse is used in conjunction with the earth-in pulse to determine an earth width. This information, coupled with orbital information, is sufficient to determine the angle of the spacecraft spin axis with respect to the nadir direction.

1.4.3   Star Sensor

The Scanning Celestial Attitude Determination System (SCADS) comprises two units: sensor and electronics. The sensor is a visible-light photomultiplier with a single slit focal plane reticle producing a fan-shaped field of view. The plane of the fan includes the spacecraft spin axis as well as the optical axis. The sensor consists of a sunshade, lens assembly, photomultiplier tube, slit reticle, high voltage supply, preamplifier, and housing assembly.

The primary functions of the electronics are to detect star signals in the sensor output, to measure the width and amplitude of the star pulse, and to indicate the precise time at which the star is centered in the field of view.

As the slit projection sweeps past each bright star in the annular scan pattern, the focused image of the star lies momentarily in the transparent focal plane slit and starlight passes through to the photomultiplier behind the

reticle. From this star transit, the photomultiplier produces an analog pulse which is in turn fed to an electronic threshold trigger. If the star has a sufficiently bright magnitude, the pulse will exceed the threshold level and the trigger will fire at conditions of star "ingress" and "egress." The resultant trigger pulses may then be used to gate out the clock times at which ingress and egress occur. The instant at which the star is centered in the slit (the average of the ingress and egress times) is called the transit time of the star. The series of star transit times, coupled with pulse width and amplitude information, form the basic operational data necessary for determining spacecraft attitude.

1.4.4   Attitude and Spin Control System

The attitude and spin control system (ASCS) consists of two air core coils, a magnetometer, and a timer. The magnetometer and timer are used to control the operation of both coils. One coil is aligned so as to produce a magnetic dipole along the spin axis for precession control, and the other is aligned so as to produce a magnetic dipole perpendicular to the spin axis for spin rate control. Under automatic control the coils will not be energized unless the field perpendicular to the coil axis is greater than 75 milligauss. The spin control coil is commutated by the magnetometer as the satellite rotates. The timer is used to turn the entire system off after a set time to reduce a possible power load on the spacecraft. The precession control magnetometer can be overridden. However, the polarity of the coil is limited to a negative sense only. The field strength is ± 9230 pole-cm for the precession coil and 2654 pole-cm for the spin coil. This system was designed to operate at or near perigee, where the system would be most efficient.

1.5   MISSION PROFILE

The primary control objectives for the SSS-A mission will be directed toward maintaining the spin axis parallel to the perigee velocity vector as long as possible. The reason for this will be to avoid the aerodynamic torque disturbances which could on certain occasions cause the spin axis to violate the sun angle or declination constraints. These problems are discussed in greater detail in Section 2.

The definitive attitude objective will be to provide definitive spin axis orientation information to an accuracy of one degree using the OA sensor data. This data will be combined with the definitive orbit data for shipment to the Information Processing Division.

SECTION 2

MISSION ANALYSIS

2.1   ATTITUDE DISTURBANCE STUDY

2.1.1   Introduction

      A nominal launch will place the spin axis within the mission constraints of the sun angle between 30° and 70° and the declination between $+10^\circ$ and -10°. Just after launch, the sun will be behind the spin axis in right ascension. If the spin axis were to remain inertially fixed, the sun angle would be reduced as the sun advances in right ascension at roughly one degree per day. However, the spin axis will precess slowly under the influence of perturbative torques such as those due to solar radiation pressure, gravity gradient, residual magnetic dipoles, and aerodynamic. Because of the low perigee altitude, aerodynamic torque will be the primary cause of attitude disturbance. Initially the disturbance will cause declination motion, followed by right ascension motion. A magnetic control system is available to move the spin axis in order to correct for the decreasing sun angle and the attitude drift. (This control system is described in Section 1.4.) Since the control coil is effective only during a perigee pass, its versatility is somewhat limited. However, since the earth's magnetic field varies from pass to pass, the required versatility may be achieved through a careful selection of the pass during which the spin axis is to be precessed.

      The variation of the magnetic control capability as a function of perigee pass is discussed in the next section. The following sections are concerned with the details of the aerodynamic perturbation and its effect on the mission.

2.1.2 Magnetic Control

After the attitude control system is enabled near apogee, a planar electromagnetic coil perpendicular to the spin axis is activated whenever the magnetometer mounted perpendicular to the spin axis senses that the geomagnetic field has exceeded 75 milligauss. This section contains the results of a study to determine the effect on the precession path of magnetic field variations resulting from longitude and latitude of perigee variations. Subsequent analysis will show that the precession path is sensitive to the initial right ascension of the spin axis. This effect has been included in the study.

The emphasis of the magnetic control study is on the ability of the coil to produce declination changes to correct for the motion produced by aerodynamic torque. For the same coil setting, the net declination motion may vary from -2 to +2 degrees, depending on the longitude of perigee and the initial spin axis right ascension. However, under the same circumstances the net right ascension motion is 7 ± 1 degrees for the negative coil and -7 ± 1 degrees for the positive coil. The larger relative variation in the declination motion requires that it be examined in greater detail.

The magnetic torque along the inertial Z axis of the geocentric frame causes the change in declination. The Z component of the torque due to the interaction of the magnetic dipole produced by the coil with the geomagnetic field is given by:

$$N_z = MB \cos \delta \cos \delta_B \sin (\alpha_B - \alpha) \qquad (2\text{-}1)$$

where: M = magnitude of the coil

B = magnitude of the geomagnetic field

α, δ = right ascension and declination of the spin axis

α_B, δ_B = right ascension and declination of the magnetic field

For nominal values of δ, ± 10°, the torque (and therefore the declination motion) is insensitive to δ. It can be shown that this independence extends to much larger values of δ. Therefore, there is no need to study the precession path as a function of the initial declination of the spin axis.

During a perigee pass, the values of B, cos δ_B, and δ_B vary considerably as the latitude and longitude of the subsatellite point varies. Since the magnitude of the field is greatest near perigee, the motion is greatest there also. Therefore, it is convenient to represent the precession paths as functions of the latitude and longitude of the subsatellite point at perigee.

Since the value of α_B usually extends to three quadrants during a pass, the term $\sin(\alpha_B - \alpha)$ changes sign somewhere during the perigee pass, thus reversing the direction of the declination motion. For a specific pass, the time of the sign change depends on the right ascension of the spin axis. Thus the initial right ascension of the spin axis must also be included as a parameter in the study.

The magnetic field of the earth may be approximated by a tilted dipole. In this case, the magnitude of the field is inversely proportional to the cube of the distance from the center of the dipole. Thus, a variation in motion is expected as the altitude of perigee fluctuates. However, the fluctuation is so small that this should produce an effect on the order of 5 percent. A spot check of precession paths at 120 nmi vs 170 nmi indicates that this is correct. Therefore, the altitude of perigee will be considered to be a constant 120 nmi.

Motion in the equatorial plane is a result of magnetic control torques along the inertial X and Y axes. The torques are:

$$N_X = MB \ (\sin \alpha \cos \delta \sin \delta_B - \sin \delta \sin \alpha_B \cos \delta_B) \qquad (2\text{-}2)$$

$$N_Y = MB \ (\sin \delta \cos \alpha_B \cos \delta_B - \cos \alpha \cos \delta \sin \delta_B) \qquad (2\text{-}3)$$

The magnitude of the in-plane torque is:

$$|N_{eq}| = MB\sqrt{\cos^2 \delta \sin^2 \delta_B + \sin^2 \delta \cos^2 \delta_B - 2 \cos \delta \sin \delta \sin \delta_B} \quad (2\text{-}4)$$

$$\times \cos \delta_B \cos (\alpha_B - \alpha)$$

Near the equator, δ_B is large, so the third term in Equation 2-4 is small and the second term is negligible. For small declinations, Equation 2-4 can be approximated by:

$$|N_{eq}| \cong MB \cos \delta \sin \delta_B + \text{Residual} \quad (2\text{-}5)$$

The first term in Equation 2-5 is independent of the right ascension of the spin axis and is not sensitive to the declination of the spin axis or the declination of the field. There will, however, be some small effects due to the residual term, which arises primarily from the third term Equation 2-4. In general, these effects will be on the order of a degree as the latitude and longitude of perigee varies.

Precession paths for various perigee passes were generated by computing the magnetic torque every 50 seconds and updating the spin axis attitude every 150 seconds. The calculations were accomplished by the magnetic control subroutines of the Multi-Satellite Attitude Prediction Program (MSAP). This combination of subroutines and step sizes has proved to be quite accurate when applied to the prediction of the spin axis motion of the SAS-1 satellite. Since SAS-1 has a 50,000 p-cm torquing coil, this same procedure should be even more accurate for SSS-A.

Examples of precession paths for one perigee pass with different values of the initial right ascension are given in Figure 2-1. This figure shows that the variation in the change of right ascension as a function of the initial
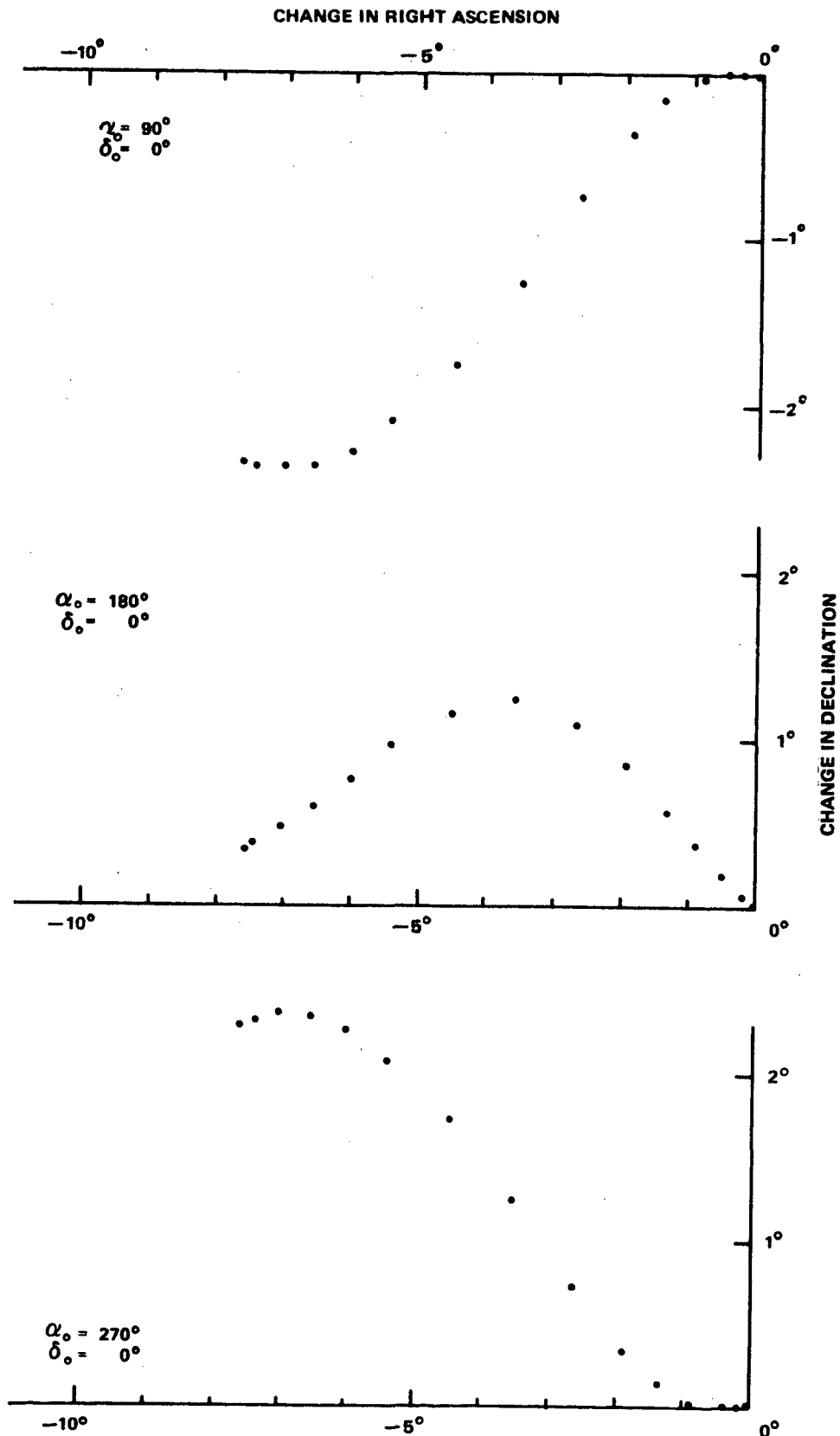
Figure 2-1. Spin Axis Precession Paths With the Coil at +8000.0 p-cm and Perigee at 90° Longitude and -2.6° Latitude. Time. Scale is Three Minutes Per Point.

right ascension is relatively small. In fact, the net right ascension change is nearly the same for most perigee passes. This is demonstrated in Tables 2-1 and 2-2. However, as predicted above, the net change in declination in Figure 2-1 varies from -2^O to $+2^O$. Thus a plot of net declination change as a function of initial right ascension is of interest.

A series of such plots is presented in Figure 2-2. These plots are for perigee passes spaced about 60° apart in longitude at roughly the same latitude of -2.6^O and the same coil strength of +8000.0 p-cm. The coil strength was revised to 9230.0 p-cm after these plots were made. The effect should increase the amplitude of these curves by about 10 percent without affecting their general shape.

Reversing the sense of the coil causes a shift of 180° in the phase of these curves. The amplitudes are the same within 0.25^O. The slight difference in amplitude is due to the fact that the precession is in the opposite direction, so that the sine term in Equation 2-1 changes sign at a slightly different time. However, the difference in amplitude is small compared with the variation due to longitude and initial right ascension. Thus the -8000.0 p-cm case is not presented here. All subsequent plots have been generated with the coil in the positive sense.

The sinusoidal variation in net declination change as a function of initial right ascension, which was predicted in Equation 2-1, is demonstrated in Figure 2-2. The amplitude and phase of the curve depend on the longitude of the perigee pass. The phase of these curves also depends on the orbit, since a different phase may be expected if the satellite sweeps through a perigee at a given longitude from high latitudes to low or from low latitudes to high.

Table 2-1. Net Right Ascension Changes for Perigees at -2.6°
Latitude With Various Initial Altitudes

LONGITUDE	CHANGE IN a (DEGREES)				
	$\delta = 0^{\circ}$	$\delta = 20^{\circ}$			
	ALL a	$a = 0^{\circ}$	$a = 90^{\circ}$	$a = 180^{\circ}$	$a = 270^{\circ}$
30°	-6.83	-6.12	-6.89	-7.58	-6.90
90°	-7.72	-6.90	-7.83	-8.57	-7.61
150°	-7.93	-7.30	-8.14	-8.50	-7.93
210°	-7.57	-7.39	-7.81	-7.76	-7.32
270°	-6.76	-6.74	-6.83	-6.78	-6.70
330°	-6.34	-6.07	-6.25	-6.60	-6.44

Table 2-2. Net Right Ascension Changes for Perigees at +2.9°
Latitude With Various Initial Altitudes

LONGITUDE	CHANGE IN a				
	$\delta = 0^{\circ}$	$\delta = 20^{\circ}$			
	ALL a	$a = 0^{\circ}$	$a = 90^{\circ}$	$a = 180^{\circ}$	$a = 270^{\circ}$
30°	-7.33	-7.30	-7.04	-7.26	-7.62
90°	-8.16	-8.14	-7.86	-8.27	-8.45
150°	-8.08	-7.97	-8.14	-8.18	-8.11
210°	-7.45	-7.42	-7.45	-7.48	-7.13
270°	-6.65	-6.77	-7.05	-6.52	-6.25
330°	-6.54	-6.77	-6.62	-6.31	-6.47
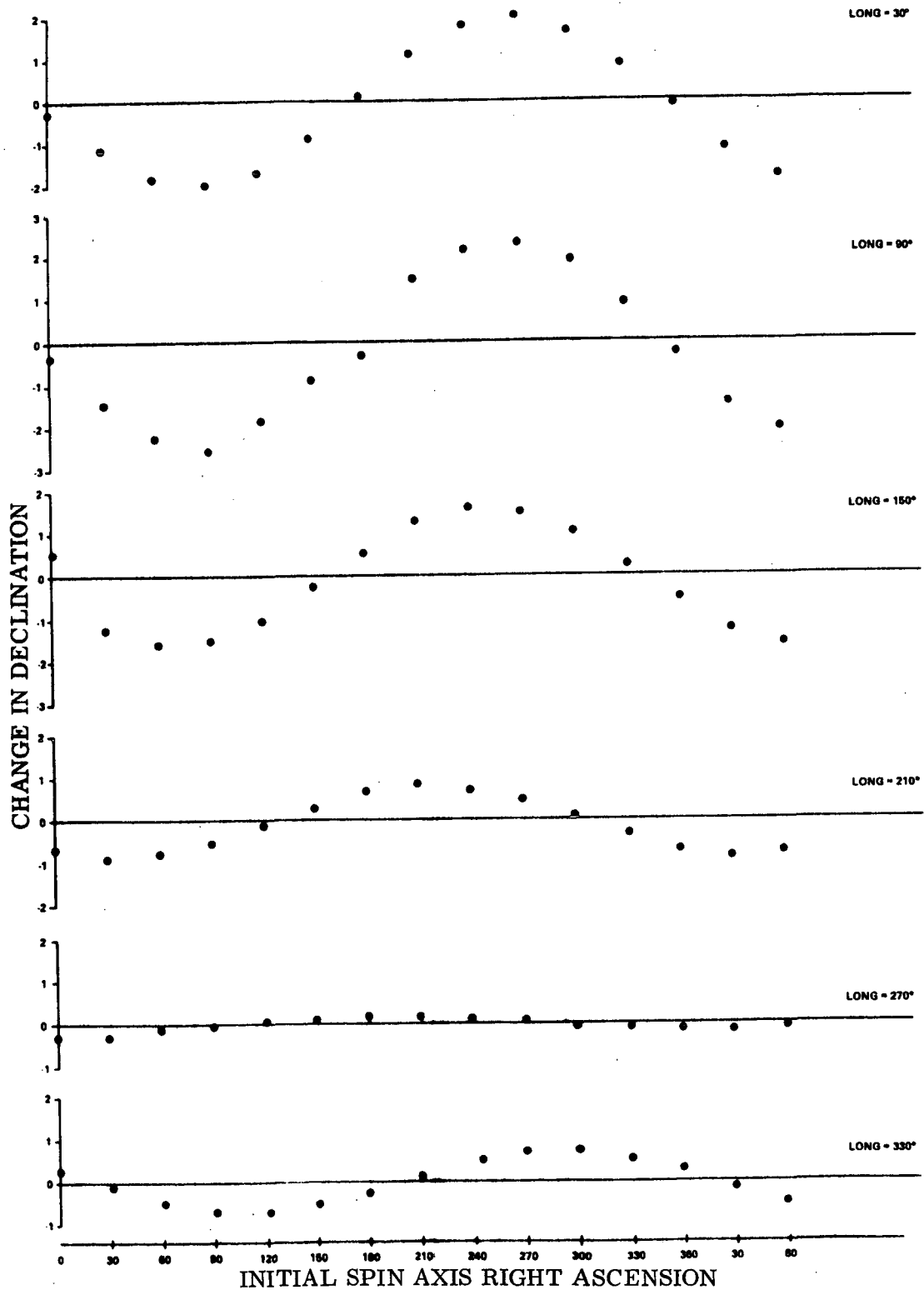
Figure 2-2. Net Change in δ Versus Initial α for Several Perigees at -2.6° Latitude

Although the curves presented in this section were generated with a specific series of orbits, they should serve to demonstrate the variety of motions available on successive perigee passes.

It appears from Figure 2-2 that, at this latitude, it is possible to obtain declination motion of about 2° over approximately one-third of the earth's surface, if the initial right ascension is located near 90° or 270°. However, a net declination change of about 1° is possible over most of the earth's surface and for nearly all right ascensions.

The large variation in the curves in Figure 2-2 as a function of longitude can be explained in part by the variation of the magnitude of the earth's field due to the variation in geographic longitude. A contour plot of the magnitude of the earth's field as a function of latitude and longitude taken from Reference 2-1 is shown in Figure 2-3. Although this plot is for 500 km altitude, it should serve to explain general trends. It is seen that longitudes 90° and 150° occur in areas of high field strengths.

The magnitude of the declination motion is sensitive to the declination of the magnetic field. Since the declination of the field near the geomagnetic equator is near 90°, the factor $\cos \delta_B$ varies rapidly. A plot of geomagnetic latitudes taken from Reference 2-1 is given in Figure 2-4. The term $\cos \delta_B$ increases rapidly with latitude. Thus at a longitude of 30°, a net declination change of 2° is possible because the declination of the field is small.

Just after launch, the latitude of perigee is roughly -2.7°. However, due to the secular advance of the line of apsides, the latitude first increases to a maximum of about $+3^{\circ}$ in five to six months and then decreases to a minimum of about -2.7°. As the latitude increases, the net declination motion decreases for longitudes 30°, 90°, and 150° because the geomagnetic field
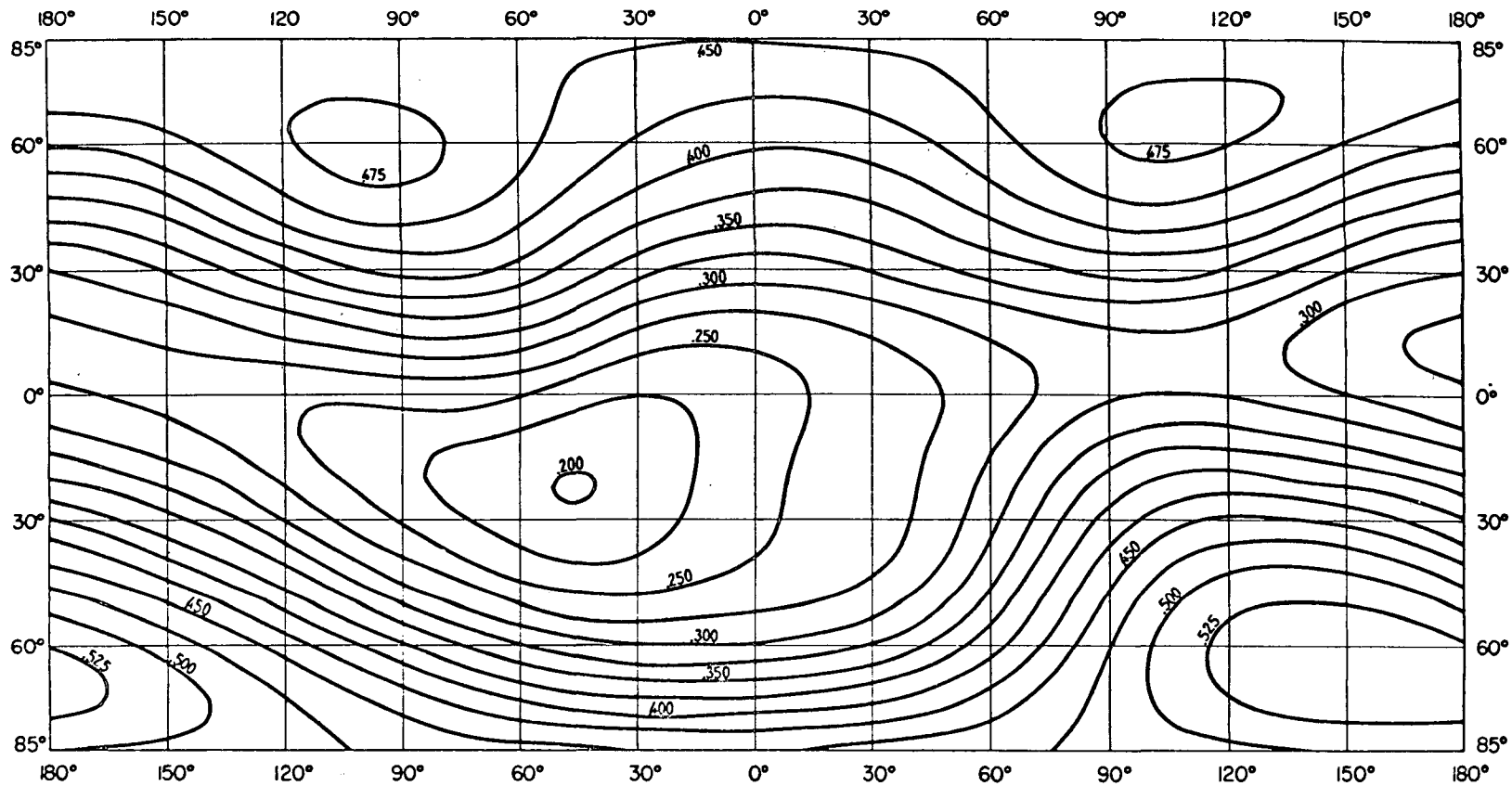
Figure 2-3. Total Intensity of the Earth's Magnetic Field, B, in Gauss, Epoch 1960, Altitude 500 km (Spherical Harmonic Analysis of Fougere)
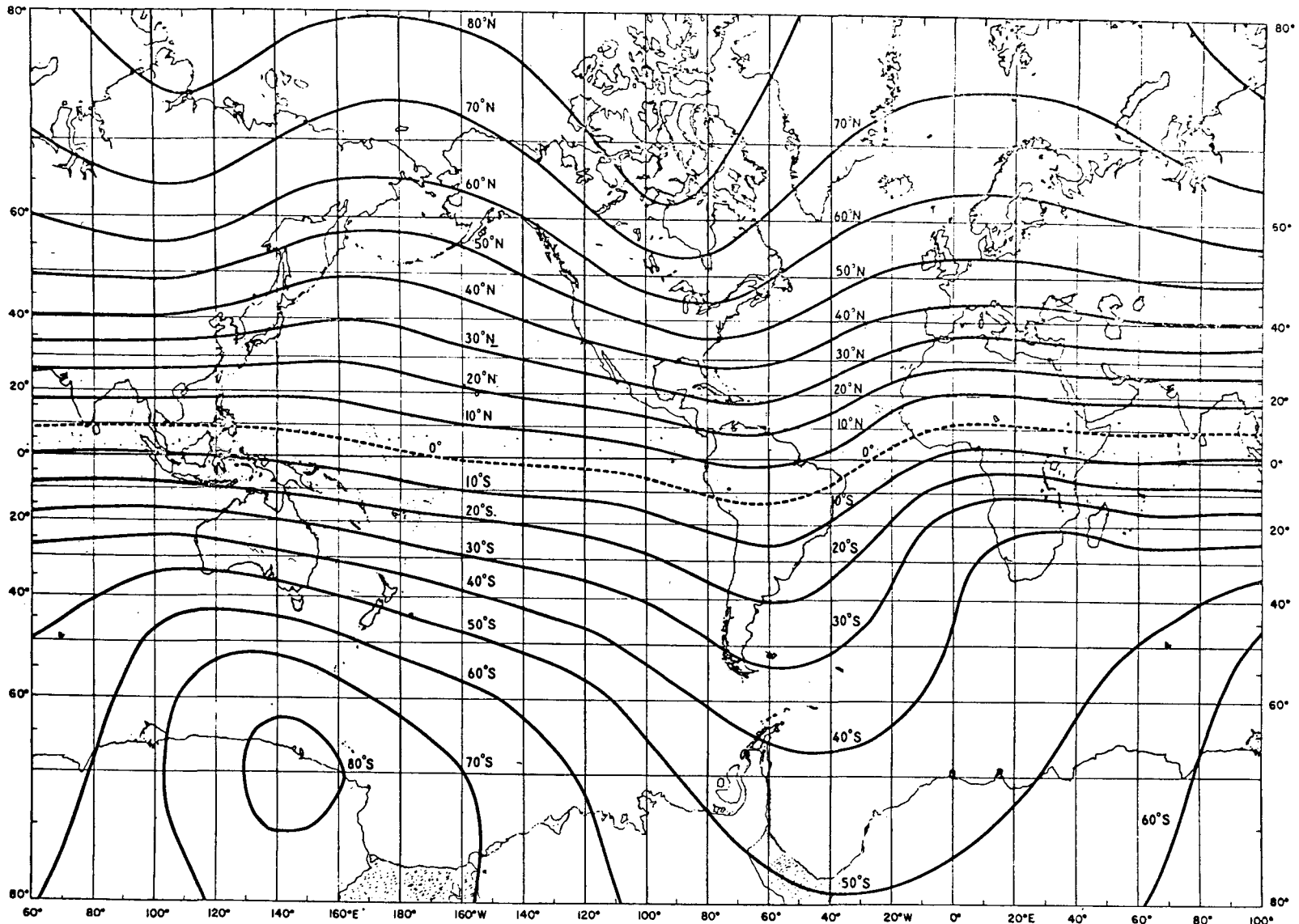
Figure 2-4. Magnetic Latitude, θ; the Dashed Line is the Dip Equator.

strength decreases. (See Figures 2-3 and 2-4.) Thus it is necessary to study the net declination motion as a function of latitude.

The six longitudes presented in Figure 2-2 are presented in Figure 2-5 through 2-10 as a function of latitude and initial right ascension. Longitudes 30° and 90° (Figures 2-5 and 2-6) can provide a maximum net declination of only 0.8^O at 2.9^O latitude, compared with the 2^O net declination possible at -2.6^O latitude. The net declination motion of longitude 150° (Figure 2-7) has deteriorated to a maximum of 0.3^O at a latitude of 2.9^O, compared to the 1.6^O maximum at -2.6^O latitude. There is very little variation of the net declination motion as a function of the latitude for longitude 210° (Figure 2-8). For a latitude of 2.9^O, the maximum net declination change is increased about 1^O for longitude 270° (Figure 2-9). It is interesting that the motion at 330° longitude undergoes a phase shift of 180° as the latitude varies from -2.7^O to 2.9^O (Figure 2-10).

In summary, it appears to be possible to obtain a net declination change of about 1^O for all latitudes and initial right ascensions. It is not possible to achieve this motion on every perigee pass, but it is possible for the majority of passes.

2.1.3   Aerodynamic Torque

In order to predict the motion of the spin axis under the effect of perturbative torques, the torques must be modeled mathematically. The aerodynamic torque model will be discussed in detail, since aerodynamic torque is the dominant perturbation.

The altitude of SSS-A will be sufficiently high so that it will be operating in an atmosphere that can be described as a free molecular flow. Thus molecules that strike the satellite surface and recoil do not affect incoming
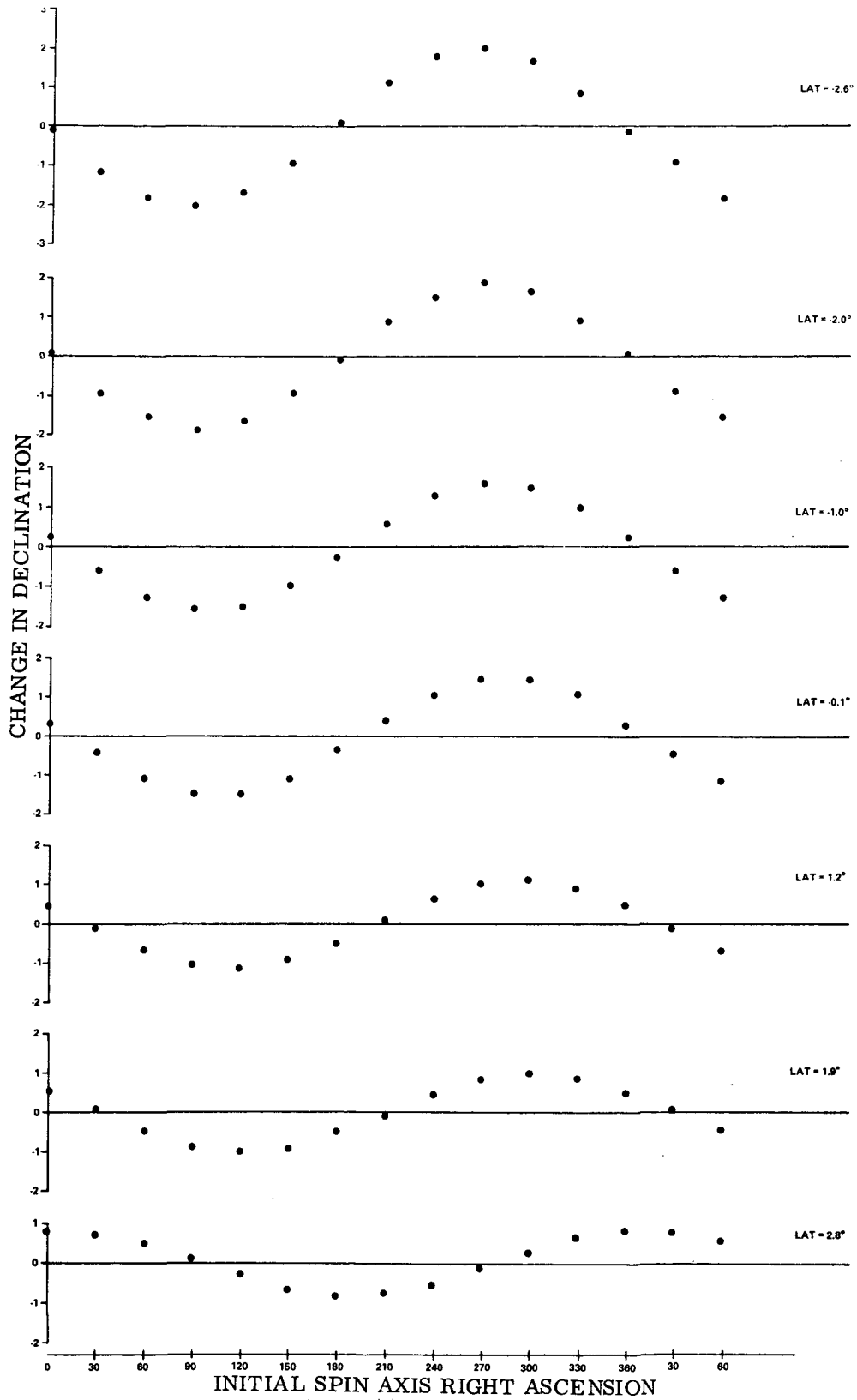
Figure 2-5. Net Change in δ Versus Initial α for Several Perigees at 30° Longitude

2-13
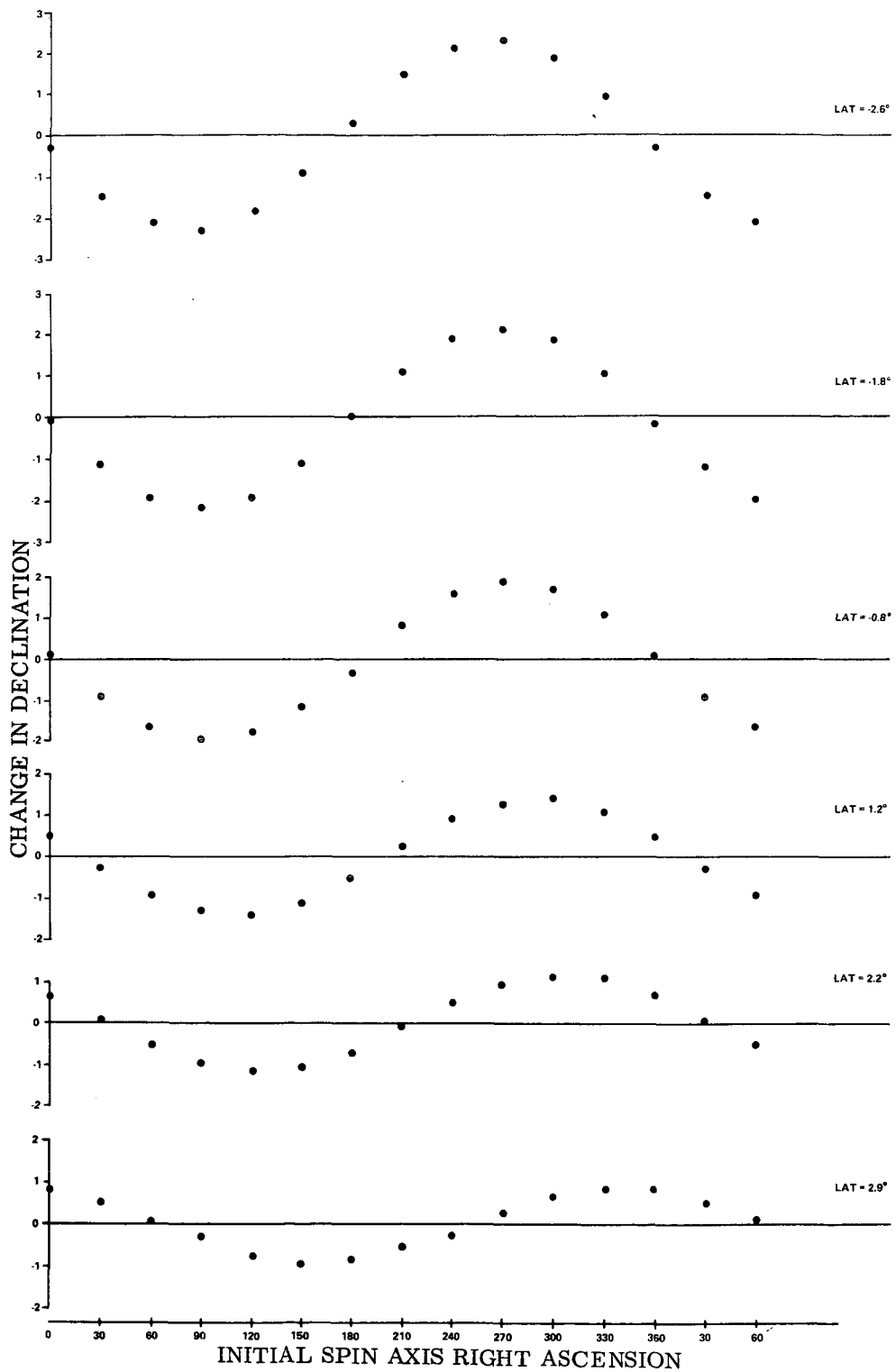
Figure 2-6. Net Change in δ Versus Initial α for Several Perigees at 90° Longitude

2-14
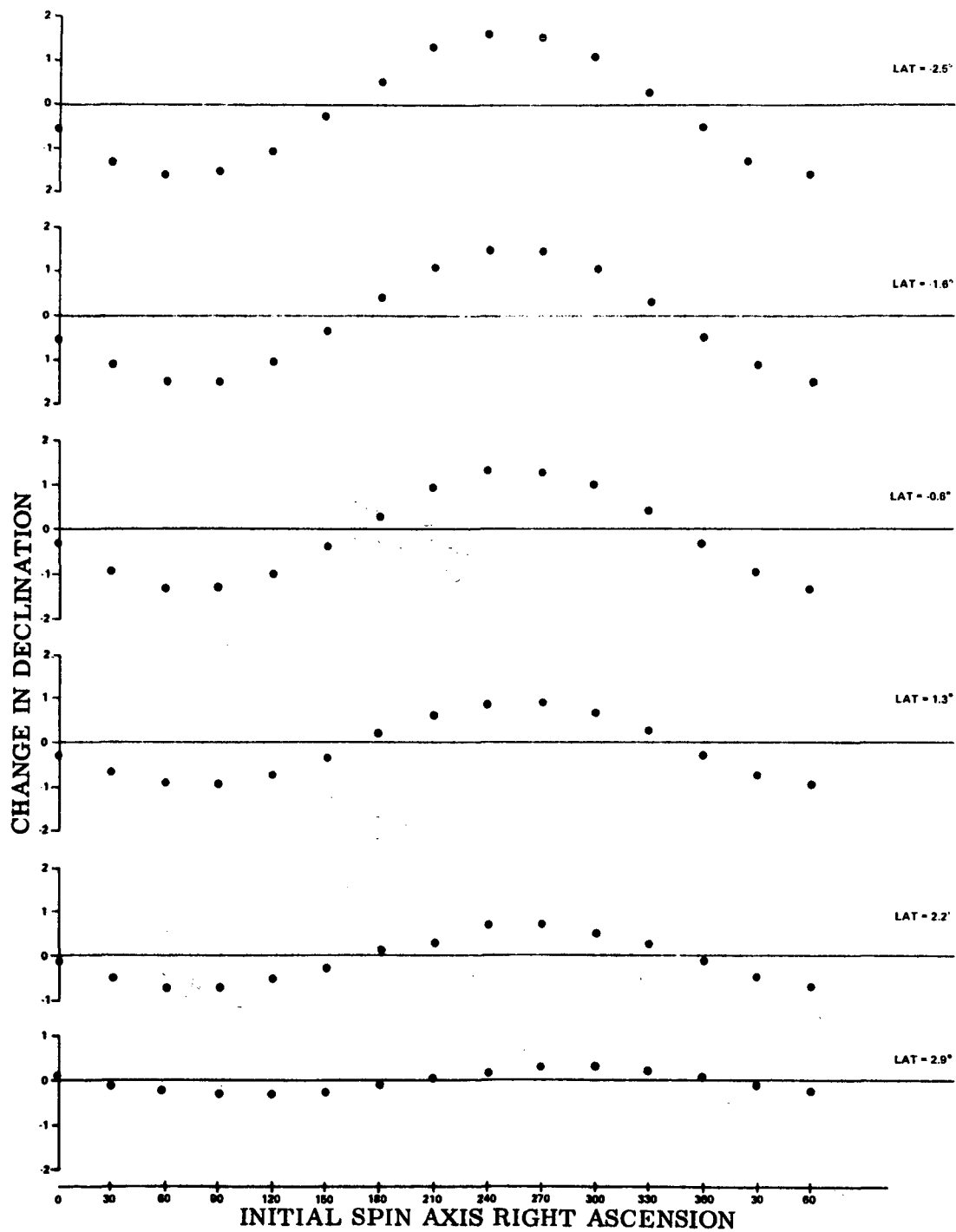
Figure 2-7. Net Change in δ Versus Initial α for Several Perigees at 150° Longitude

2-15
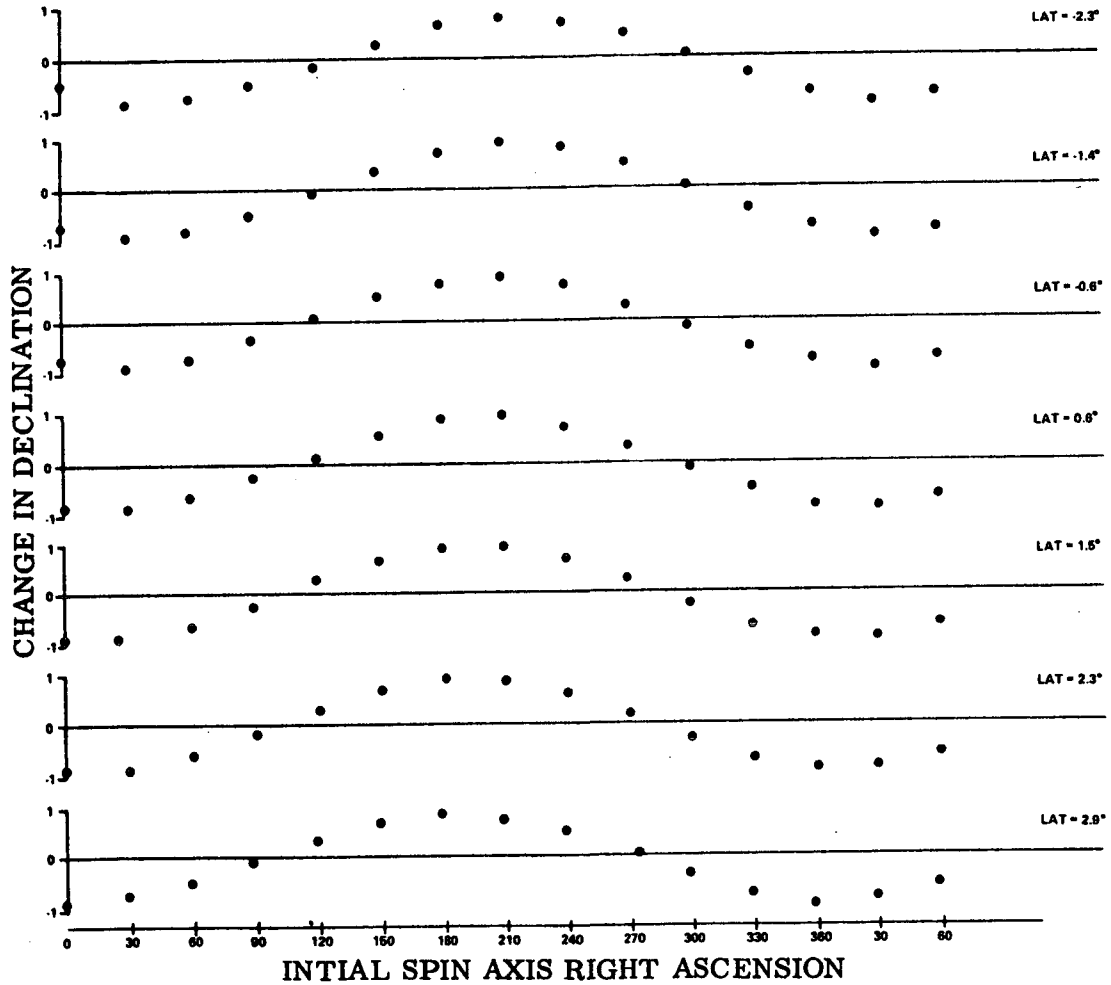
Figure 2-8. Net Change in δ Versus Initial α for Several Perigees at 210° Longitude
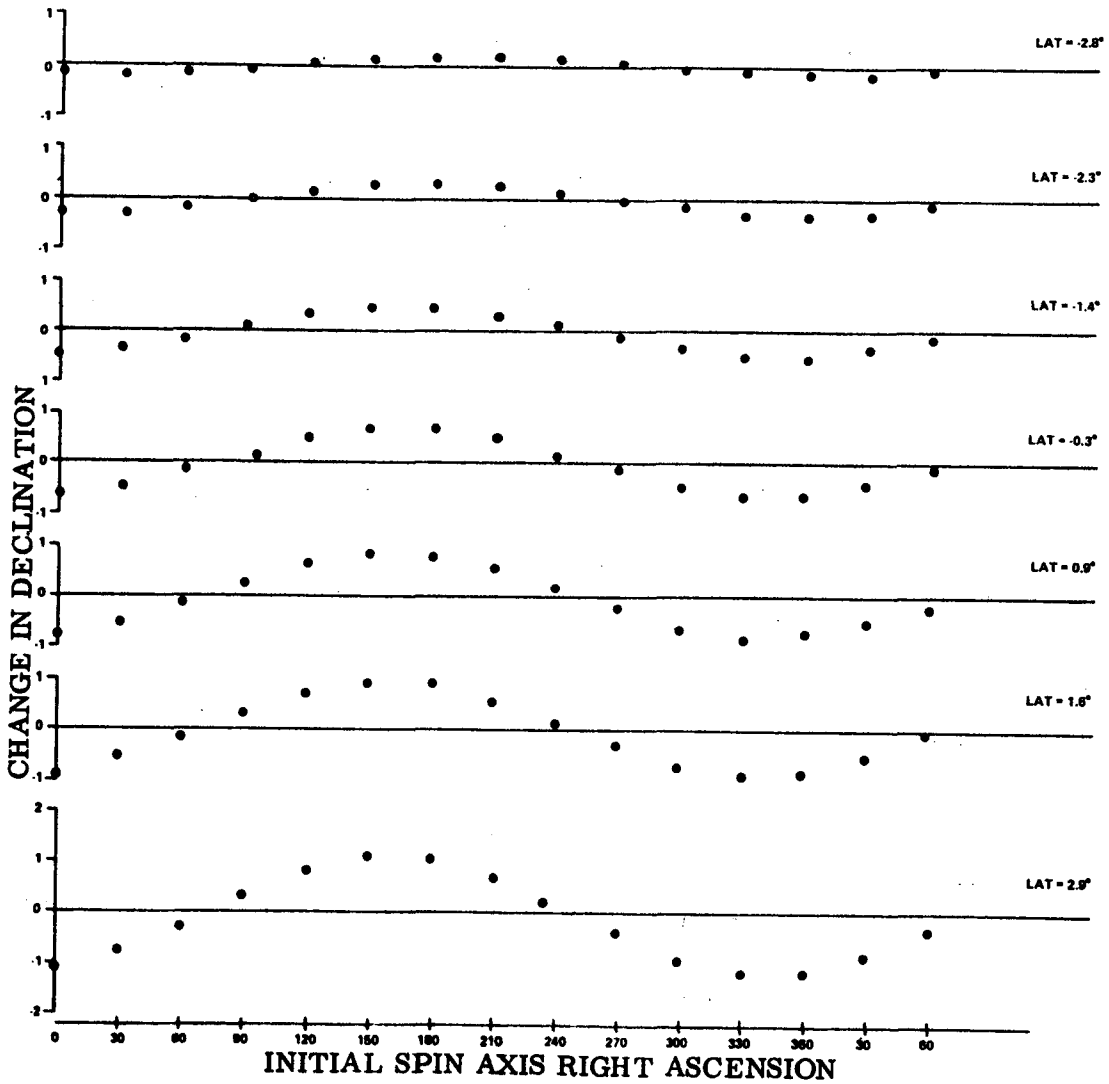
Figure 2-9. Net Change in δ Versus Initial α for Several Perigees at 270° Longitude
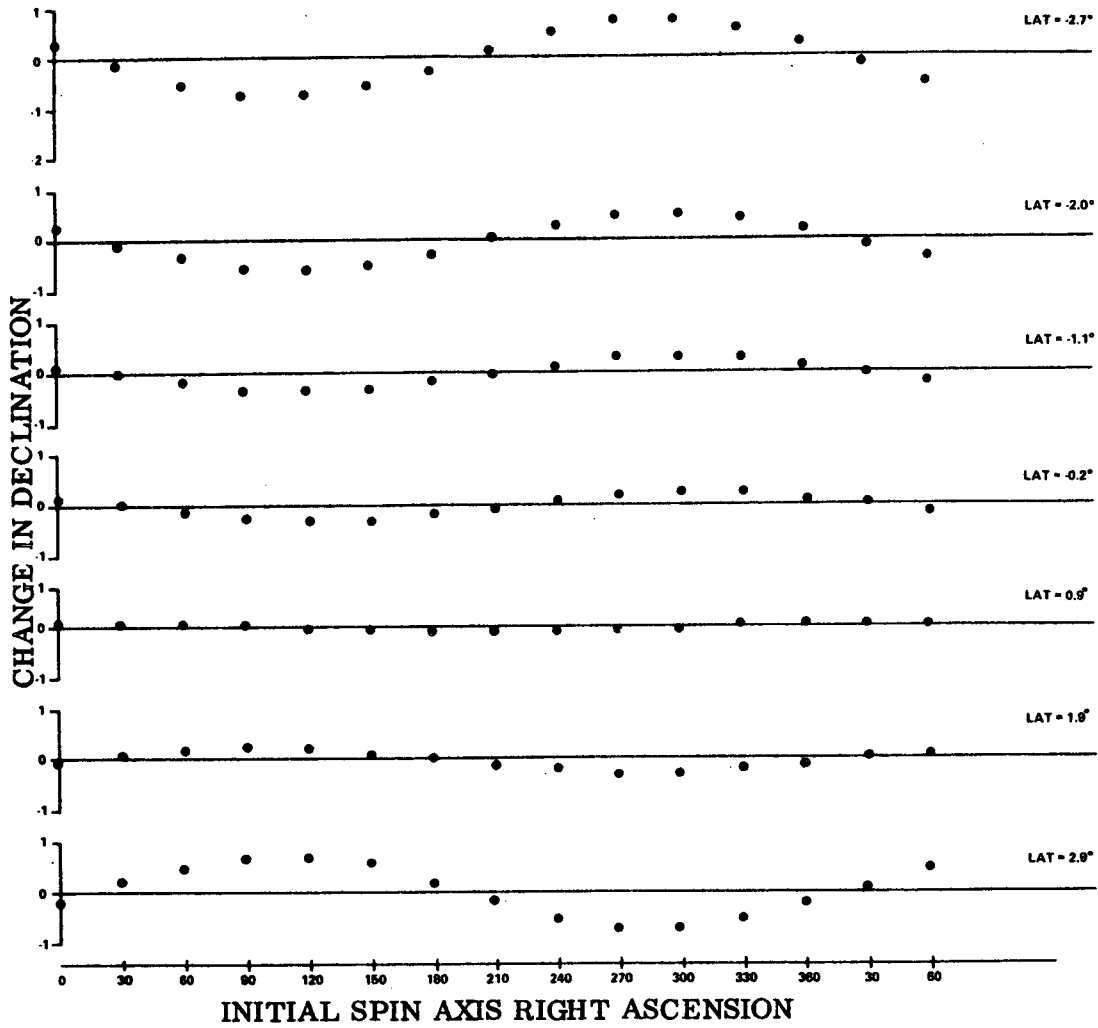
Figure 2-10. Net Change in δ Versus Initial α for Several Perigees at 330° Longitude

2-18

molecules. In addition, the thermal velocity of the molecules is much smaller than the velocity of the satellite. Therefore, as viewed from the satellite, the molecular flow appears as a nearly parallel flow moving in the opposite direction to the satellite's velocity, but with the same magnitude.

Under these assumptions, the force exerted by the atmosphere on the satellite is given by:

$$\vec{F} = C_D \left(\rho \frac{V^2}{2} \right) A_P \left(-\hat{v} \right) \tag{2-6}$$

where:

C_D = drag coefficient $\cong 2.0$

ρ = atmospheric density

V = magnitude of the satellite velocity

A_P = surface area of the satellite projected on the plane perpendicular to $\hat{v}$

$\hat{v}$ = unit vector in the direction of satellite velocity

The satellite surface is usually complex, so that it is difficult to determine its projected area A_P. However, if the satellite can be described as an aggregate of simple surfaces, it should be possible to determine the torque due to the aerodynamic force on each of the components. If some of the components of the satellite surface shadow the components which lie behind them along the molecular stream, the shadowed components should not be subjected to the aerodynamic force and should not contribute to the total torque. However, due to the random thermal motion of the air molecules, the stream as viewed by the satellite is not perfectly parallel. Thus it is highly probable that a number of air molecules strike the "shadowed" surfaces because their random velocity component is such that they miss the shadowing object. If the shadowing object is small enough and

far enough away, its effect may be negligible. In the following discussions, it will be assumed that shadowing effects are negligible for SSS-A.

The decomopostion of SSS-A into flat plates, spheres, and cylinders is given in Appendix B. The aerodynamic force on a flat plate is:

$$\vec{F}_P = C_D \left(\rho \frac{V^2}{2} \right) A \, (\hat{n} \cdot \hat{v}) \, (-\hat{v}) \quad \text{for } \hat{n} \cdot \hat{v} > 0 \tag{2-7}$$

The term $A \, (\hat{n} \cdot \hat{v})$ is the projected area of the plate where A is the area of the plate and $\hat{n}$ is a unit vector normal to the plate directed out from the center of mass. When the term $\hat{n} \cdot \hat{v}$ is positive, the plate will "see the wind." When the term $\hat{n} \cdot \hat{v}$ is negative, the plate will not "see the wind" because it is being shadowed by the body of the satellite. Thus:

$$\vec{F}_P = 0 \quad \text{for } \hat{n} \cdot \hat{v} < 0 \tag{2-8}$$

The force on a sphere is:

$$\vec{F}_S = C_D \left(\rho \frac{V^2}{2} \right) \frac{A_S}{4} \, (-\hat{v}) \tag{2-9}$$

where A_S is the surface area of the sphere.

The projected area of a cylinder when the velocity vector is normal to its axis is the product of the diameter of the cylinder and its length. At some other angle of incidence, the projected area is given by:

$$A_P = DL \sin \Theta \tag{2-10}$$

where: D = diameter of cylinder

L = length of cylinder

Θ = angle between $\hat{v}$ and cylinder axis

2-20

The force acting on the cylinder is then:

$$\vec{F}_C = C_D \left(\rho \frac{V^2}{2} \right) DL \sqrt{1 - (\hat{a} \cdot \hat{v})^2} \, (-\hat{v})$$

(2-11)

where $\hat{a}$ is a unit vector along the cylinder axis.

The torque due to each component is:

$$\vec{N} = \vec{r} \times \vec{F}$$

(2-12)

where $\vec{r}$ is the vector from the center of mass of the satellite to the centroid of a plate, the center of a sphere, or the center of the cylinder. The force $\vec{F}$ is determined by Equation 2-7, 2-9, or 2-11, respectively. The total torque exerted on the satellite about the center of mass is then the vector sum of the torques due to each component.

The spin axis is expected to be parallel to the velocity vector at injection into the orbit. Since injection occurs at perigee, this is the same as saying that initially the spin axis will be parallel to the perigee velocity vector v_P. Since the atmosphere is densest at perigee, the spin axis motion can be explained as though the aerodynamic force occurs only at perigee and is opposite to the velocity vector at perigee. The force is applied to the centroid of the projected area. The offset of the centroid from the center of mass is the moment arm for the torque. As the orientation of v_P relative to the spin axis changes, the projected area and the location of the centroid relative to the center of mass varies. When the spin axis is parallel to v_P, the projected area of the satellite is symmetrical, so that the centroid coincides with the center of mass. Therefore, no torque is expected. However, the perigee advances in right ascension because of the effect of the oblate earth on the orbit. Thus v_P leaves the spin axis behind in right ascension. As it does so, the centroid of the projected area moves away from the center of mass, causing an increase in the aerodynamic torque.

2-21

The effect of the increasing aerodynamic torque on the spin axis attitude was studied by incorporating the aerodynamic model, consisting of Equations 2-7 to 2-11, and the decomposition in Appendix B into MSAP. Ultimately, the system was used to simulate the history of the spin axis during the course of a year-long mission. That simulation included the effects of solar gravity on the orbit, magnetic control torques, and gravity gradient torque, as well as aerodynamic torque.

The aerodynamic force equations require knowledge about the velocity vector of the satellite and about the atmospheric density at the satellite's position. MSAP can obtain the velocity and position vectors either from an orbit generator or from an ephemeris tape. The first simulations were made with an orbit generator using the following elements:

Epoch	May 1, 1971
Epoch time	5.0 hours U.T.
Semi-major axis	23051.28 km.
Eccentricity	0.713740
Inclination	2.94°
Mean anomaly	0.0°
Argument of perigee	290.71°
Right ascension of ascending node	60.04°

The orbit generator includes the effects of the earth's oblateness, but not the effects of solar gravitation. Therefore, the early simulations included the secular advance of the perigee in right ascension, but not the variation of the perigee altitude expected for the SSS-A orbit. The effect of the varying perigee height was studied by changing the semi-major axis to achieve the desired perigee altitude.

2-22

The atmospheric density model provided with MSAP is based on the COSPAR International Reference Atmosphere (CIRA) 1965. It consists of 12 tables, one for every two hours of the day. Since the effects of the atmosphere occur primarily at perigee, which occurs at roughly the same local time, only one table was needed. In order to determine which table was best suited, the tables were compared with the 1970 model of the atmosphere by Jacchia (Reference 2-2).

The fundamental parameters in his model are the altitude and the exospheric temperature. The exospheric temperature is primarily dependent on the local time of day. The mission requirements are such that the satellite will be launched with perigee occurring at approximately 11 a.m. local time. During the course of the mission this time will gradually decrease. The densest table provided by MSAP was used in the study and corresponds to an exospheric temperature of roughly $900^{\circ}K$. In May 1971, this corresponds to a local time of about 8 a.m. At 120 nmi, the MSAP atmosphere is 70 percent of the Jacchia atmosphere at 11 a.m.

The drag coefficient, C_D, was set to a value of 2.0. The z axis moment of inertia was taken as 7.05×10^7 g-cm^2, with the distance from the separation plane to the center of mass as 38 cm. Below an altitude of 850 km, the aerodynamic torque was computed every 30 seconds and the spin axis was updated every 3 minutes. The perturbations due to gravity gradient and solar radiation pressure were found to be negligible. Thus, the only perturbing torque considered for the study was the aerodynamic torque. The initial attitude was parallel to v_p.

A plot of the resultant spin axis motion for a 120-nmi perigee altitude is presented in Figure 2-11. As expected, the attitude drift is very slow during the first few days. The perigee velocity vector is advancing in right
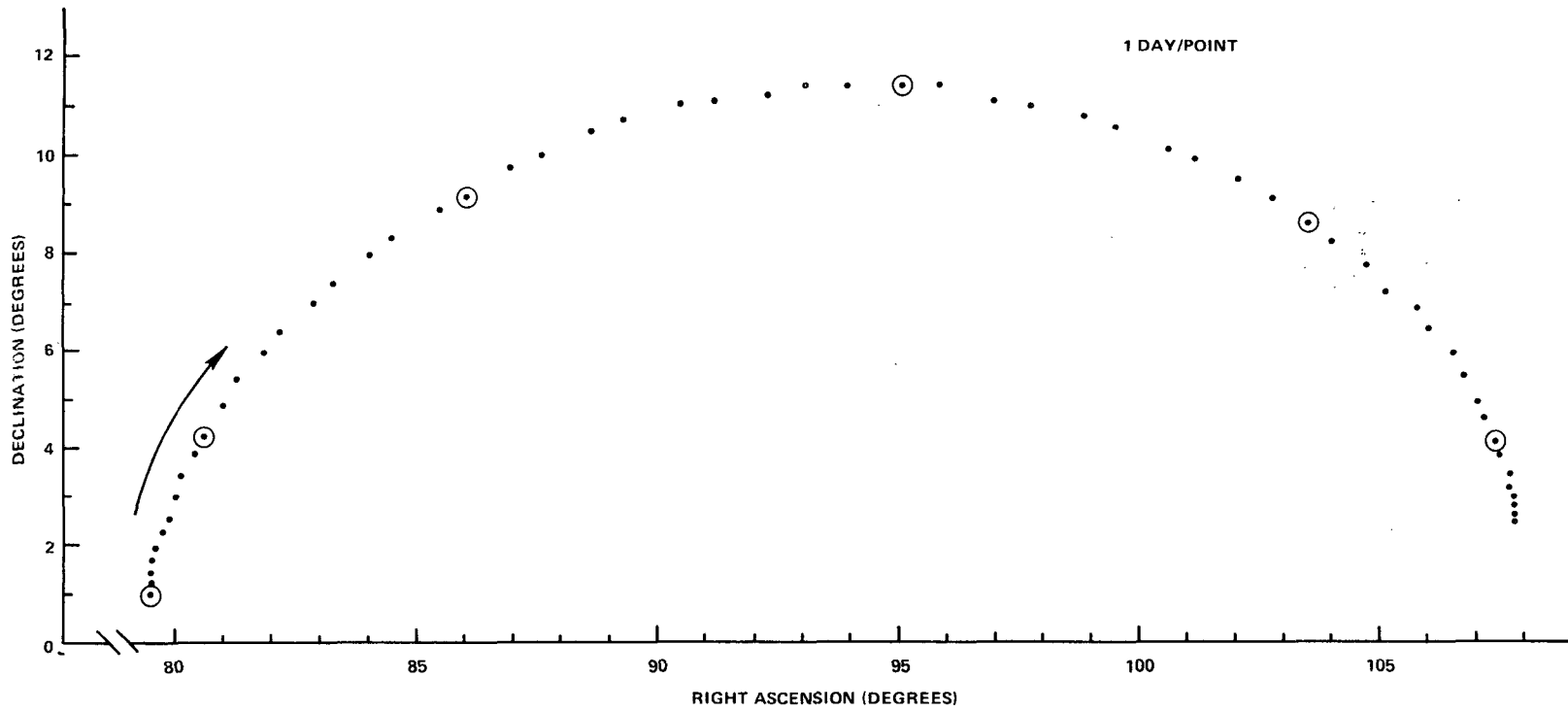
Figure 2-11.   Spin Axis Drift for a Perigee Altitude of 120 nmi

ascension at about 0.5° per day. After a few days, v_P is ahead of the spin axis. In 29 days, the spin axis has caught up with the perigee velocity vector.

The relationship of the spin axis to the perigee velocity vector is presented in Figure 2-12, where the declination of the spin axis is plotted versus the right ascension relative to the perigee velocity vector. As the spin axis lags behind v_P in right ascension, the centroid or center of pressure slips below the center of mass along the axis of symmetry. The force applied at the center of pressure causes a torque in the direction of the positive orbit normal, causing a positive declination drift. As the declination increases, the center of pressure drops below the orbit plane, so that a component of the torque in the orbit plane develops. At an altitude of 120 nmi, the aerodynamic torque causes a right ascension drift rate that is higher than the advance of v_P. After 29 days, the spin axis has drifted to the same right ascension as v_P. At that time, the component of the center of pressure offset in the orbit plane coincides with the center of mass, so the declination motion ceases. However, due to the high declination, the right ascension drift rate is at a maximum. The spin axis therefore drifts ahead of v_P. As the relative right ascension increases, the component of the center of pressure offset in the orbit plane increases. At this time, however, the aerodynamic force is applied in the opposite direction, since the spin axis is ahead of v_P. Therefore, a negative declination drift results. After about 56 days, the spin axis returns to a position nearly parallel to v_P. Thus it can be said that the spin axis is captured about the perigee velocity vector.

The aerodynamic force is proportional to the atmospheric density at perigee. The drift rate is proportional to the force and the offset of the centroid from the center of mass. Thus as the altitude of perigee increases, the atmospheric density at perigee decreases, consequently reducing the drift rate. A right ascension drift rate that exceeds the secular advance of perigee will then
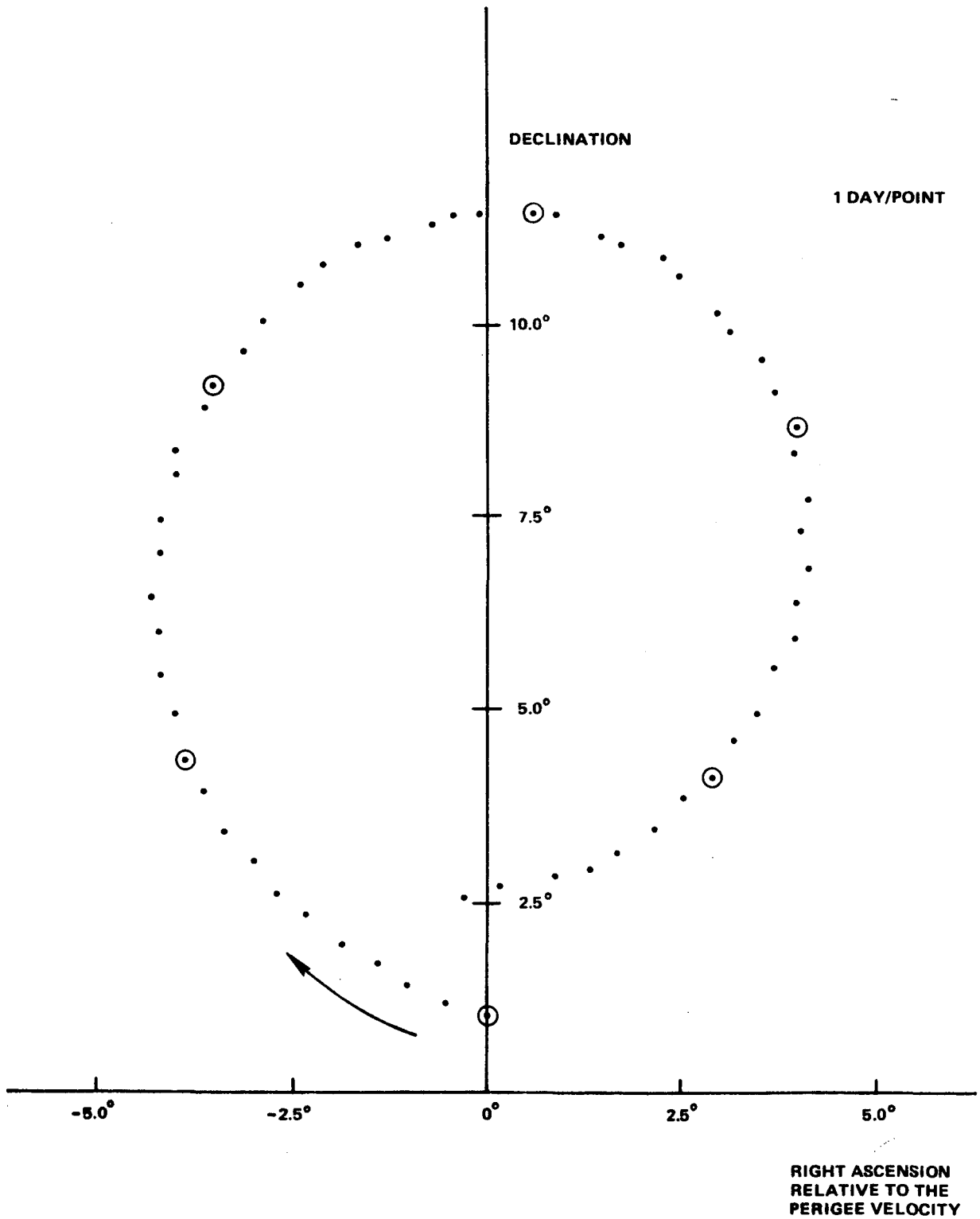
Figure 2-12. Spin Axis Drift Relative to the Perigee Velocity Vector for a Perigee Altitude of 120 nmi

occur at a larger centroid offset, i.e., at a higher declination. Eventually, the atmospheric density at perigee may become so low that a large centroid offset cannot compensate. Thus the spin axis will not catch up with v_P and capture will not occur.

At a perigee altitude of 140 nmi, the atmospheric density is about 1/3 that at 120 nmi. Thus it would be expected that the drift rate at this altitude would be three times slower and the maximum declination three times higher than at 120 nmi. An MSAP simulation for a perigee altitude of 140 nmi is presented in Figure 2-13. As expected, it takes the spin axis about 170 days to return to v_P.

An MSAP simulation for a perigee altitude of 170 nmi is presented in Figure 2-14. The density of the atmosphere at 170 nmi is one-tenth the density at 120 nmi. Increasing the capture circle of the 120 nmi perigee shown in Figure 2-12 by a factor of 10 would lead to a declination of greater than 100°. Thus the spin axis is probably not captured about the perigee velocity vector at 170 nmi. There is little evidence of capture in Figure 2-14.

In brief, then, the expected motion of the spin axis is toward a higher declination when the spin axis is behind v_P in right ascension and toward a lower declination when the spin axis is ahead of v_P in right ascension. As the declination increased from zero, the spin axis moves ahead in right ascension. If the altitude of perigee is low enough, the right ascension drift rate can exceed the secular advance of v_P.

A successful completion of the SSS-A mission places two constraints on the orientation of the spin axis. First, the attitude must be within 10° of the equatorial plane. Second, the angle between the spin axis and the sun must be between 30° and 70°. It was learned above that aerodynamic torque may cause
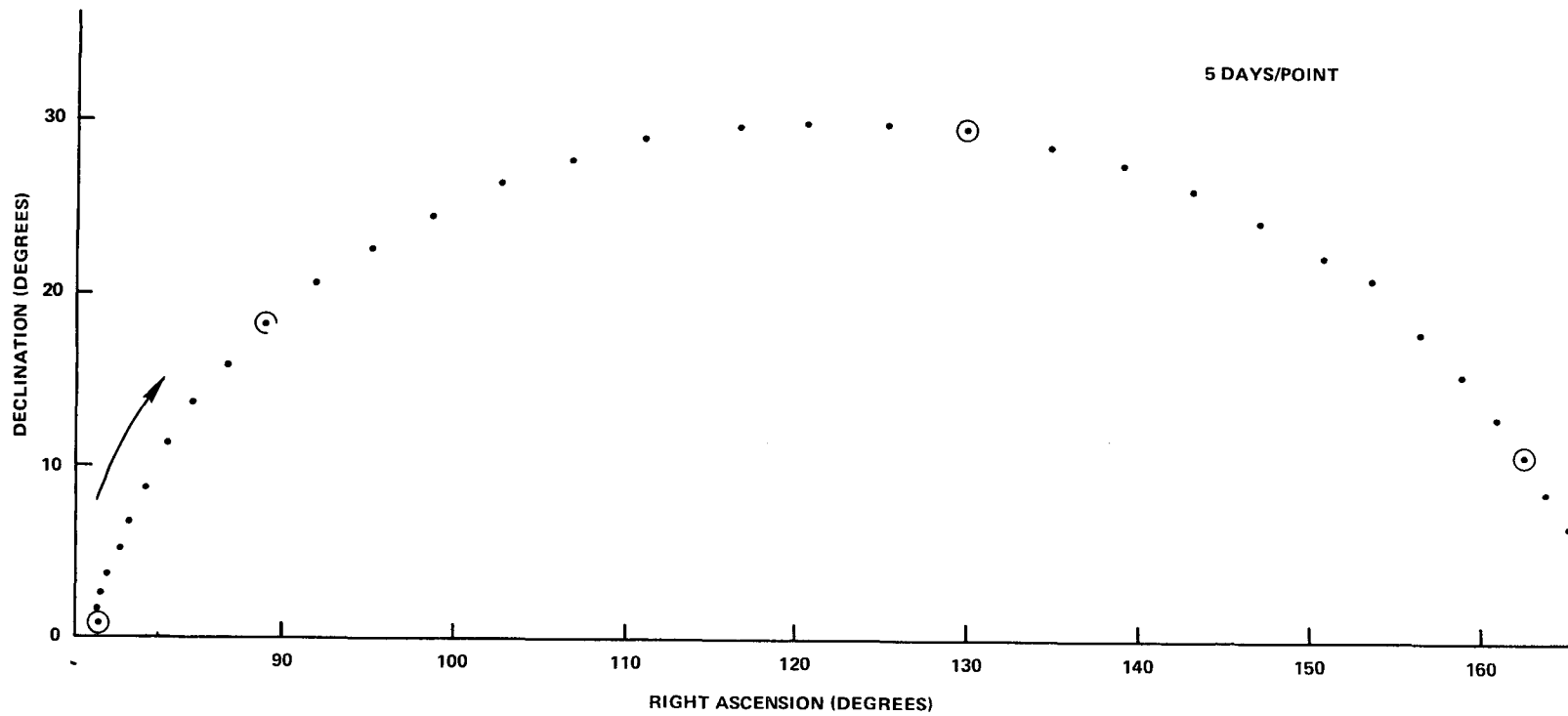
Figure 2-13.   Spin Axis Drift for a Perigee Altitude of 140 nmi
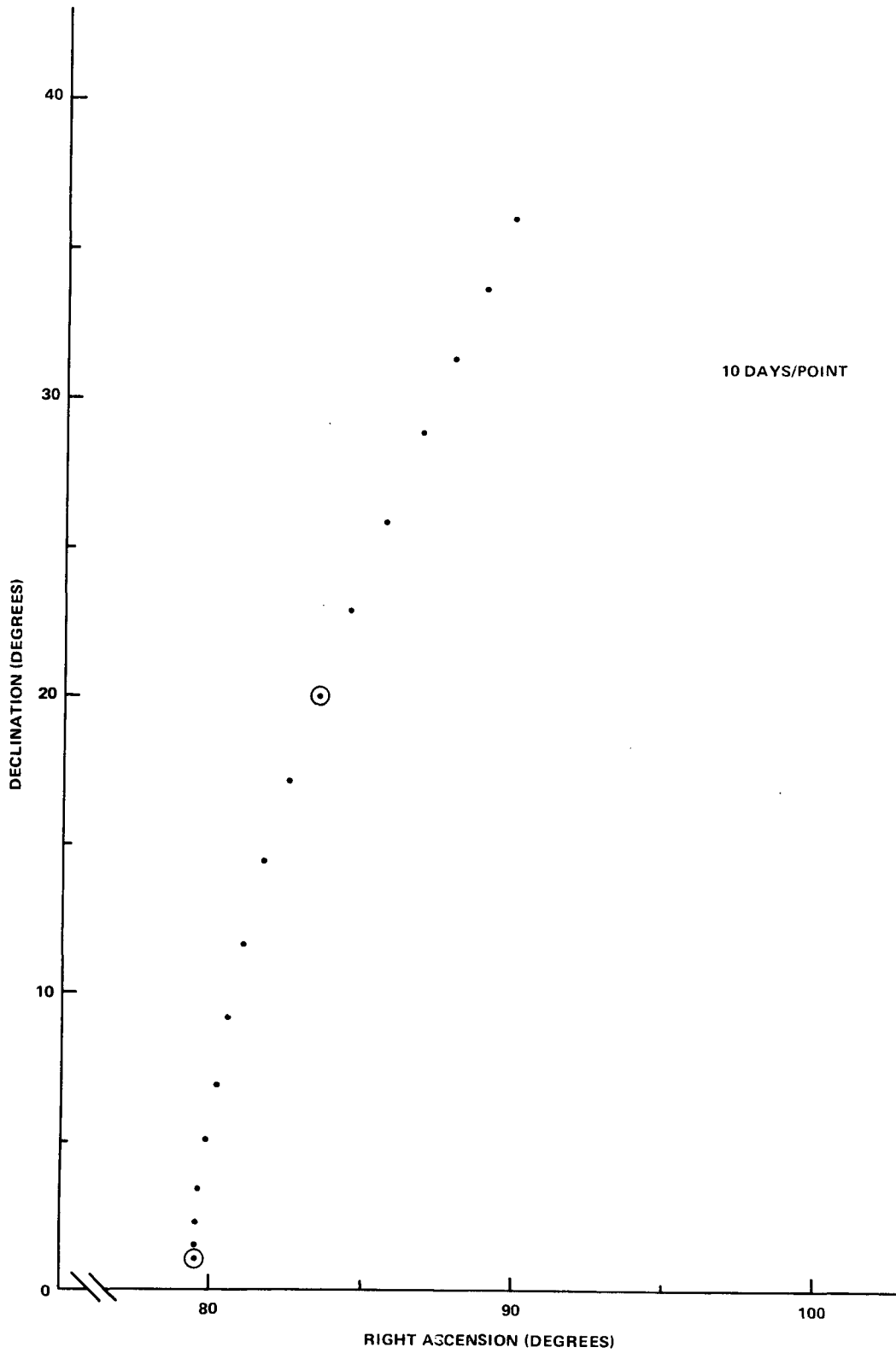
Figure 2-14. Spin Axis Drift for a Perigee Altitude of 170 nmi

a violation of the first constraint. However, the magnetic torquing coil may be used to move the spin axis ahead of the perigee velocity vector before the declination exceeds 10°. The aerodynamic torque will then cause a decrease in declination. Thus by tracking v_P, the effects of aerodynamic torque may be controlled.

A nominal launch will ensure the fulfillment of both attitude constraints and will place the sun behind the spin axis in right ascension. The nominal orbit is such that the perigee velocity vector will advance at about 0.5^O per day. Since the sun is advancing in right ascension at about 1^O per day, the sun will eventually catch v_P. Unless this occurs at the summer or winter solstice, a violation of the 30° sun angle constraint will occur. At a solstice, however, it might be possible to let the sun pass while the spin axis is at a high positive or negative declination and still maintain a sun angle greater than 30°. Even if this initial encounter is successfully carried out, the sun will be advancing away from v_P so that a sun angle of greater than 70° is inevitable if the spin axis continues to track v_P. Therefore, at some time in the course of the mission, it will be necessary to precess the spin axis away from v_P.

The simulations presented in Figures 2-11 to 2-14 indicated that when the spin axis is not parallel to v_P, the aerodynamic torque causes it to drift out of the equatorial plane. In order to plan a successful mission, it is necessary to know what sort of drift rates may be expected as a function of the spin axis attitude relative to the perigee velocity vector and as a function of the perigee altitude.

Drift rates for a series of attitudes relative to v_P are presented in Tables 2-3 and 2-4 for a perigee pass at an altitude of about 120 nmi. Table 2-3 shows that when the spin axis is at the same declination as v_P, there

Table 2-3. Right Ascension Drift Rates for Various Attitudes
Relative to the Perigee Velocity Vector for a
Perigee Altitude of 120 nmi

| RELATIVE RIGHT ASCENSION | RELATIVE DECLINATION | |
| | 0° | 10° |
DEGREES	DEGREES/ORBIT	DEGREES/ORBIT
0	0.00	+0.44
5		+0.44
10	-0.00	+0.41
20	-0.01	+0.37
30	-0.02	+0.31
40	-0.03	+0.23
50	-0.03	+0.15
60	-0.02	+0.08
70	-0.01	+0.02
75		+0.00
80	-0.01	-0.01
85		-0.00
90	+0.00	+0.00
95		+0.00
100	-0.00	-0.00
105		-0.02
110	-0.01	-0.04
120	-0.02	-0.12
130	-0.04	-0.23
140	-0.05	-0.32
150	-0.16	-0.41
160	-0.07	-0.48
170	-0.09	-0.54
175		-0.56
180	-0.10	-0.57

Table 2-4. Declination Drift Rates for Various Attitudes Relative to the Perigee Velocity Vector for a Perigee Altitude of 120 nmi

RELATIVE RIGHT ASCENSION	RELATIVE DECLINATION	
	0°	10°
DEGREES	DEGREES/ORBIT	DEGREES/ORBIT
0	0.00	-0.00
5		-0.22
10	-0.43	-0.42
20	-0.81	-0.79
30	-1.09	-1.08
40	-1.26	-1.25
50	-1.25	-1.24
60	-0.93	-0.94
70	-0.45	-0.46
75		-0.22
80	+0.01	+0.00
85		+0.20
90	+0.31	+0.31
95		+0.24
100	+0.01	+0.04
105		-0.20
110	-0.51	-0.46
120	-1.04	-0.95
130	-1.35	-1.28
140	-1.37	-1.32
150	-1.19	-1.14
160	-0.88	-0.84
170	-0.47	-0.46
175		-0.24
180	0.00	-0.01

is very little right ascension drift. However, at a relative declination of 10°, the right ascension drift reaches a maximum at 0° relative right ascension, a minimum at 90°, and another maximum at 180°.

On the other hand, the declination drift in Table 2-4 appears to be independent of the relative declination. The declination drift rate has maxima at 45° and 135° relative right ascension and is nearly zero at 0°, 80°, 100°, and 180°. The positive declination drift at 90° is an indication that the centroid is ahead of the center of mass on the spin axis (i.e., toward the fluxgate magneto- meter) at this angle of attack, whereas, for the other angles, the centroid is behind. A relative right ascension of 80° or 100° may prove to be a useful orientation for the spin axis when it can no longer remain parallel to v_p, because the aerodynamic torque vanishes at those points.

These tables can be extended to other relative attitudes because the satellite is symmetric about 0° relative right ascension and 0° relative declination. The direction of the drift can be determined by visualizing the orientation of the negative perigee velocity vector to the centroid--center-of- mass offset. In this way the direction of the torque, hence the drift, can be determined. The drift rate for a perigee pass at a different altitude can be es- timated by multiplying the appropriate drift rate from Tables 2-3 and 2-4 by the ratio of the atmospheric density at that perigee to the density $(1.41 \times 10^{-13}$ g/cc) at the perigee used to compile the tables. This ratio is part of the Perigee History Program output described in Section 8.3.

The z axis moment of inertia was changed to 7.47×10^7 g-cm^2 and the center of mass was moved to 36.3 cm from the center of mass. These changes reflect the mass parameters of the satellite as of March 2, 1971, and were incorporated into MSAP prior to generating Tables 2-3 and 2-4. In addi- tion, the atmospheric model in MSAP was changed to one patterned after Reference 2-3. This revision allows for the slow regression of perigee away

from the diurnal bulge as the sun advances in right ascension away from perigee. Previously, the regression had to be calculated by hand and the atmospheric tables switched accordingly.

2.2   LAUNCH WINDOW

The launch times to be considered in this section are from 4:30 to 7:00 U.T. on November 1, 1971. Injection will be at 120 nmi, with an apogee altitude of 5.9 earth radii. The orbital elements used are:

Epoch	November 1, 1971
Epoch time	4.5 – 7.0 hours U.T.
Semi-major axis	22114.17 km
Eccentricity	0.70153000
Inclination	2.892°
Mean anomaly	0.0°
Argument of perigee	289.540°
Right ascension of ascending node	235.630°–273.230°

With the approximation that the orbital inclination is zero, the perigee will advance in right ascension at 0.50° per day under the influence of the oblate earth. The perigee altitude will first increase and then decrease under the influence of solar gravitation. The length of time before a maximum or minimum perigee altitude depends on the orientation of the sun to the major axis of the orbit at the time of launch: the later the launch, the later and higher the perigee maximum and minimum.

The perigee maxima and minima for six launch times are listed in Table 2-5. The requirement of small aerodynamic torques leads to the

Table 2-5. The Effects of the Sun on the Orbit
Achieved at Various Launch Times
on November 1, 1971

LAUNCH TIME	INITIAL SUN ANGLE (DEGREES)	SOLAR DECLINATION AT INITIAL ENCOUNTER (DEGREES)	MINIMUM PERIGEE ALT (nmi)	MAXIMUM PERIGEE ALT (nmi)
4:30	42	-22	82	133
5:00	49	-20	89	135
5:30	56	-16	98	137
6:00	63	-11	105	138
6:30	70	-5	111	141
7:00	77	+3	113	145

choice of 6:30 as the best time to launch, since its minimum perigee altitude is the highest. A launch at 7:00 violates a sun constraint and therefore will not be discussed further.

Another consideration in choosing a launch time is the probable accuracy of the attitude determination for a given launch time. Therefore, a study was conducted to determine the effect of uncertainties in the observables -- sun angle, sensor mounting angle, rotation angle, angular radius of the earth, angular error in space in spacecraft position, and distance from the earth -- on attitude determination of SSS-A. For the first orbit following launch, four different launch times were considered. The Optical Aspect Data Predictor (Section 8.2) was used, with the following input parameters:

> Date - November 1, 1971
>
> Launch time (hours/min/sec, GMT) 4/0/0, 5/0/0, 6/0/0, 7/0/0
>
> SSS-A orbit - nominal
>
> Sensor mounting angle - 135 degrees
>
> Attitude - parallel to velocity vector at perigee
>
> Time interval - 60 seconds/frame
>
> Uncertainties applied -
>
>> sun angle, 0.25 degrees
>>
>> sensor mounting angle, 0.1 degrees
>>
>> rotation angle, 0.1 degrees
>>
>> angular radius of the earth, 0.1 degrees
>>
>> angular error in spacecraft position, 0.1 degrees
>>
>> distance from the earth, 1.0 kilometers

The results are shown in Table 2-6. Almost all useful data during the first orbit after launch is obtained while the spacecraft is near perigee. The smallest

Table 2-6. Error Study Results

LAUNCH TIME (HOURS/MIN/SEC)	SUN ANGLE	ATTITUDE		MAXIMUM ANGULAR ERROR IN ATTITUDE (DEGREES)	AVERAGE ANGULAR ERROR IN ATTITUDE (DEGREES)	MINUTES OF USEFUL DATA
		R.A.	DEC.			
4/0/0	34.90	247.63	0.97	3.49	.6	47
5/0/0	48.66	262.67	0.97	8.83	1.1	27
6/0/0	62.91	277.71	0.97	7.83	1.3	27
7/0/0	77.35	292.75	0.97	7.59	1.5	26

average error occurs for the 4/0/0 launch time, with the worst data occurring approximately 10 minutes after perigee.

To determine a range of launch times acceptable from the standpoint of aerodynamic torque, some estimate must be made of the torques to be expected during the course of the mission as a function of the launch time. The estimate can be made using Tables 2-3 and 2-4 and the perigee density ratios from the Perigee History Program. The method requires in addition a rough estimate of the expected position of the spin axis relative to the perigee velocity vector, v_P, during the course of the projected mission.

There are two considerations with respect to the position of the spin axis: the requirement that the declination be within 10° of the equatorial plane implies that the spin axis should track v_P, and the requirement that the sun angle be kept between 30° and 70° implies that the spin axis should track the sun. Some combination of the two will probably be employed.

Initially, the spin axis will track v_P until the sun angle reaches 30°. If at that point, the sun is at the same right ascension as v_P and is at a declination of -20° or lower, it should be possible to let the sun pass under the spin axis if the spin axis is at $+10^O$ declination. Then the spin axis could continue to track v_P until the sun angle reached 70°. At that point, the spin axis could be moved under the sun to about 90° ahead of v_P and allowed to drift there. When the sun reaches 110° ahead of v_P, the spin axis could be precessed under it to 180° ahead of v_P and could track $-v_P$ for the remainder of the year. Table 2-5 indicates that this approach may be possible for launches earlier than 5:00. This procedure was carried out in an MSAP simulation of a one-year mission for a July 15 launch. The results are contained in Appendix A.

For launches later than 5:00, the procedure of letting the sun pass under the spin axis fails because the sun catches v_P at a later time and at a higher declination. There are then two possible choices for these later launches. The first is to leave v_P when the sun angle reaches 30° and track the sun. The second is to precess the spin axis behind v_P over the sun to a relative right ascension of -80 or -100°. This maneuver would have to be accomplished when the sun was at winter solstice and before the sun angle reached 30°. In both cases, the remainder of the mission would consist of either tracking v_P when the spin axis is near a point of zero aerodynamic torque or tracking the sun when a possible sun angle violation conflicts with tracking v_P.

The details of this procedure are presented in Table 2-7 for the first choice and in Table 2-8 for the second choice. In these tables, γ is the sun angle, v_P is the position of the perigee velocity vector, and α_R is the right ascension of the spin axis relative to v_P. The tables are divided into phases distinguished by whether the spin axis is tracking the sun or tracking the perigee velocity vector at some angle relative to it.

The tracking of the sun at 35° and 65° rather than 30° and 70° allows for the necessity of zigzagging magnetic torques to control declination drift during those periods. The change in tracking the sun from 35° to 65° is done to avoid the aerodynamic drift maxima that occur at $\alpha_R = 45^O$ and 135°.

Under the approximation that the sun, v_P, and the spin axis move in the equatorial plane, the position of the spin axis can be estimated for the course of the mission. The anticipated spin axis histories for the five launch times were generated. The histories for both choices for a 6:00 launch are presented in Figures 2-15 and 2-16. These figures are meant to be only an estimate of the trend of the spin axis motion. In practice, the spin axis will

Table 2-7. Movement of the Spin Axis Relative to the Sun and to the Perigee Velocity Vector, v_P, While Staying Ahead of the Sun. The Spin Axis – Sun Angle is Given by γ and the Right Ascension of the Spin Axis Relative to v_P is Given by α_R.

PHASE	TRACK	AT	UNTIL	TORQUE TO
I	v_P	$\alpha_R = 0°$	$\gamma = 30°$	
II	SUN	$\gamma = 35°$	$\alpha_R = 30°$	$\alpha_R = 60°$
	SUN	$\gamma = 65°$	$\alpha_R = 80°$	
III	v_P	$\alpha_R = 80°$	$\gamma = 35°$	$\alpha_R = 100°$
	v_P	$\alpha_R = 100°$	$\gamma = 35°$	
IV	SUN	$\gamma = 35°$	$\alpha_R = 120°$	$\alpha_R = 150°$
	SUN	$\gamma = 65°$	$\alpha_R = 180°$	
V	v_P	$\alpha_R = 180°$	$\gamma = 35°$	

Table 2-8. Movement of the Spin Axis Relative to the Sun and to the Perigee Velocity Vector, v_P, While Dropping Behind the Sun. The Spin Axis – Sun Angle is Given by γ and the Right Ascension of the Spin Axis Relative to v_P is Given by α_R.

PHASE	TRACK	AT	UNTIL	TORQUE TO
I	v_P	$\alpha_R = 0°$	DECLINATION OF SUN = -23°	$\alpha_R = -80°$
	v_P	$\alpha_R = -80°$	$\gamma = 65°$	
II	SUN	$\gamma = 65°$	$\alpha_R = -60°$	$\alpha_R = -30°$
	SUN	$\gamma = 35°$	$\alpha_R = 0°$	
III	v_P	$\alpha_R = 0°$	$\gamma = 65°$	
IV	SUN	$\gamma = 65°$	$\alpha_R = 30°$	$\alpha_R = 60°$
	SUN	$\gamma = 35°$	$\alpha_R = 80°$	
V	v_P	$\alpha_R = 80°$	$\gamma = 65°$	$\alpha_R = 100°$
	v_P	$\alpha_R = 100°$	$\gamma = 65°$	
VI	SUN	$\gamma = 65°$	$\alpha_R = 120°$	$\alpha_R = 150°$
	SUN	$\gamma = 35°$	$\alpha_R = 180°$	
VII	v_P	$\alpha_R = 180°$	$\gamma = 65°$	
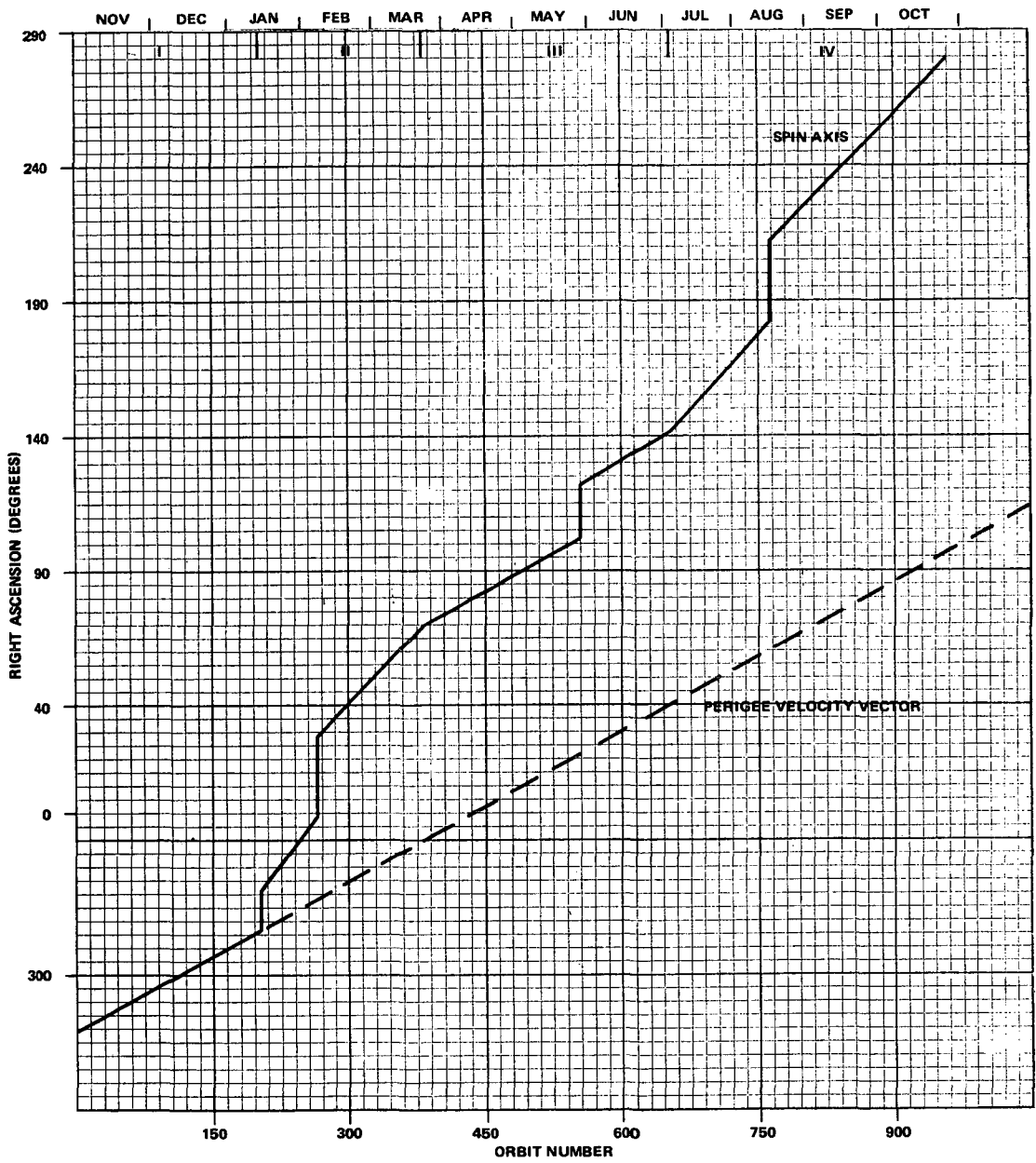
Figure 2-15. Anticipated Spin Axis Position for a 6:00 Launch.
The Spin Axis Stays Ahead of the Sun.
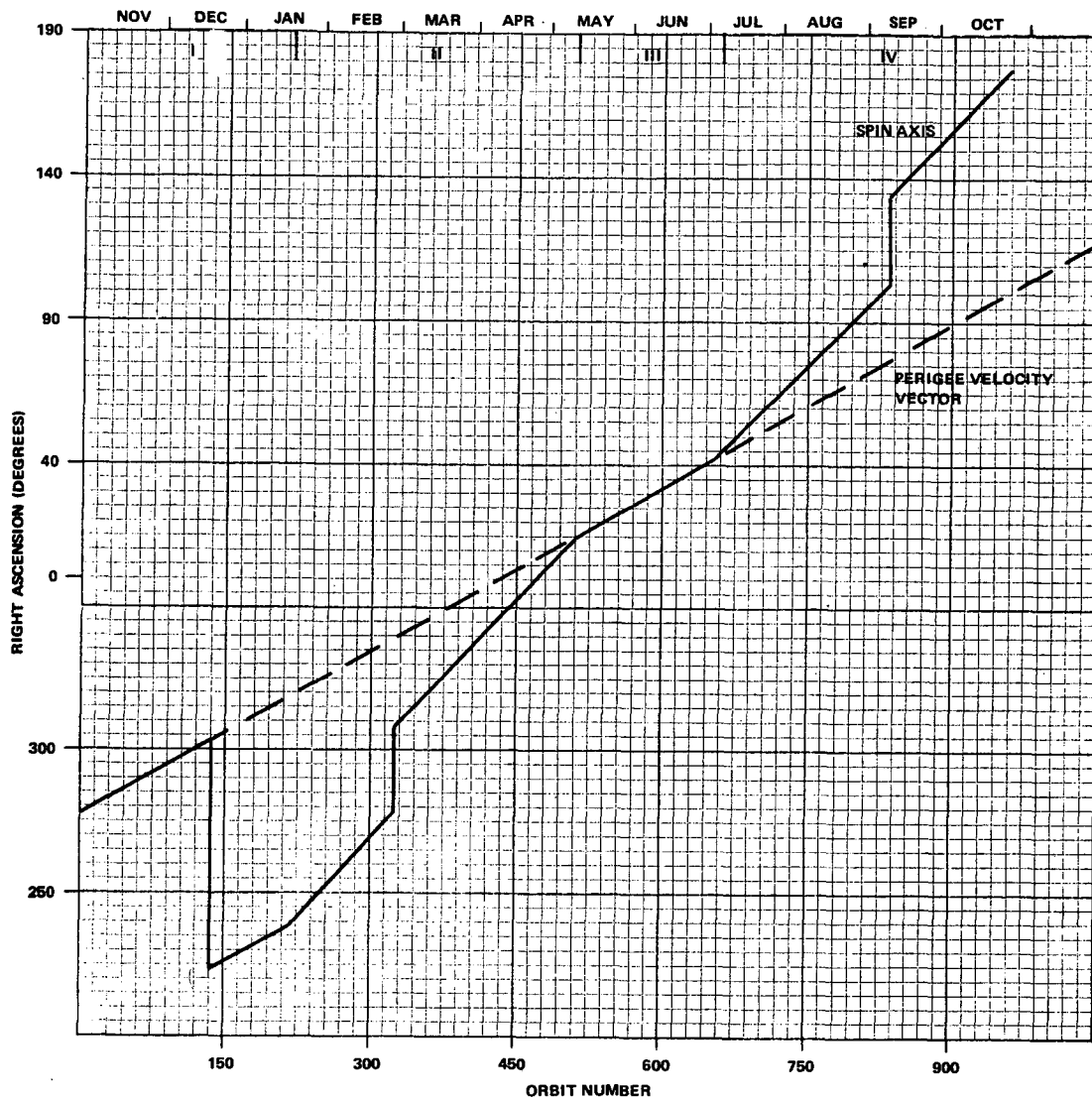
Figure 2-16. Anticipated Spin Axis Position for a 6:00 Launch.
The Spin Axis Stays Behind the Sun After Orbit 136.

oscillate about the line in Figure 2-15. Often the change to a new phase can be delayed or advanced by taking advantage of the sun's declination. However, the history generated in this manner should be adequate for estimating the attitude drift due to aerodynamic torque.

These projected attitudes were used in conjunction with the drift rate tables (Tables 2-3 and 2-4) and the atmospheric density ratios to compile drift rate histories for five launch times. The drift rate histories calculated for the procedure of keeping ahead of the sun are presented in Figures 2-17 to 2-21. The torques listed in Tables 2-7 and 2-8 are indicated by "T" in the figures.

When the spin axis is tracking v_P at a relative position of low aerodynamic torque, the control procedure will be to let v_P advance, leaving the spin axis behind. Eventually, the spin axis will drift in declination. The drift can be corrected by torquing ahead of the zero torque point and taking advantage of the drift in the opposite direction. In order to reflect this process, those phases where the spin axis tracks v_P are represented by vertical lines centered on zero declination drift rate. The length of the vertical lines indicates the drift rate that can be expected if the spin axis drifts no more than 5° away from the zero torque point. In some cases, this drift rate can be quite high, although the net drift will be kept small by torquing back and forth across the zero torque point.

When the spin axis is tracking the sun, the declination drift due to aerodynamic torque will have to be compensated for by the magnetic control system. It was found in Section 2.1.2 that a declination change of about 1° can usually be achieved within a few orbits. Associated with the declination change is a right ascension change of 7°-8°. When tracking the sun, the right ascension motion will almost certainly leave the spin axis at a worse relative position for aerodynamic torque. Thus a torque away from the sun to recover from
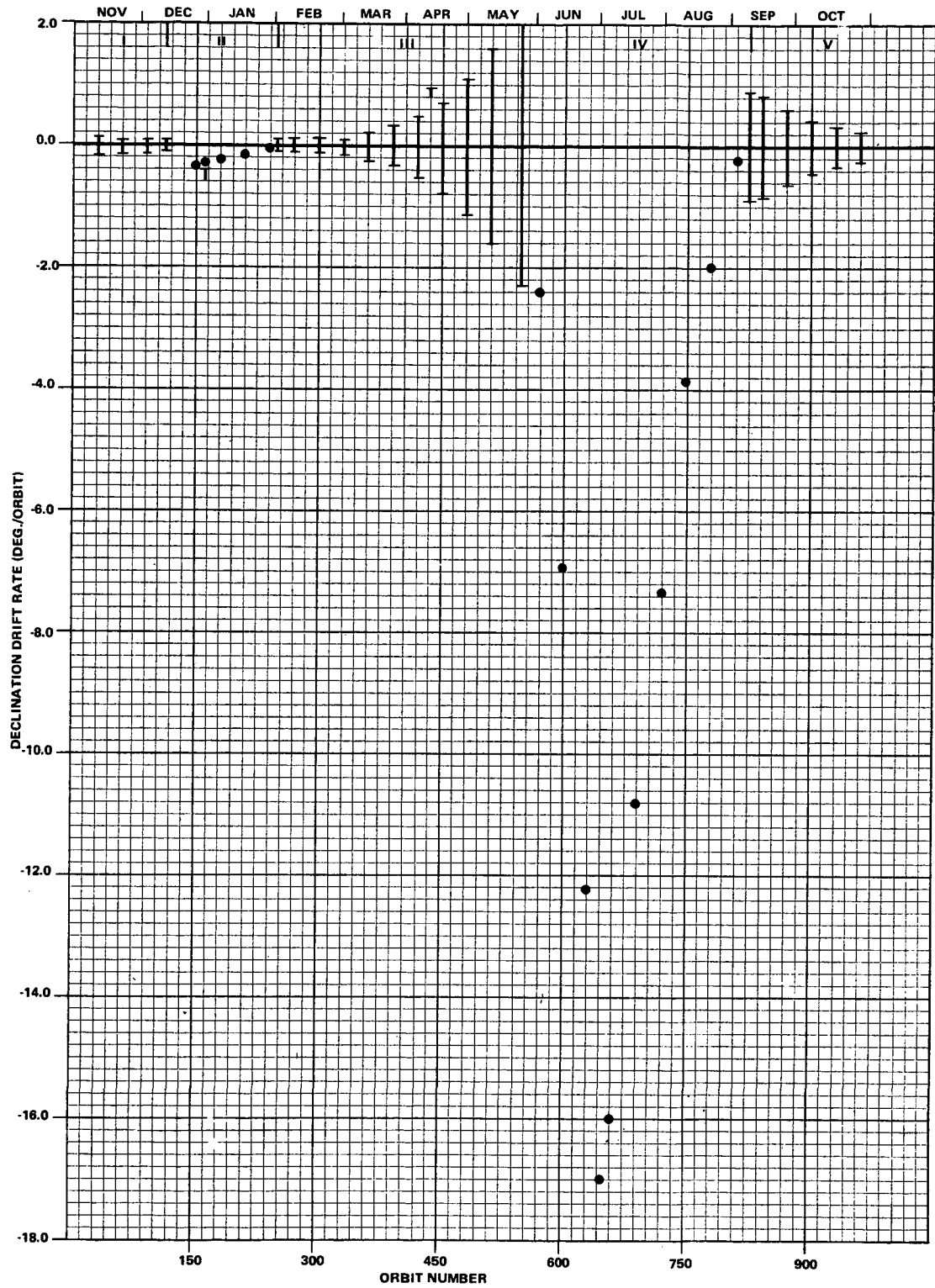
Figure 2-17. Expected Drift Rates for a 4:30 Launch.
The Spin Axis Stays Ahead of the Sun.
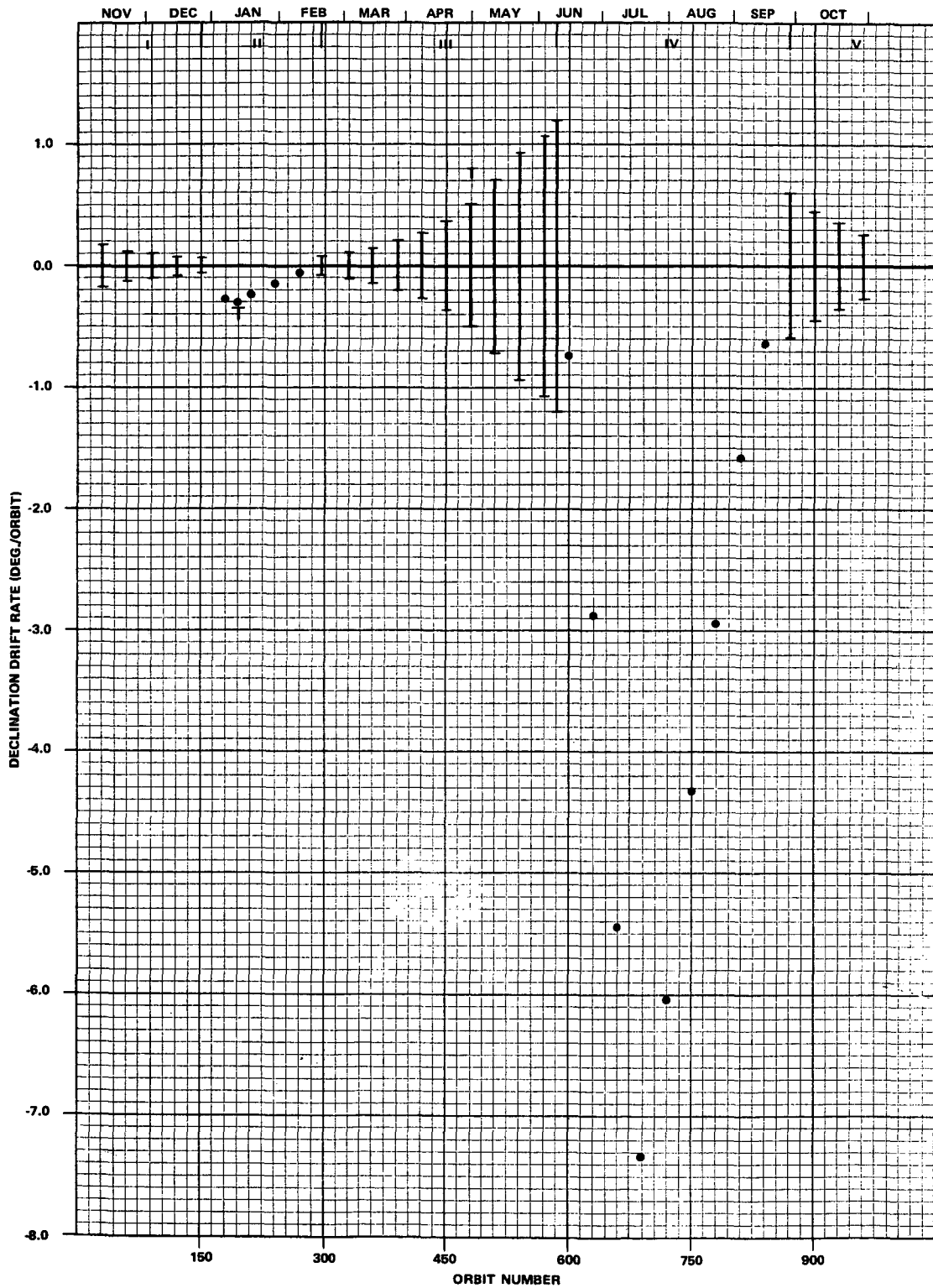
Figure 2-18. Expected Drift Rates for a 5:00 Launch.
The Spin Axis Stays Ahead of the Sun.

2-46
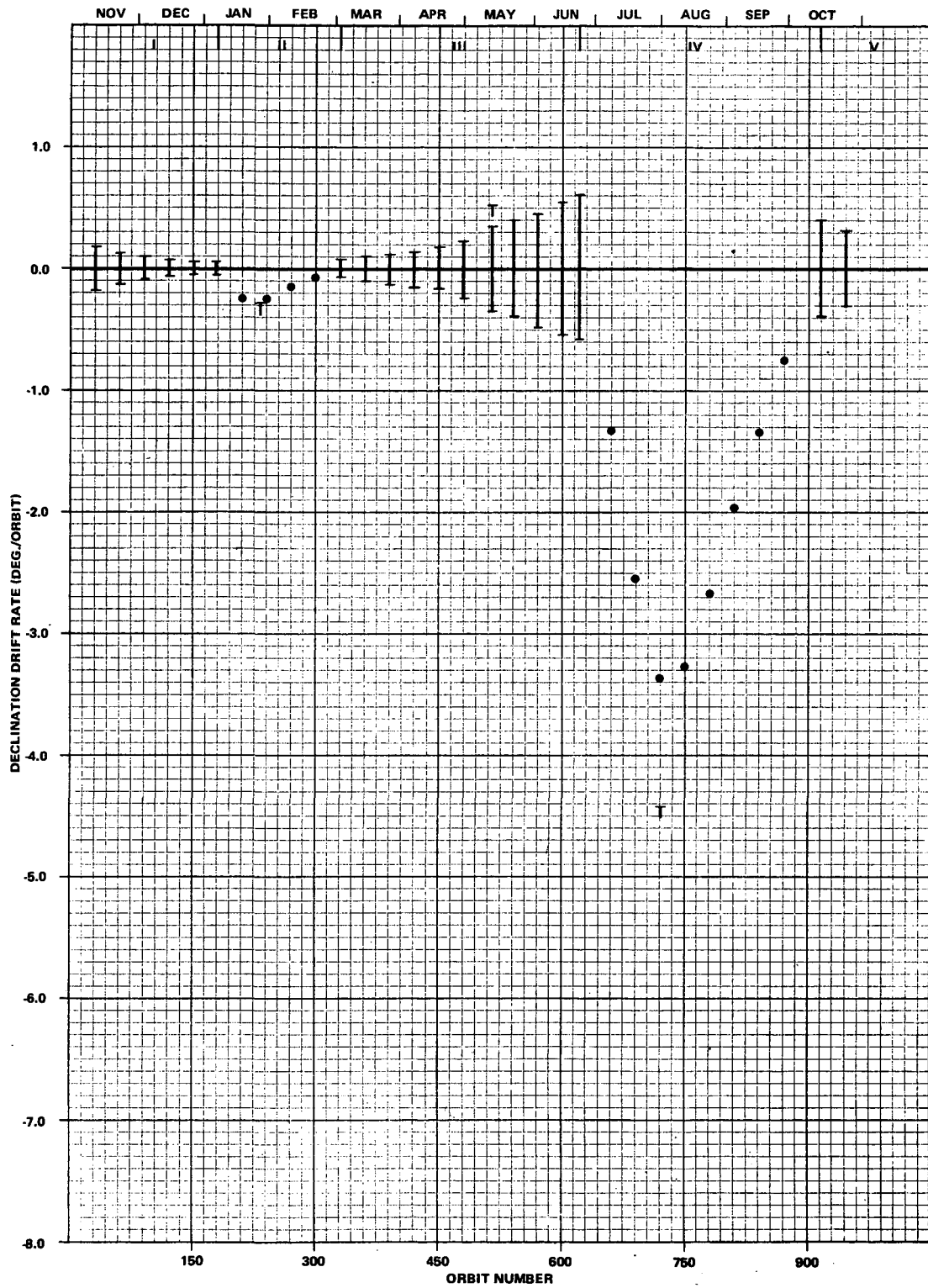
Figure 2-19. Expected Drift Rates for a 5:30 Launch.
The Spin Axis Stays Ahead of the Sun.
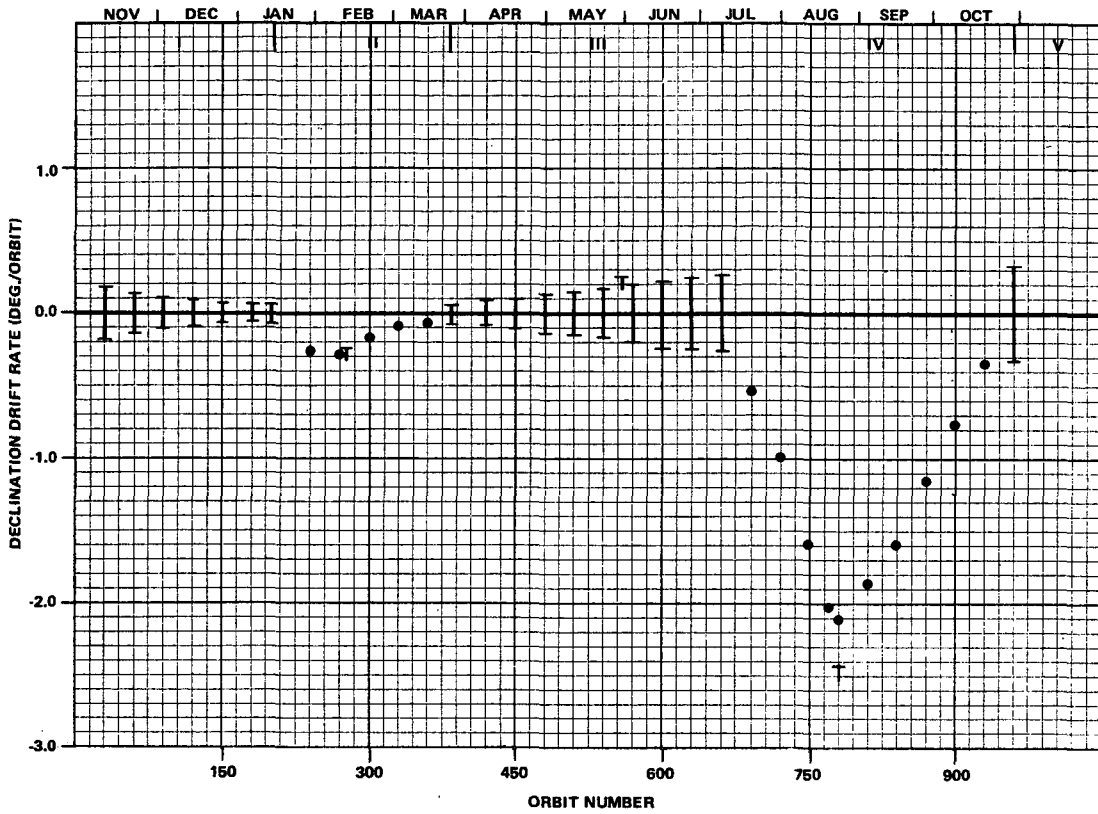
Figure 2-20. Expected Drift Rates for a 6:00 Launch.
The Spin Axis Stays Ahead of the Sun.
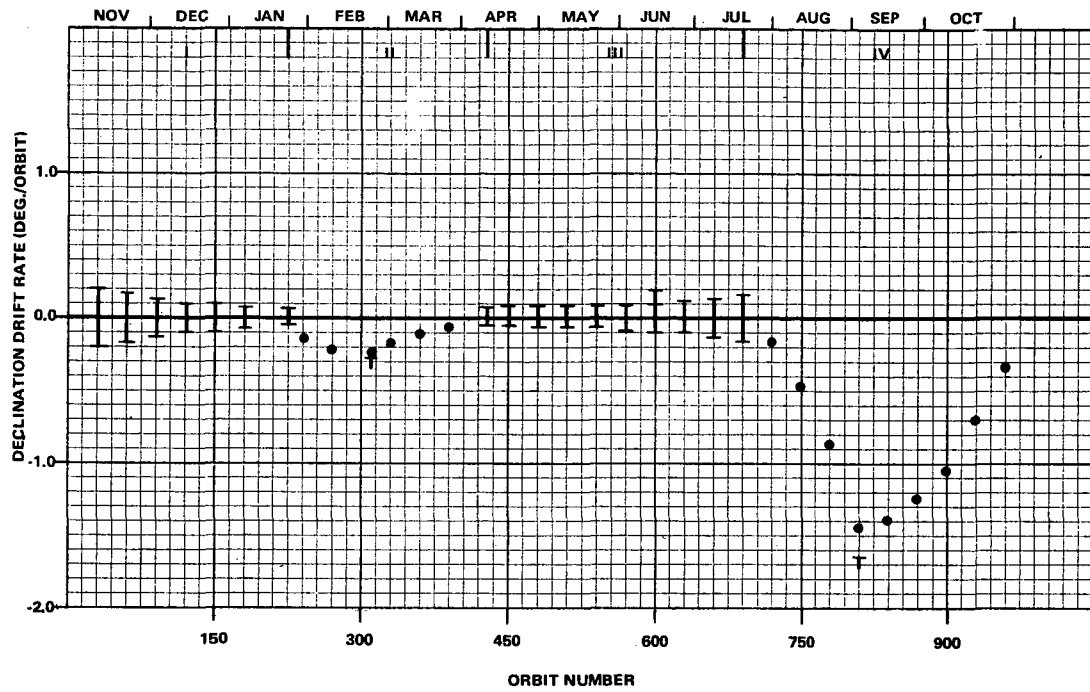
Figure 2-21. Expected Drift Rates for a 6:30 Launch.
The Spin Axis Stays Ahead of the Sun.

a high declination will usually be followed by another torque to regain the original right ascension and the advantage of a lower drift rate. Such a maneuver will be referred to as a zigzag. Several examples of these maneuvers are given on page A-15.

It is often possible to achieve a total of 2^O declination change by means of a zigzag. Thus drift rates much larger than 1^O per orbit probably cannot be controlled. According to Figures 2-17 to 2-21, high drift rates are to be expected in the summer of 1972 for all launch times. The earlier launches will be completely uncontrollable with drift rates as high as 17° per orbit for the 4:30 launch time. The launch at 6:00 will probably lead to a violation of the declination constraint, but it will perhaps not be too severe. The drift rate for the 6:30 launch can probably be controlled. Thus later launches are desirable because the high drift rates in the summer occur later and are not as large as the earlier launches.

The approach of getting behind the sun was examined for a 5:00 and a 6:00 launch. The results are presented in Figures 2-22 and 2-23 and can be compared with those in Figures 2-18 and 2-20. As can be seen, there is very little advantage to this maneuver. In fact, the Phase III tracking of v_p region is much shorter for this method than it is for the stay ahead method.

The aerodynamic drift difficulties that will occur in the summer of 1972 are due to the low altitude of perigee during this time. The previous figures were generated under the assumption of a nominal launch. A non-nominal launch that could lead to even lower perigee altitudes is possible. In order to investigate this, a $3-\sigma-$low orbit was selected from the available launch window program outputs for comparison with the nominal cases. The drift rate history for a 5.4 earth radii apogee orbit for a launch time at 5:30 on November 4, 1971, is presented in Figure 2-24. The lower minimum perigee causes
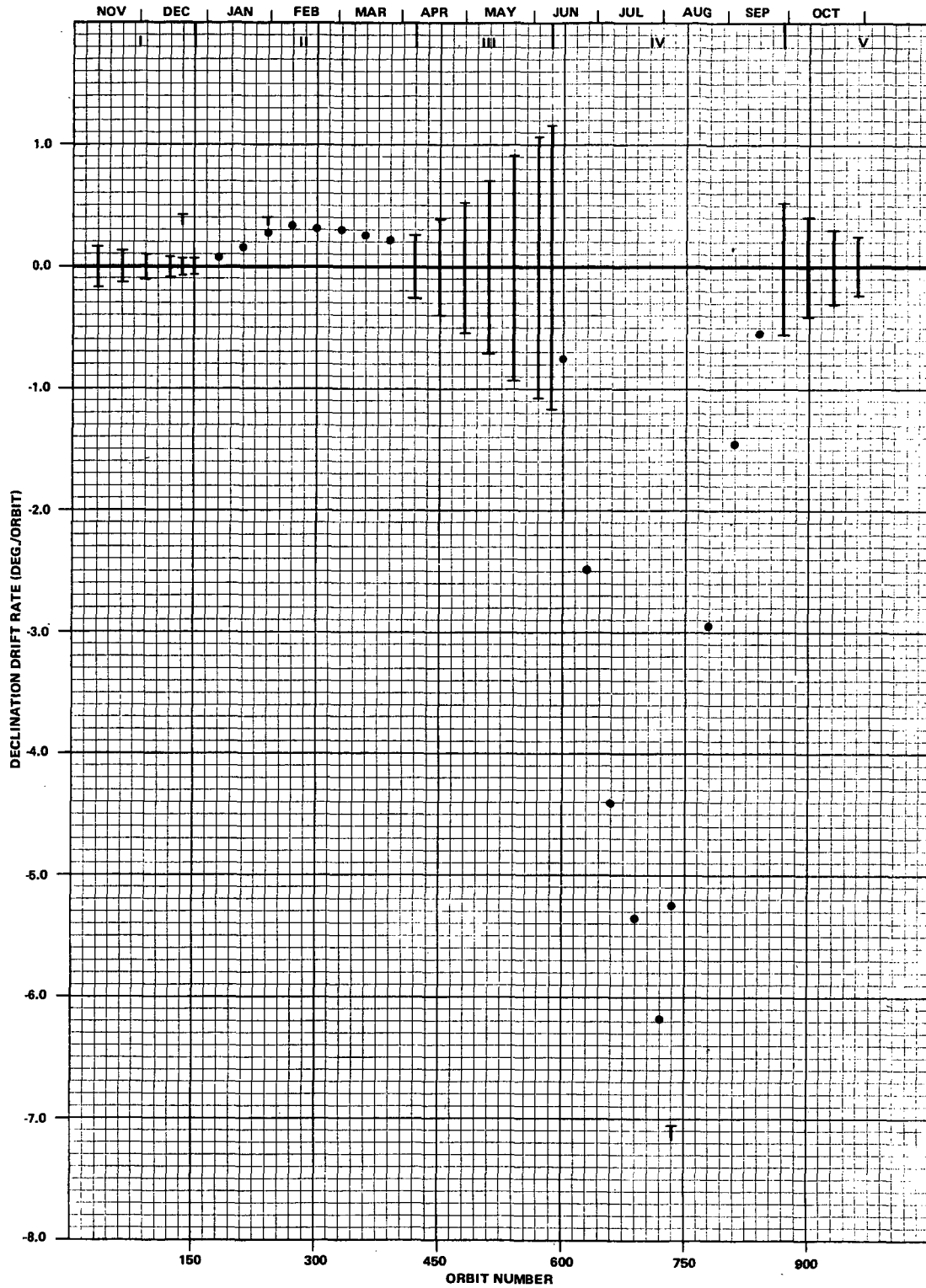
Figure 2-22. Expected Drift Rates for a 5:00 Launch. The Spin Axis Stays Behind the Sun After Orbit 136.

2-51
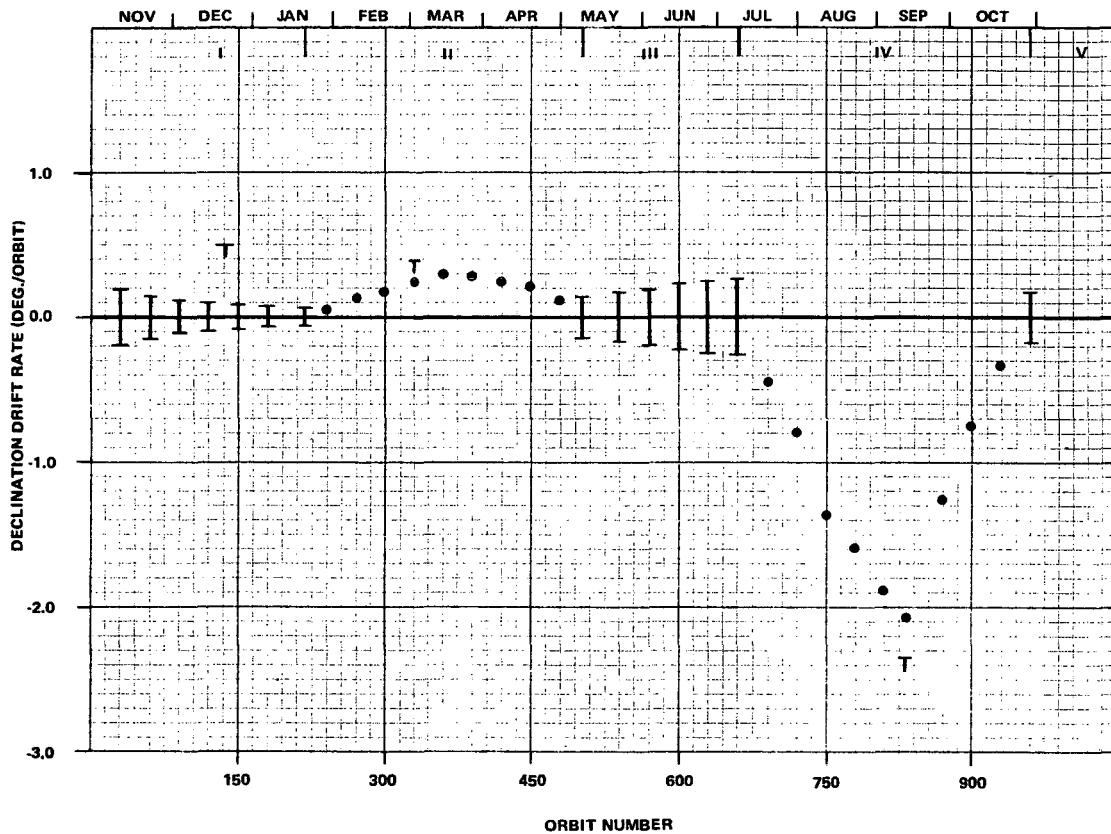
Figure 2-23.   Expected Drift Rates for a 6:00 Launch.
The Spin Axis Stays Behind the Sun After
Orbit 136.

2-52
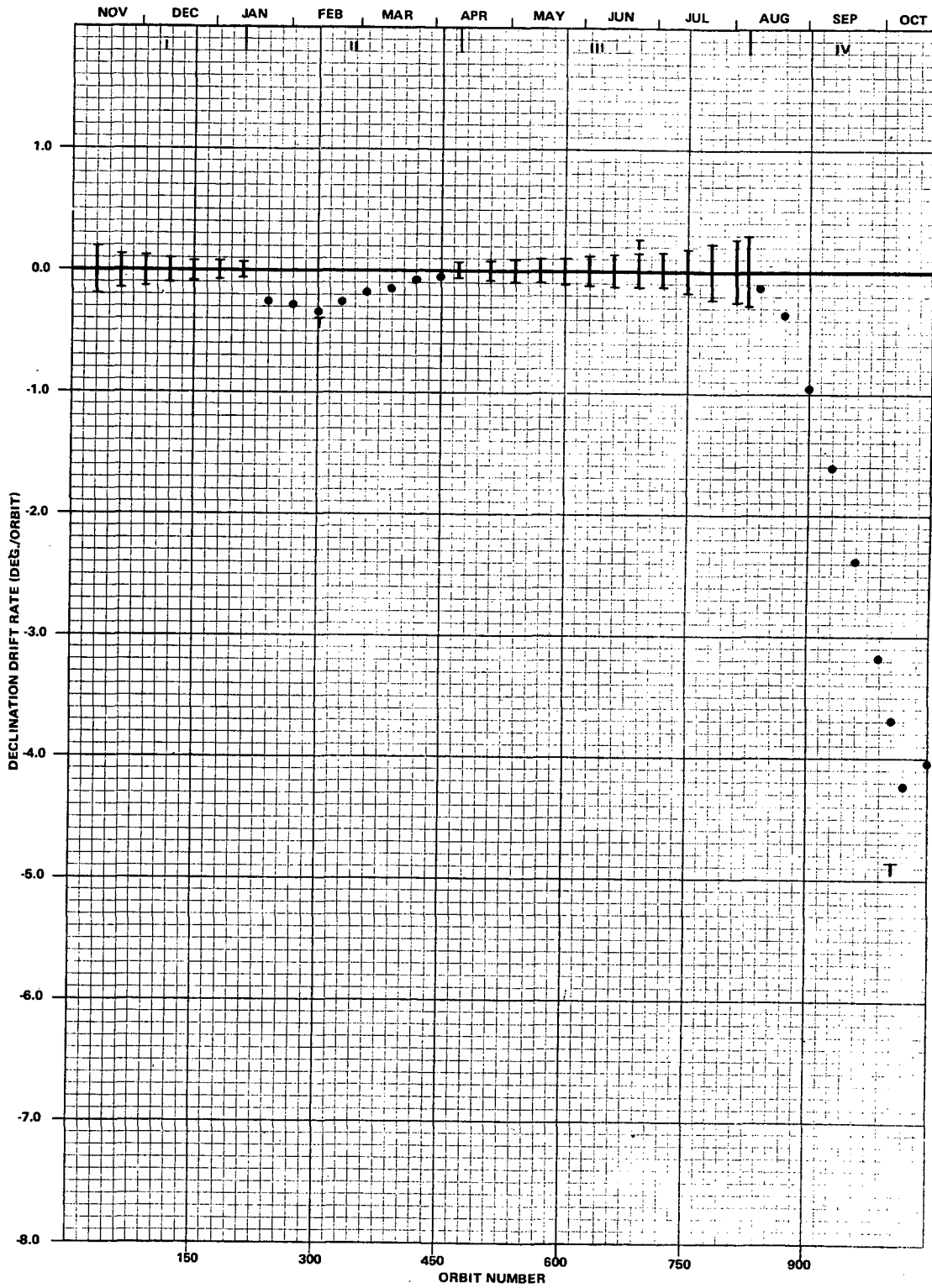
Figure 2-24. Expected Drift Rates for a 5:30 Launch into a 3-σ-low Orbit. The Spin Axis Stays Ahead of the Sun.

2-53

a higher maximum drift rate than observed in the nominal case represented in Figure 2-19. The most significant feature, however, is the fact that the high drift rates occur about one and a half months later than in the nominal case. This is due to the larger rate of advance of perigee that results from the smaller semi-major axis. Thus a launch into a lower orbit may actually be an improvement over a launch into the nominal orbit, at least for the early launch times.

In conclusion, all launch times will lead to a period of large aerodynamic drift. These drifts, however, occur later and may be controlled for the later launches under nominal conditions. In the interest of low attitude drift rates, the latest launch time possible without violating a sun constraint is to be recommended. Unfortunately, this conflicts with the requirement of accurate attitude determination. A launch into a lower orbit does not reduce the aerodynamic drift but does postpone the inevitable period of high drift rates. The effect of such a launch on the attitude accuracy has not been determined.

2.3 A MISSION SIMULATION

The previous section gives a rough estimate of the magnitude of aerodynamic drift problems that may be encountered under the assumption of two control philosophies: first, stay ahead of the sun; second, drop behind the sun. The approach does not give a feel for the types or frequency of control maneuvers that will be necessary during the various phases of the mission. The possibility of launches earlier than 5:00 tracking v_P at a high declination while the sun passes underneath was ignored in the previous section. Therefore, a mission beginning with a launch at 5:00 was simulated with MSAP to see if such a maneuver is advantageous. It can be seen from Table 2-5 that 5:00 is as late as the satellite can be launched with the possibility of letting the sun pass. However, since the encounter occurs with the sun increasing its declination toward the vernal equinox, the closest approach of the sun to v_P occurs after

the initial encounter when the sun is at -13° declination. At that time, the spin axis will have to be behind v_P. This requirement will lead to an understanding of the control torques necessary during the Phase II portion of a mission.

The path of the spin axis in inertial coordinates over the course of the simulation is presented in Figures 2-25 to 2-29. The points represent the position of the spin axis at three-day intervals for Figures 2-25 and 2-26 and at three-orbit intervals for the remaining figures. The straight lines connecting points represent the motion due to magnetic control torques. The number on the line is the perigee pass during which the control maneuver was accomplished. Numbers near points represent the perigee pass associated with that point. The small x's represent the position of the perigee velocity vector corresponding to that perigee pass. The small circles with rays extending out represent the position of the sun at the time of perigee pass indicated by the number associated with the circle. The altitude and date for selected perigee passes are given in tables in the figures.

The first control on pass 36 was necessary to control the upward drift of the spin axis. (See Figure 2-25.) A high declination is needed to allow the spin axis to pass under the sun, but until that time, the declination has to be carefully controlled or violation of a sun constraint could occur. For example, if the spin axis were allowed to drift higher, then two magnetic torques would be necessary to get ahead of v_P and achieve a negative declination drift. The negative drift would bring the spin axis to a low declination just about the time of the initial encounter. A backward torque at that time to obtain a positive declination drift would violate the 30° sun constraint. Therefore, the torques on orbit 36 and 79 were designed to get just ahead of v_P in order to reduce the net upward drift rate.
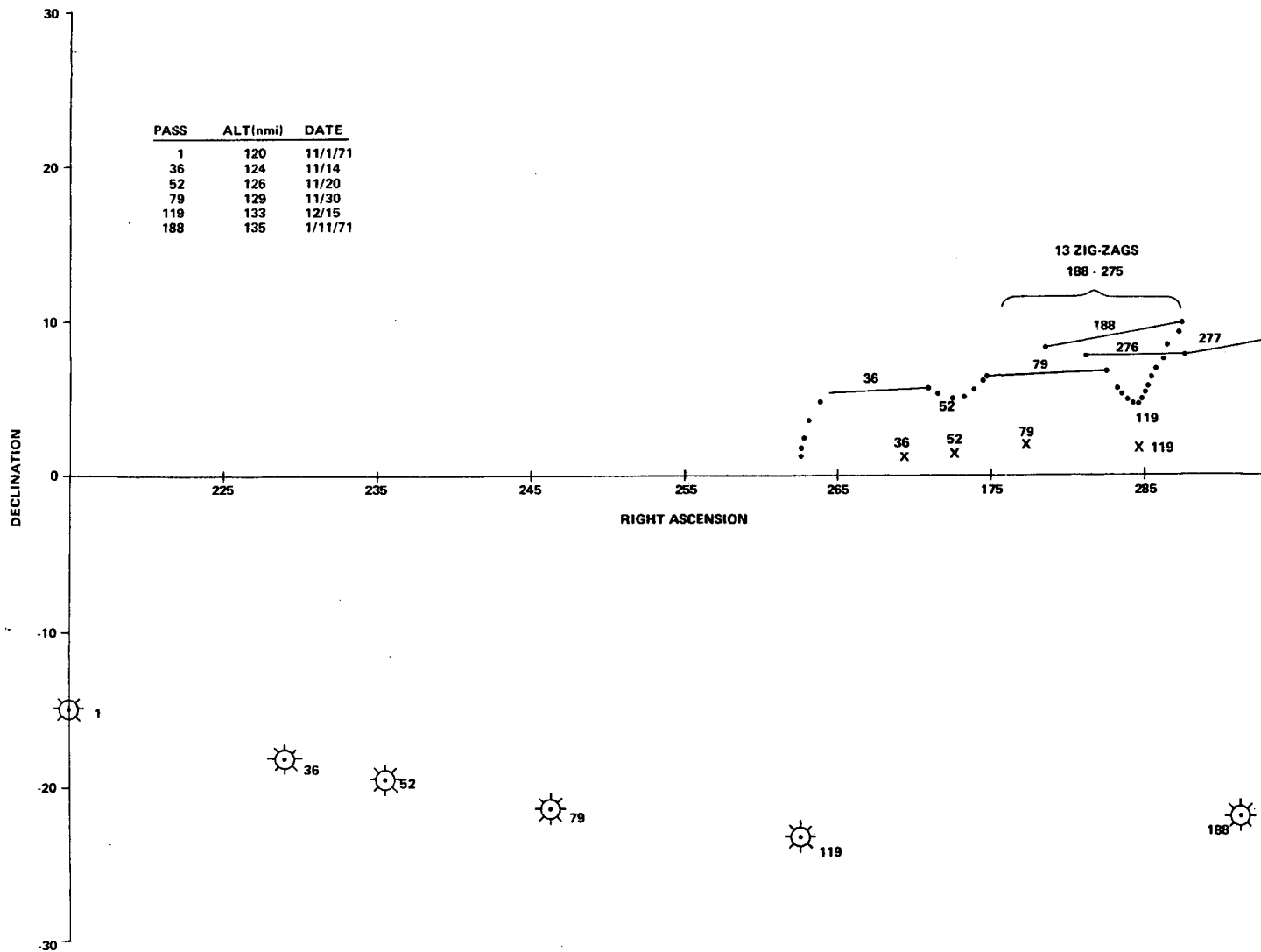
Figure 2-25. Mission Simulation for a 5:00 Launch.
November 1 to February 13. Three
Days Per Point.

30 —

20 —

18 ZIG-ZAGS AND 7 FORWARD MANEUVERS
278 - 402

10 —

188

276   277

79

119

DECLINATION

X 79   X 119   X 188   X 277   403·   X 403   435

0 —
      285   295   305   315   325   335   ·345
                              RIGHT ASCENSION

435

-10 —

☼ 277

PASS	ALT(nmi)	DATE
277	131	2/13
403	114	4/1
435	109	4/13

-20 —

☼ 188

-30 —
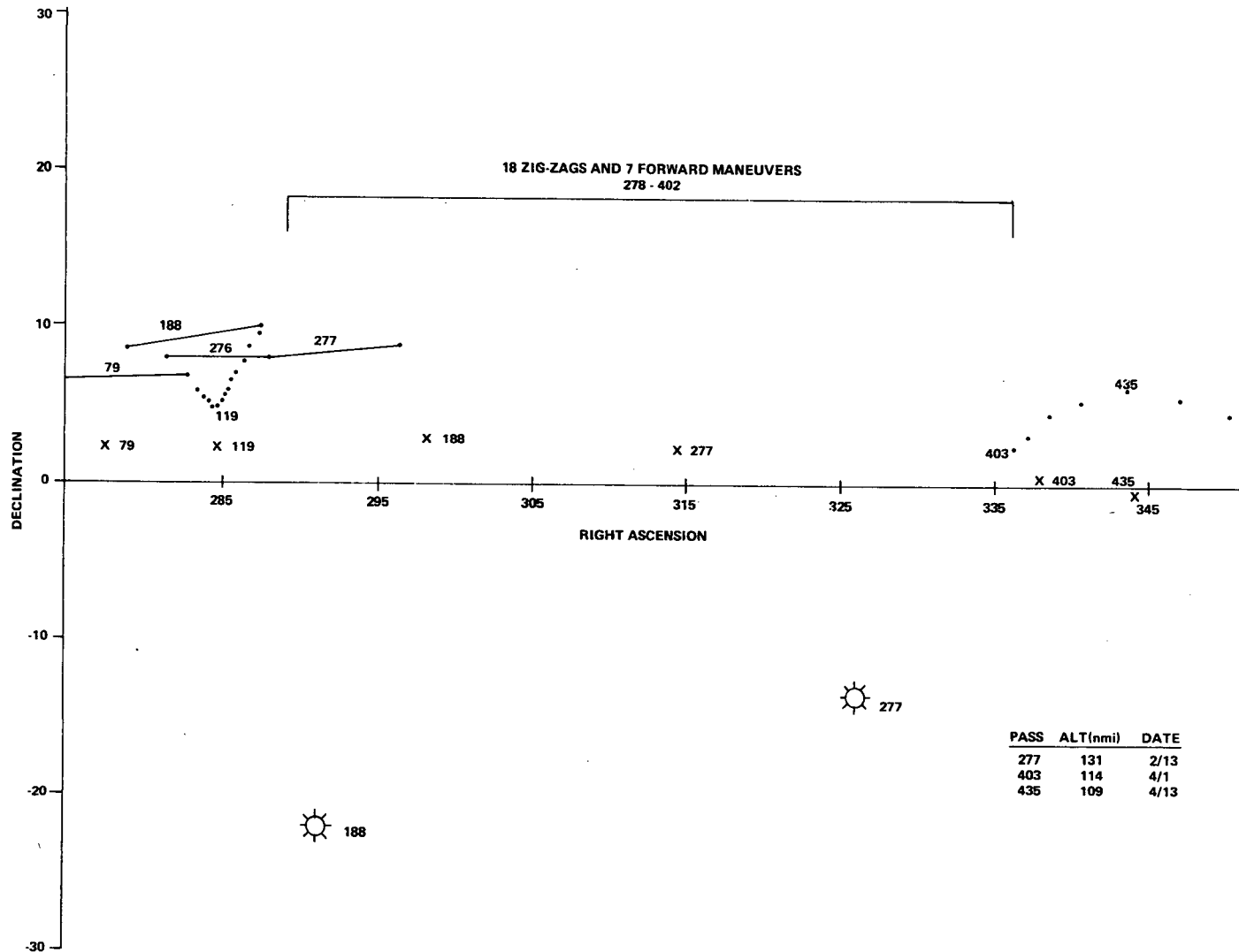
Figure 2-26. Mission Simulation for a 5:00 Launch.
November 30 to April 19. Three Days
Per Point.
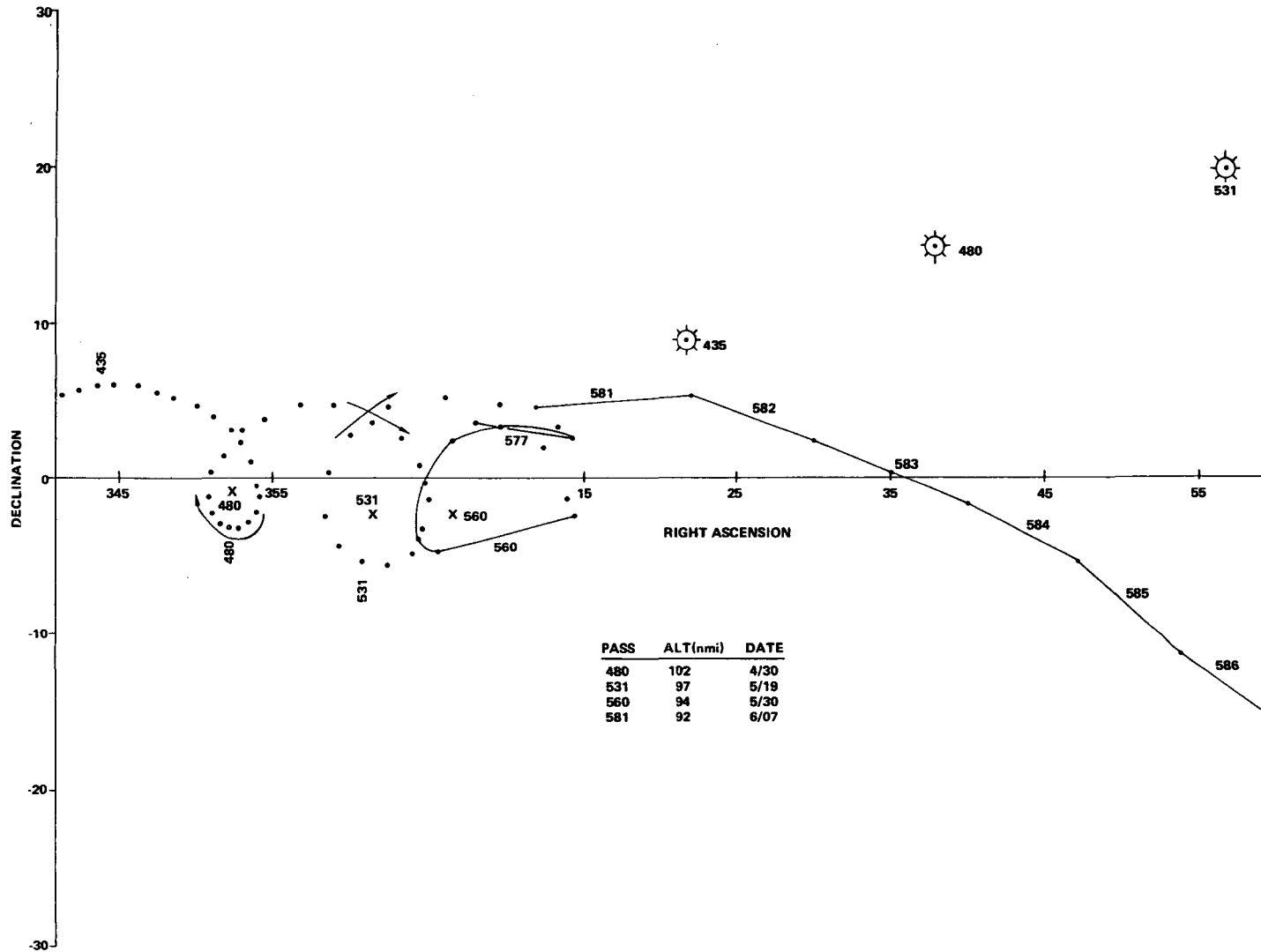
Figure 2-27. Mission Simulation for a 5:00 Launch. April 10 to June 9. Three Orbits Per Point.
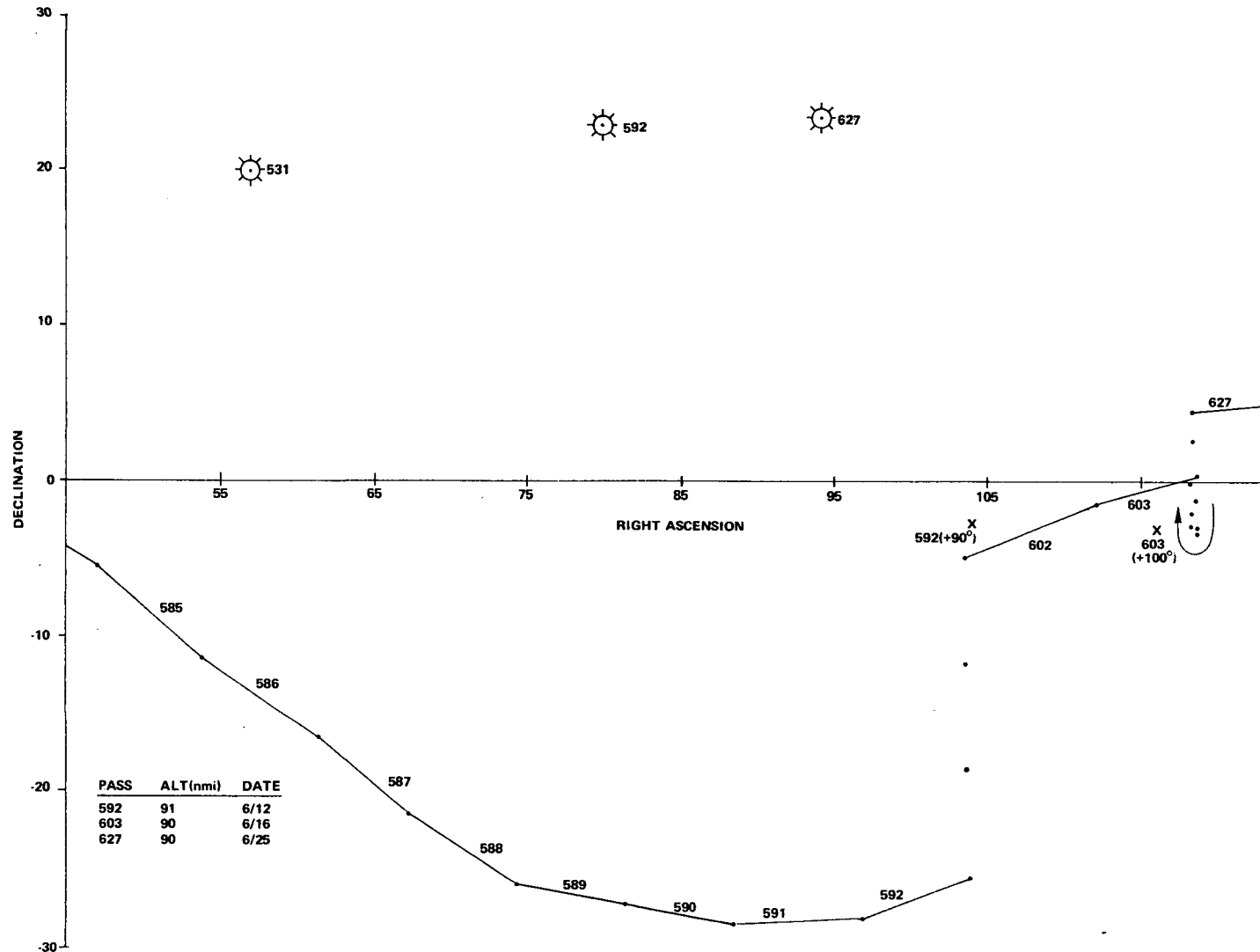
Figure 2-28. Mission Simulation for a 5:00 Launch.
June 9 to June 25. Three Orbits Per
Point.

PASS	ALT(nmi)	DATE
658	89	7/7
665	89	7/9
669	89	7/11
681	89	7/15
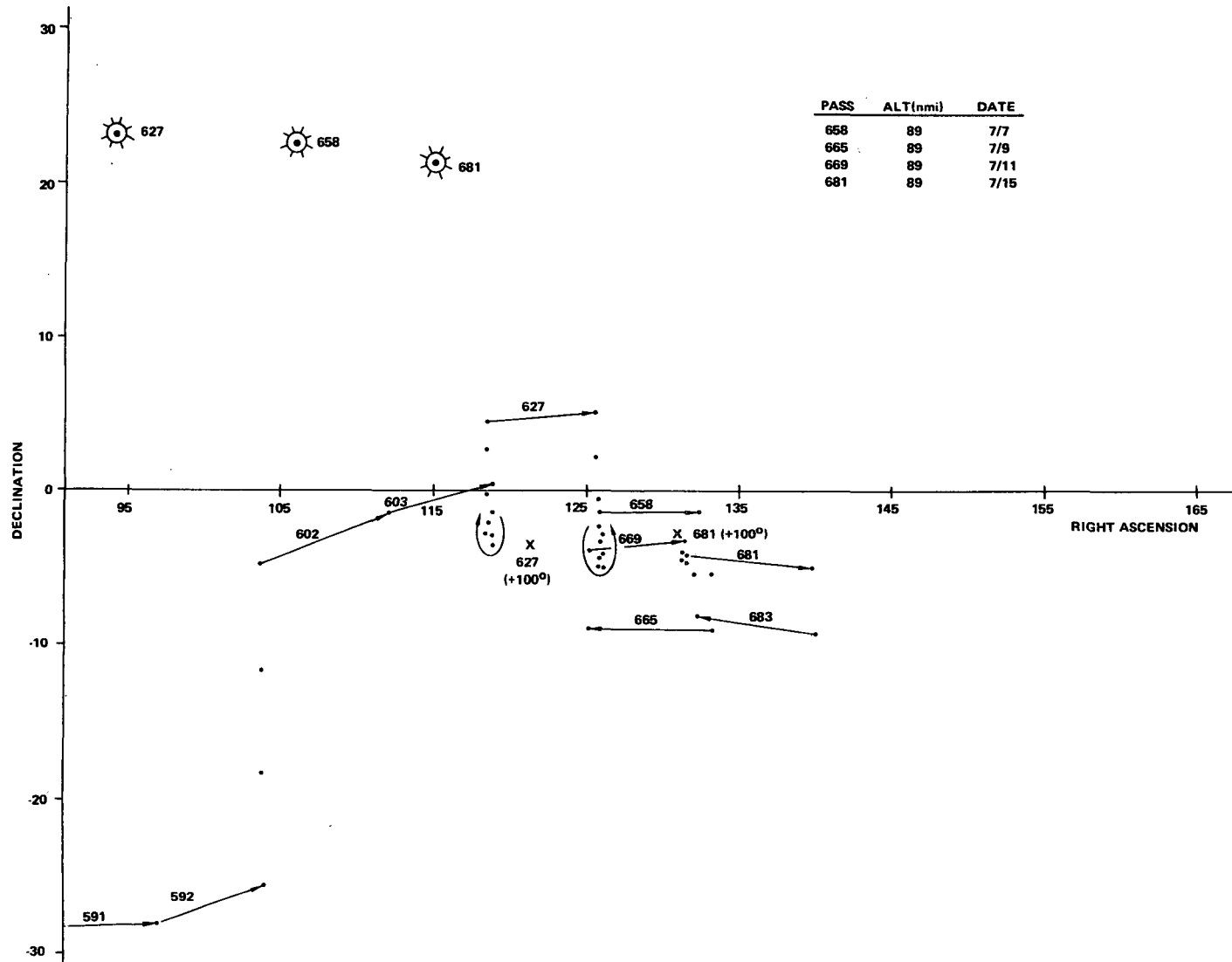
Figure 2-29. Mission Simulation for a 5:00 Launch.
June 11 to July 18. Three Orbits Per
Point.

After the control on pass 79, the spin axis was allowed to drift as the sun passed it between orbits 157 to 167. The sun angle during this time reached a minimum of 30.5^O. Since the spin axis had lagged behind v_P at this point, it was drifting upward in declination. On pass 188, it had reached a declination of 9.8^O. Since the sun had not yet passed v_P, the spin axis could not be precessed ahead of v_P to reduce its declination because that would lead to a violation of the sun constraint. (See Figure 2-26.) Therefore, the spin axis was torqued back on pass 188 and torqued ahead on pass 189. This zigzag resulted in a net decrease in declination of about 1^O, with no increase in the right ascension relative to v_P.

At this point, the mission philosophy is represented by Phase II in Figure 2-22. The major maneuver to a relative right ascension of -80° was not performed, because the extra week of tracking v_P was not worth the complications of such a maneuver. Although the first part of Phase II in Figure 2-22 was calculated under the assumption that the spin axis was tracking the sun at an angle of 65°, the graph represents fairly well the drift rates experienced in this simulation when the sun angle was kept around 35°.

On passes 276 and 277, the spin axis was precessed ahead in order to track the sun and at the same time get closer to v_P so that the aerodynamic torque would be reduced. Until pass 403, seven of these forward maneuvers were carried out. In addition, 18 zigzag maneuvers were required to maintain declination control. These controls amounted to one maneuver every three perigee passes between orbits 276 and 403. During this time, the declination drift rate was between 0.3^O to 0.4^O per orbit in good agreement with Figure 2-22.

On pass 403, the spin axis was moved close to v_P and was allowed to track v_P until pass 560. (See Figures 2-26 and 2-27.) During this time, the perigee altitude is low enough so that the capture phenomenon discussed in

Section 2.1.3 causes the spin axis to track v_p without violating any mission constraints. The drift rate toward the end of this period was about 1° per orbit, as predicted by Figure 2-22. In order to reduce the rate, the spin axis was moved closer to v_p on pass 560.

During this time, the sun angle was approaching 70°. Since the angle between the sun and v_p would reach 70° on pass 594, the spin axis had to be moved toward the sun away from v_p. Figure 2-22 shows that if the spin axis moves away from v_p while tracking the sun at 35°, declination drift rates on the order of 5° per orbit can be expected. Therefore, it was decided to take advantage of the sun's approach to the summer solstice and precess the spin axis under it to get ahead of the sun at a right ascension of about 90° relative to v_p.

Since large negative drift rates were expected during such a maneuver, the spin axis was precessed back on pass 577 in an attempt to maintain a high declination prior to beginning the maneuver. On pass 581, the maneuver to 90° relative right ascension was begun. The spin axis was advanced by the magnetic control coil on every pass until pass 593. Due to the -5° and -6° drifts experienced during this maneuver, the -10° declination constraint was violated. (See Figure 2-28.) However, due to the fairly large positive declination drifts at 90° relative right ascension, the spin axis was outside the constraints for only about 14 orbits.

On orbits 602 and 603, the spin axis was precessed to a right ascension of about 102° relative to v_p in order to stop the upward drift which would have led to a sun constraint violation. This process was repeated several times until it was no longer possible to control the satellite without an extended violation of one or more of the mission constraints. (See Figure 2-29.)

If the spin axis were to be precessed ahead of the sun away from the zero torque point at 100° right ascension relative to v_p, then a large

negative declination would result, as it did in getting to the zero torque point. In this case, however, there would be no quick recovery because it would be necessary to track the sun at that angle for some time. Precessing the spin axis ahead to $-v_P$ leads to a violation of the 70° constraint for an extended period of time. Precessing the spin axis back to a right ascension of 80° relative to v_P would lead to a violation of the 30° sun constraint, again for an extended period of time. Therefore, the simulation was terminated.

Several things were learned from the simulation. First, when the spin axis was away from v_P in Phase II and experiencing drift of about 0.3^O to 0.4^O per pass, magnetic control torques were required about every three passes.

Second, since for the early launches the sun will be at a high declination toward the end of Phase III, the onset of the catastrophic drift rates of Phase IV can be postponed. In the case of the 5:00 launch simulation, this postponement amounted to about 100 orbits. Since Phase IV begins with the sun at a lower declination, for the later launches, the postponement effect tends to equalize the time of the beginning of Phase IV. However, only the later launches allow any hope of controlling the spin axis during this period.

Third, since the sun had passed the winter solstice at the time of the initial encounter, a period of tracking the sun away from v_P was necessary. Thus there was no clear advantage gained by this technique over the stay-ahead-of-the-sun approach. Therefore, the later launch times must still be recommended over the earlier ones.

2.4 SENSOR MOUNTING ANGLE STUDY

The Sensor Mounting Angle Study was conducted to determine whether a sensor mounting angle of 135° would provide sufficient optical aspect data for attitude determination. The Optical Aspect Data Predictor Program (Section 8.2) was used for the study. The right ascension and declination of the spin axis and the argument of perigee were varied for a number of cases.

The conclusion was that the optical aspect telescope mounted at an angle of 135° will provide sufficient optical aspect data for attitude determination under all mission conditions, subject to the following restrictions:

1. The declination of the spin axis lies within the interval -45° to $+45^\circ$.

2. The angle between the spin axis and the sun vector is less than 90°.

2.4.1 Assumptions Regarding the Optical Aspect System

The Optical Aspect System on board the satellite consists of a telescope mounted at 135° to the spin axis. An optical sensor triggers whenever the telescope scan crosses a sunlit area of the earth. However, the sensor is disabled when the azimuthal angle of the telescope, measured from the sun line, is less than 45° or greater than 315°.

Therefore, the sensor can be triggered (on or off) by three different types of events:

1. Sensor triggers at a sunlit horizon.
2. Sensor triggers at a terminator.
3. Sensor triggers at a cutoff angle.

Of the three types of sensor triggerings, only the first provides data useful for attitude determination. Therefore, a pair of sensor triggerings is useful for attitude determination only if at least one of the triggerings occurs at a sunlit horizon crossing.

The presence of a terminator crossing combined with a horizon crossing does not interfere with attitude determination, provided that the terminator crossing can be identified and rejected. The Attitude Determination Subsystem can make this rejection, provided that it has a sufficiently large block of data or a rough attitude estimate. Therefore, data obtained while a terminator is visible is only slightly less useful than data obtained with the earth fully sunlit.

It is possible for an optical sensor to record more than one pair of triggerings in a single scan (e.g., two terminator crossings and two horizon crossings). However, the electronics of the Small Scientific Satellite (SSS) sensor can record only one pair of triggerings per spin period. The first pair of crossings following a sun crossing is recorded, and no further triggerings are recorded until after another sun crossing.

In summary, OA data can be classified according to the cause of the earth-in triggering and the cause of the earth-out triggering. There are nine possibilities:

H	-	H	best; two useful triggerings
H	-	T	
T	-	H	
H	-	C	one useful triggering
C	-	H	
T	-	C	
C	-	T	
T	-	T	no useful data
C	-	C	

where H = sunlit horizon, T = terminator, and C = sensor cutoff.

2.4.2 Range of Study

The presence of Optical Aspect data at a given time depends on three factors: spacecraft attitude, spacecraft position, and sun position.

2.4.2.1 Spacecraft Attitude

The spacecraft attitude is subject to the following mission constraints:

1. Declination between -10° and $+10^{\circ}$

2. Sun angle (angle between spin axis and sun vector) between 30° and 70°

For this study, the declination was assumed to lie between -45° and $+45^{\circ}$ and the sun angle to lie between 0° and 90°. The set of all attitudes with declinations between -45° and $+45^{\circ}$ consists of a band extending around the celestial sphere, 45° either side of the equatorial plane. If the position of the sun is fixed, then those attitudes with sun angles between 0° and 90° are just those points within this band that lie within 90° of the sun, or that line on the hemispherical surface which has the sun direction at its pole. Therefore, with the sun's position fixed, the following method was used to generate the desired set of attitudes:

1. The declination was varied from -45° to $+45^{\circ}$ in steps of 15°.

2. The right ascension was varied from 0° to 345° in steps of 15°.

3. For each of these attitudes, the sun angle was computed. If the sun angle was greater than 90°, then the attitude was rejected.

2.4.2.2   Spacecraft Position

The following orbital elements for the mission were used:

Semi-major axis – 23064.3 km

Eccentricity – 0.7138

Inclination – 2.92°

Argument of perigee – unknown

Right ascension of ascending node – unknown

Since orbital inclination is small, all orbits for which the argument of perigee plus the right ascension of the ascending node is a constant, will be nearly identical. Therefore, without loss of generality, the right ascension of the ascending node was set to zero and the argument of perigee was varied. In this study, the argument of perigee was varied from 0° to 315° in steps of 45°.

2.4.2.3   Sun Position

The position of the sun was taken for July 1, 1971. Results will differ slightly for other months of the year. The sun position determines the earth lighting conditions.

2.4.3   Results

Results for 692 cases were obtained, tabulated, and plotted (Reference 2-4 contains a complete description of the results). In every case at least 14 minutes of useful data was obtained. The plotted results are presented in Appendix C.

SECTION 3

ATTITUDE SUPPORT SYSTEM

3.1   SYSTEM OVERVIEW

The SSS-A Attitude Support System consists of four subsystems (see Figure 3-1): the Telemetry Data Handling Subsystem, the Attitude Determination Subsystem, the Multi-Satellite Attitude Prediction (MSAP) Subsystem, and the Merge Subsystem. The functions of these subsystems are discussed in the following paragraphs.

3.1.1   Telemetry Data Handling Subsystem

The function of the Telemetry Data Handling Subsystem is to provide a direct interface between the raw telemetry data being transmitted from the XDS 930 computer and the Multi-Satellite Operations Control Center to the S/360-95 at Goddard Space Flight Center via a direct data link facility. The subsystem places the data into a satellite-dependent data set on disk.

3.1.2   Attitude Determination Subsystem

The primary function of the Attitude Determination Subsystem is to determine attitude accurately from the raw telemetry data obtained from the spacecraft. Specific objectives of the subsystem are to:

- Provide necessary interface with the Telemetry Data Handling Subsystem and the MSAP Subsystem

- Approximate the spacecraft attitude using the Quick-Look procedure available in the Optical Aspect (OA) Attitude Determination module
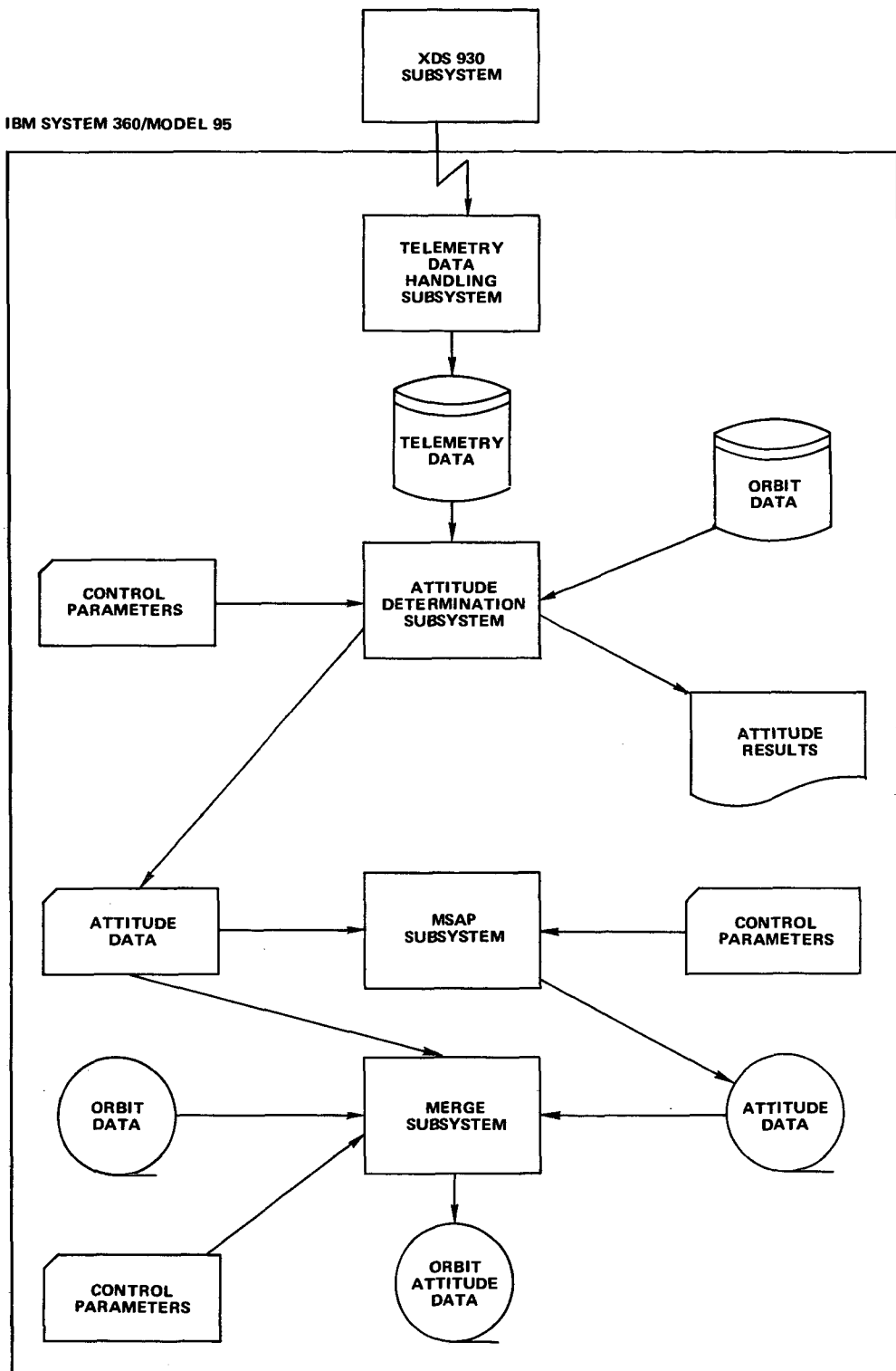
Figure 3-1. SSS-A Attitude Support System Overview

- Determine the spacecraft attitude to within one degree of accuracy using the Differential Correction procedure available in the OA Attitude Determination module

- Determine the spacecraft attitude to within 0.1 degrees from the SCADS telemetry data using the STAR module

- Provide an interactive graphics capability via the IBM 2250 or 2260 Display Unit to monitor and control the subsystem flow

- Provide attitude determination results in a readily usable format for evaluation

3.1.3   Multi-Satellite Attitude Prediction Subsystem

The major functions of the Multi-Satellite Attitude Prediction Subsystem are to predict the spacecraft attitude over some specified time span and to assist in the generation of control commands required to maintain the satellite within the attitude constraints. A secondary function of the subsystem is to generate a data set containing the satellite's spin axis vector in inertial coordinates at one-minute intervals to be used in the determination of definitive attitude.

3.1.4   Merge Subsystem

The purpose of the Merge Subsystem is to generate an orbit attitude tape containing definitive orbit and attitude data. Attitude data supplied by the MSAP Subsystem is compared, in conjunction with definitive orbit data, to attitude data generated by the Attitude Determination Subsystem. An error estimate is then calculated and inserted in the output data records.

3.2   SYSTEM DATA FLOW

The Small Scientific Satellite Attitude Support System (SSSASS) has three main functions:

1. Prediction, determination, and control of the satellite spin axis attitude

2. Evaluation of the star sensor and recommendations for sensor operation

3. Determination of definitive satellite spin axis attitude

Successful performance of these functions involves the transfer of data between the interrelated components of SSSASS. The logical flow of data within SSSASS is determined by the function that is being performed. The data flow for each function is described in the following sections.

3.2.1   Non-Definitive Data Flow

The non-definitive function of SSSASS is to predict and determine satellite attitude and to generate control commands for necessary spacecraft maneuvers. During the non-definitive phase, definitive orbit information is not available to the Attitude Determination Subsystem (ADS) and a definitive orbit attitude tape is not generated by SSSASS.

Input to ADS consists of a raw telemetry data set, ephemeris information, a priori right ascension and declination, and input parameters. The Multi-Satellite Operations Control Center (MSOCC) supplies, via a data link, raw telemetry data to the Telemetry Data Handling Subsystem, which generates the disk telemetry data set used by ADS. MSOCC also supplies ADS with injection parameters from which an approximate orbit, and therefore ephemeris information, is generated. The MSAP Subsystem

supplies ADS with a priori right ascension and declination values. The input parameters are supplied by the ADS operations system.

Primary output from ADS is a printout of computed attitude values. The MSAP Subsystem, using these computed attitude values as input, aids in determining the control commands which will effect any necessary satellite repositioning. This subsystem also predicts the resulting right ascension and declination values. The predicted attitude values are used as the a priori attitude input values during a subsequent pass through the Attitude Determination Subsystem. Secondary output from ADS consists of a SCADS disk data set, which is used as input by an independent SCADS program, and data displays on the 2250 or 2260 Display Unit. An overview of the non-definitive data flow is shown in Figure 3-2.

3.2.2.   Definitive Data Flow

The definitive function of SSSASS is to produce a definitive orbit attitude tape. Input to ADS is similar to that for the non-definitive phase, consisting of a raw telemetry data set, ephemeris information, a priori right ascension and declination, and input parameters. However, unlike the non-definitive phase, definitive orbit and calculated attitude information is also available to ADS in this phase. Ephemeris information, residing on magnetic tape, is supplied to ADS by the Orbit Determination Subsystem. Attitude values calculated during the non-definitive phase of SSSASS are used by ADS as the a priori attitude input values. The raw telemetry data is supplied by MSOCC in the form of a telemetry data tape, rather than via a data link. The input parameters are supplied by the ADS operations system as in the non-definitive phase.
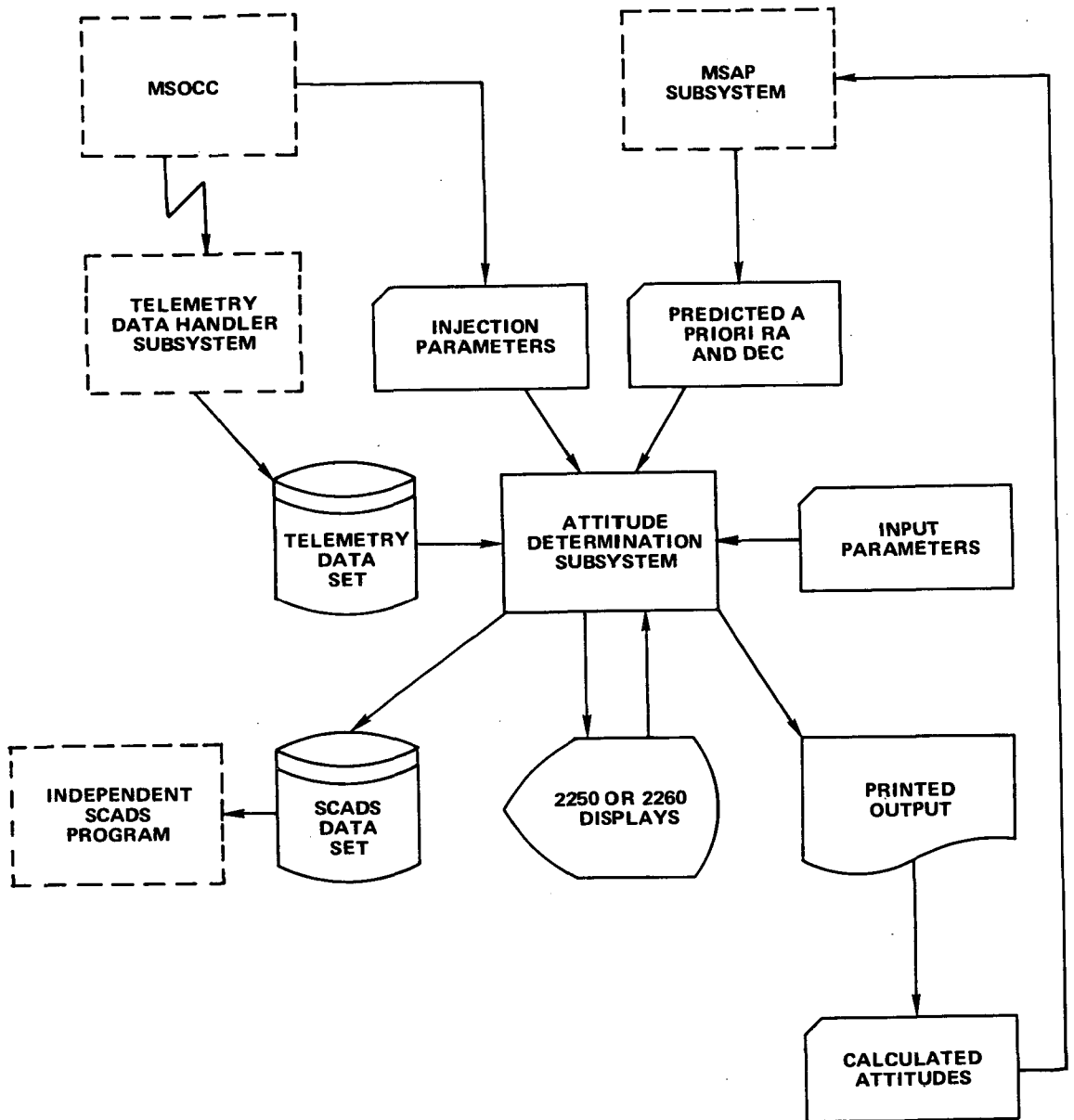
Figure 3-2. SSSASS Non-Definitive Data Flow

Primary output from the ADS is calculated attitude values, which serve as input to the MSAP Subsystem. This subsystem generates a definitive attitude tape which, together with a definitive orbit tape supplied by the Orbit Determination Subsystem and the attitude values calculated by ADS, comprises the input to the Merge Subsystem. The Merge Subsystem then generates a definitive orbit attitude tape. Secondary output from ADS consists of a SCADS disk data set and data displays on the 2250 or 2260 Display Unit, as in the non-definitive phase. An overview of the definitive data flow is shown in Figure 3-3.
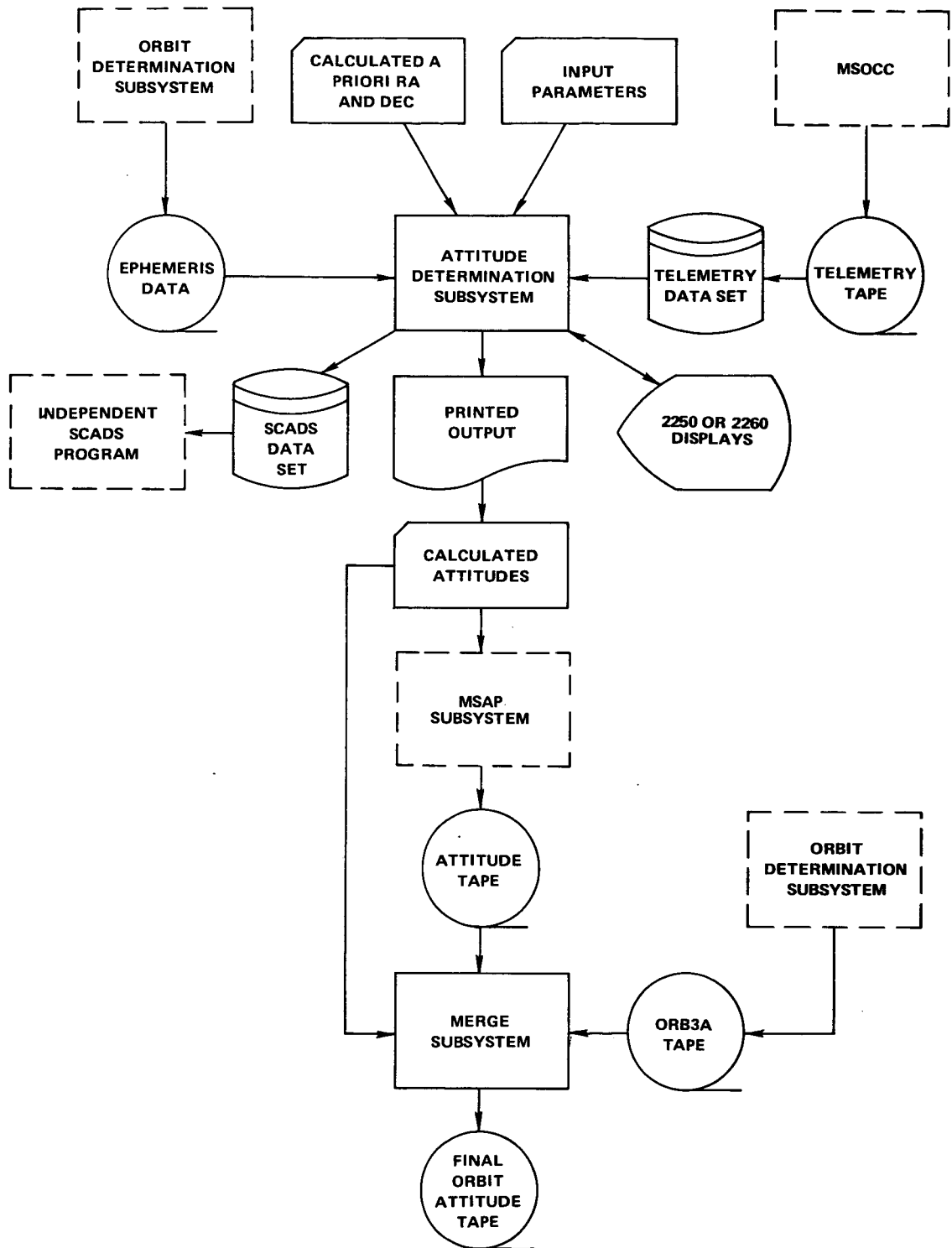
Figure 3-3. SSSASS Definitive Data Flow

SECTION 4

ATTITUDE DETERMINATION SUBSYSTEM

4.1   INTRODUCTION

The objective of the Attitude Determination Subsystem is to determine spacecraft spin axis attitude from optical aspect and SCADS telemetry data obtained from the on-board attitude sensing system. The system consists of a digital solar sensor, a single horizon detecting optical sensor, and a star sensor.

Utilizing the telemetry data obtained from these sensors, the Attitude Determination Subsystem has been designed to perform the following functions in order to achieve its objective:

- Process raw telemetry data residing on either a magnetic tape or disk

- Calculate spin rate in units of revolutions per minute or degrees per second

- Calculate the right ascension and declination of the spin axis in the inertial coordinate system

- Optionally utilize the 2250 or 2260 Display Unit as a means of directing the subsystem flow

The subsystem is a combination of FORTRAN and Assembler Language Code (ALC) to be executed on the IBM System 360 Model 95 under MVT. The subsystem is designed in a modular structure in order to avoid redundant coding and to provide flexibility. The subsystem consists of six main modules (see Figure 4-1):

1.   SSSMON – executive module

2.   TELPRO – telemetry processor module

3.   DISPLY – display module
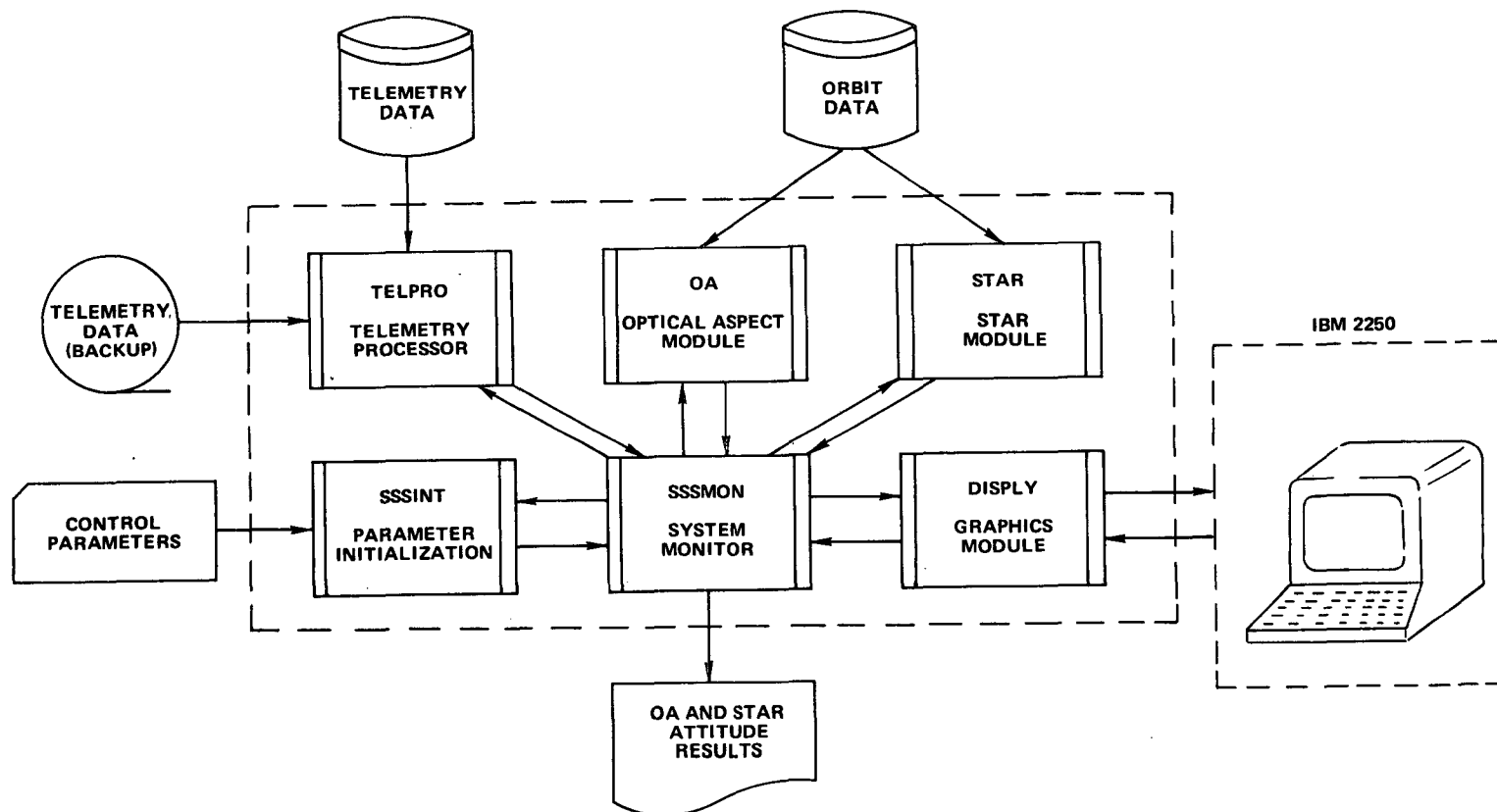
Figure 4-1. Attitude Determination Subsystem Overview

4. SSSINT – parameter initialization module

5. OA – optical aspect attitude determination module

6. STAR – star sensor attitude determination module

4.2   EXECUTIVE MODULE

The primary functions of the executive module are to provide the necessary interface among modules of the subsystem and to control subsystem flow. The subsystem can operate in either a noninteractive or an interactive graphics mode, requiring the executive module to either automatically specify subsystem processing or to permit the user to control program flow. The primary modules with which the executive module must interface are the telemetry processor, parameter initialization, optical aspect, star, and graphics display modules. Since the subsystem is operated in an overlay environment, the executive must retain the appropriate information for the desired operation, allowing for the flexibility of user-specified program flow in the interactive graphics mode.

Secondary functions of the executive module are:

- The calculation of spin rate from optical aspect telemetry data

- The creation of an independent SCADS telemetry data set

- The conversion of telemetry and attitude data from engineering to display units

- The compression of telemetry samples

- The summarization of attitude information for input to the MSAP subsystem

These functions are performed by support routines of the executive module as needed during program execution.

4.3 TELEMETRY PROCESSOR MODULE

The basic requirement to be satisfied by the Telemetry Processor module is to provide the Attitude Determination Subsystem with OA and SCADS attitude telemetry data in the format and organizational structure expected by the OA and Star modules. The following functions are performed by the Telemetry Processor module in satisfying this requirement:

- Reading a raw telemetry input data set, residing on either tape or disk, over a specified interval

- Unpacking a telemetry bit string and extracting items of data

- Associating related telemetry words, which together describe a data event occurrence

- Grouping data event occurrences to form data samples

- Verifying the quality of data items

- Converting data items from telemetry counts to engineering units

- Filling output arrays with converted data samples

These functions are performed using raw telemetry data transmitted in either the primary mode or the backup mode (see Figures D-3 and D-4). Telemetry data transmitted in the primary mode differs in both form and content from that transmitted in the backup mode.

A telemetry data word consists of a four-bit ID byte followed by 3 four-bit bytes when the primary transmission mode is employed. Three types of OA data event occurrences are possible:

1. A sun event

2. An earth-in event

3. An earth-out event

A sun event, described in three telemetry words, consists of a sun angle, a sun time fine, and a sun time coarse. Earth-in and earth-out events, each described in two telemetry words, consist of an earth-in and an earth-out time fine and an earth-in and earth-out time coarse. The one SCADS data event occurrence, a star sighting, is described in three telemetry words and consists of an ingress time fine, an ingress time coarse, and an amplitude-duration. Coarse and fine time telemetry words contain a readout of the low-order part of the contents of the spacecraft clock at the time at which a particular data event occurred.

A telemetry word occurring in the backup mode consists of 3 four-bit bytes, the rightmost of which comprises the ID byte. The leftmost ten bits, two of which overlap the two leftmost ID bits, comprise the data portion of the telemetry word. Possible OA data event occurrences are the same as in the primary mode of transmission. However, the time of a data event occurrence is described in a single telemetry word which contains a count of the number of bits transmitted between the time at which the event occurred and the end of the telemetry quarter-frame during which the event occurred. SCADS data are not available in the backup transmission mode.

An input data set containing raw telemetry data transmitted in one of the modes described above is read by the Telemetry Processor module into a buffer area. The telemetry bit string comprising each record is unpacked, and extracted data items are stored in an intermediate array. Data samples, in a format appropriate for processing by the OA and Star modules, are constructed from the telemetry words contained in this intermediate array. The method used is to associate telemetry words which together describe a data event occurence and then group data event occurences to form data samples.

The association of related telemetry words to form a data event is accomplished by flagging those words which cannot be so associated. Each telemetry frame contained in the intermediate array of unpacked telemetry data is examined in order to determine if, for one of the following reasons, the entire frame should be disregarded:

- Zero attached time, indicating fill by MSOCC
- Poor quality
- Inconsistent STATA value (transmission mode indicator)

The quality test is optional. An initial STATA value is established each time the processing of a new telemetry interval is requested. The occurrence, within the interval, of a STATA byte which deviates from this value results in the flagging of the frame containing that byte. A frame that is determined to be invalid in its entirety is flagged, and processing of the next telemetry frame is initiated. Otherwise, the individual data items contained in the current frame are examined as described below.

The techniques for processing primary and backup OA data and SCADS data are similar. When the availability of a desired data type has been established, the ID associated with the first telemetry word of that type is examined. If its value is not one of the permissible ID values for that type, the telemetry word is flagged. Otherwise, tests are performed, based on the value of the ID and of status flags, to determine if the current telemetry word should be associated with a previous telemetry word (words) in describing the occurrence of a data event. A telemetry word is so associated if the following conditions are satisfied:

- The last data event described by a previously encountered telemetry word has not been fully described.
- The current and previous telemetry words describe a data event of the same type.

- In the case of SCADS and primary OA data:

    1. The previously encountered telemetry word is immediately prior to the current telemetry word.

    2. The previous and current telemetry words are from the same data table.

    3. A failure of the spacecraft clock has not occurred between the previous and current telemetry words.

The current telemetry word is considered to describe the occurrence of a new data event if any of the above conditions is not satisfied. If the last data event has not been fully described, all previous telemetry words associated with that event are flagged. This examination of telemetry words within a frame is performed for both OA and SCADS data, if both are requested. The examination continues until the availability of each is exhausted, at which time the process is repeated using the next telemetry frame.

The grouping of data event occurrences to form data samples assumes the existence of an array of unpacked telemetry data in which all data items that cannot be associated with completely described data event occurrences have been flagged. This array is scanned, proceeding through one telemetry frame to the next, in a search for complete data events. The construction of an output data sample is initiated upon the identification of either a sun event, in the case of OA data, or an ingress time, in the case of SCADS data. Successive data events are added to the sample until one of the two following conditions arises.

- All data events comprising a complete telemetry sequence are encountered, in the expected order of occurrence.

- A data event type is encountered more than once.

Appropriate unit conversions, determined from the data event type and the mode of telemetry transmission, are performed and the data sample is stored in an output array. The construction of the next data sample then is initiated. This cycle is continued until the entire array has been scanned.

4.4 OPTICAL ASPECT MODULE

The Optical Aspect Attitude Determination Module is designed to handle data from a single on-board horizon detecting optical sensor in conjunction with a solar aspect detector. The measurements available from the sensor complement are the time that the sun was sensed, the time that the earth was sensed, the width of the earth scan in units of time, and the spin axis-sun direction cone angle. Only horizon crossings are processed for the attitude determination calculations; therefore, terminator crossing data must be logically rejected. The module has as its primary input a file of preprocessed telemetry information consisting of a string of sensor output times directly transformable to attitude information and an instrument-measured solar aspect readout. This information is made available to the module in blocks, the extent of which is specified at execution time. The attitude calculation is based on single horizon crossing data. Also incorporated into the module is a least-squares differential correction procedure based on the generalized cones program GCONES (Reference 4-1). The output of the deterministic procedure for attitude determination is passed to the GCONES procedure as an initial estimate if a differential correction is desired. The central body for the attitude calculations will be considered as either the earth or the moon. In most cases the module will function without benefit of an initial a priori estimate of the spacecraft attitude. Certain pathological data cases will require an initial estimate. Data flow for the Optical Aspect Module is given in Figure 4-2.
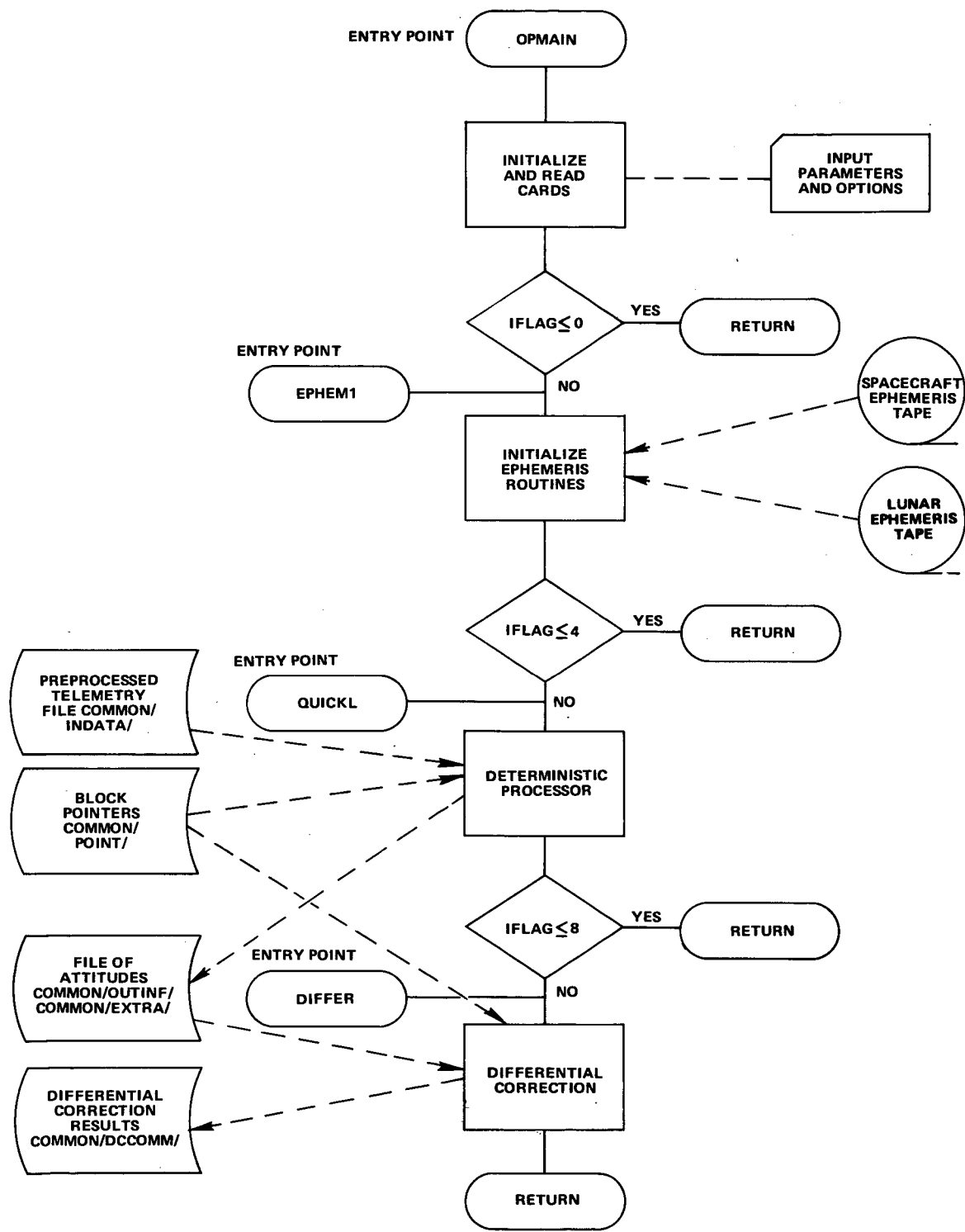
Figure 4-2. Optical Aspect Module Data Flow

4.4.1   Analytical Techniques

4.4.1.1   Sun Angle Processing

        The purpose of the sun angle processing is to smooth sun angles and reject outliers and invalid data. Any telemetry frame with a negative sun time or sun angle less than zero or greater than 180° is rejected. The remaining frames are used to compute a linear least squares fit of the sun angles versus the sun times. The standard deviation of the sun angles from the fitted curve is computed. Spurious values are rejected and the computation of the linear fit is repeated.

        After the linear fit is complete, the smoothed sun angle corresponding to each valid sun time is saved for use in the differential correction. In addition, the sun angle is evaluated at each sensor triggering time and saved for use in the single frame processing. Thus the data can be considered to have been simultaneously measured at the horizon sensor triggering time.

        The utility of this procedure depends on a number of factors. The user may wish to turn off the option to smooth sun angles if the spacecraft is undergoing nutation, or if for any reason the sun angle is varying more rapidly with time than would be expected to result from a constant attitude.

4.4.1.2   Single Horizon Crossing Computation

        As many as two possible attitudes are calculated from a single horizon crossing event, with the corresponding nadir angles and dihedral angles.

        Three spherical triangles must be solved to obtain the required nadir angles and corresponding dihedral angles (see Figure 4-3). Each nadir angle defines a cone around the vector from the spacecraft to the central body, and each sun angle defines a cone around the sun vector. The utility routine is used to compute the two attitude vectors defined by the intersection of these
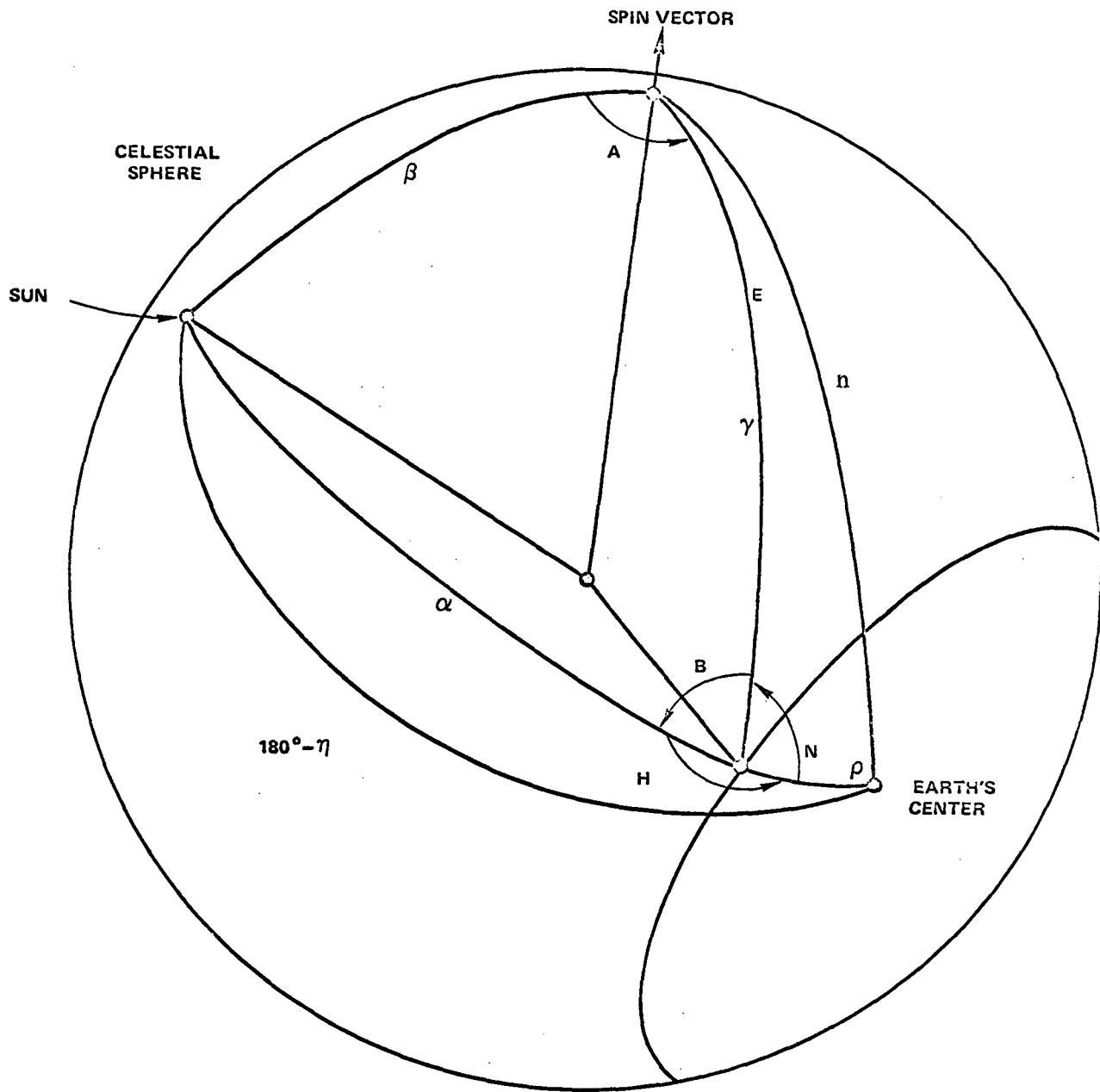
Figure 4-3. Single Horizon Crossing Geometry

two cones. As can easily be seen, one of the attitude vectors corresponds to a dihedral angle greater than pi and the other attitude corresponds to a dihedral angle less than pi. The computed dihedral angle must be used to choose between the two attitude vectors obtained for each nadir angle in order to avoid a four-fold ambiguity. The fact that a two-fold ambiguity remains will be shown below.

The first spherical triangle is formed by the spin axis, the sun vector, and the horizon crossing point, as shown in Figure 4-4.

The sun angle, β, the sensor mounting angle, γ, and the spacecraft rotation angle from the sun, A, are given so that α and B can be determined. From the law of cosines:

$$\cos \alpha = \cos A \sin \beta \sin \gamma + \cos \beta \cos \gamma.$$

If abs $(\cos \alpha) > 1$, no solution is possible. Otherwise:

$$\alpha = \text{arcos} (\cos \alpha)$$

and:

$$\cos B = (\cos \beta - \cos \alpha \cos \gamma)/\sin \alpha \sin \gamma$$

Again if:

$$\sin \alpha \sin \gamma = 0 \text{ or abs } (\cos B) > 1$$

no solution is possible. Otherwise:

$$B = \text{arcos} (\cos B)$$

Putting the solution into the proper quadrant, if the dihedral angle A is greater than pi, it is necessary to set:

$$B = -B$$
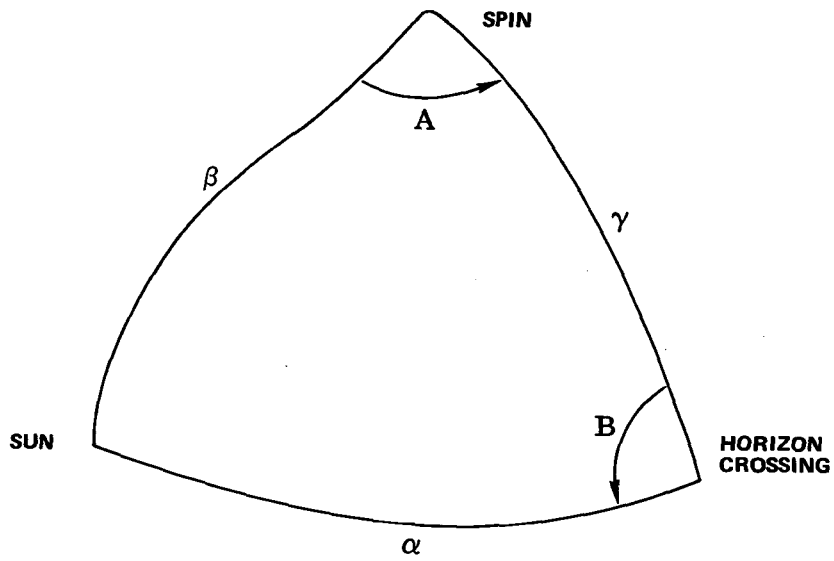
Figure 4-4. Horizon Crossing Spherical Triangle

The second spherical triangle is formed by the sun vector, the horizon crossing point, and the vector to the center of the central body, as shown in Figure 4-5.

The angular radius of the central body, ρ, and the arc length from the sun to the center of the central body, $(\pi-\eta)$, can be computed from spacecraft and solar ephemeris. The angle α is as computed above. Calculations for H are:

$$\cos H = (\cos (\pi-\eta) - \cos \alpha \cos \rho)/\sin \alpha \sin \rho$$

If $\sin \alpha \sin \rho = 0$ or abs $(\cos H) > 1$, no solution is possible, Otherwise, there are two solutions for H:

$$H_1 = \text{arcos } (\cos H) \text{ and}$$
$$H_2 = -H_1$$

The remaining calculations must be performed for $i = 1$ and $i = 2$. If solutions are obtained for both cases, then there will be two possible attitudes, two nadir angles, and two dihedral angles for this crossing. If one of the solutions is rejected in the computations which follow, then there may be a single unambiguous attitude, nadir angle, and dihedral angle for the crossing.

The third spherical triangle is formed by the spin axis, the horizon crossing point, and the center of the central body, as shown in Figure 4-6.

The angles ρ, the central body angular radius computed from ephemeris information, and γ, the sensor mounting angle, are known. Therefore, the angle N can be computed, since:

$$B + H_i + N = 2\pi$$
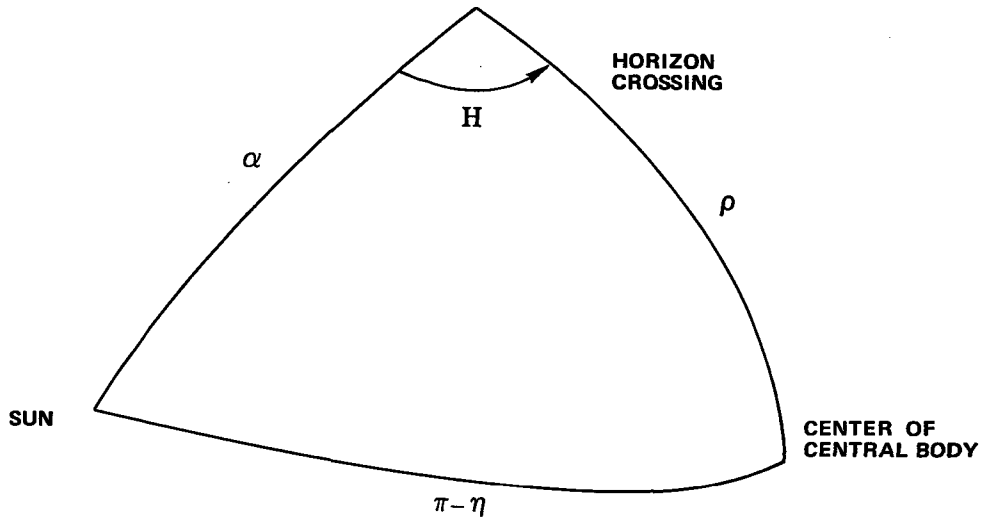
Figure 4-5. Sun Vector, Nadir Vector Spherical Triangle
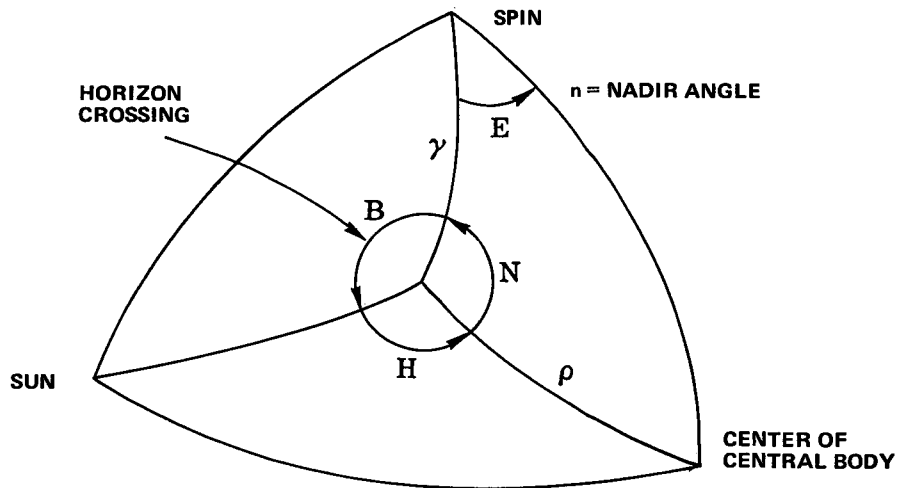
Figure 4-6. Schematic Drawing of the Three Relevant
Spherical Triangles

that is, the angles around a point on the celestial sphere sum to 360°. So:

$$N = 2\pi - B - H_i - 2\pi k$$

where:

$$k = 0, 1, \text{ or } 2$$

k can be chosen such that:

$$-\pi < N \leq \pi$$

For an earth-in crossing, N must be positive and for an earth-out crossing, N must be negative. If the sign of N is incorrect, the solution is rejected. Otherwise, the third spherical triangle is solved for N and E. Again, using the law of cosines:

$$\cos n = \cos N \sin \gamma \sin \rho + \cos \gamma \cos \rho$$

If abs (cos n)>1, no solution is possible. Otherwise, the nadir angle is computed from:

$$n = \text{arcos (cos n)}$$

and the dihedral angle E is computed from:

$$\cos E = (\cos \rho - \cos \gamma \cos n)/\sin \gamma \sin n$$

If $\sin \gamma \sin n = 0$ or abs (cos E)>1, no solution is possible. Otherwise,

$$E = \text{arcos (cos E)}$$

If this is an earth-out crossing, E must be negative. Therefore, E is set equal to -E. The dihedral angle:

$$D = A + E$$

is the meaningful angle in the attitude calculation. If D<0 then:

$$D = D + 2\pi$$

If D>2π, then:

$$D = D - 2\pi$$

Now the two possible attitude vectors may be determined, given the nadir angle, sun angle, and the cone axes. From the first attitude vector obtained, the corresponding dihedral angle, D', is computed. If D and D' are both less than π or both greater than π, then the choice of attitude vector is correct. Otherwise, the alternate choice is correct.

4.4.1.3   Single Frame Processing

A single input frame consists of a sun crossing time, an earth-in time, an earth-out time, a spin rate, and two processed sun angles.

If the sun time or the spin rate is less than or equal to zero, the frame is rejected. Otherwise each sensor triggering time is processed as follows:

- If the triggering time is less than or equal to zero, the triggering is rejected.

- If the sun angle is less than zero or greater than pi, the triggering is rejected.

- The spacecraft rotation angle, A, is computed by:

    A = (triggering time – sun time) x spin rate

- The angle is checked against the sensor cutoff angle. If A is less than the cutoff angle or greater than 2π minus the cutoff angle, the triggering is rejected.

For each central body under consideration (earth, moon), the following steps are performed:

1.   The lighting conditions on the central body are computed from ephemeris data. If the central body is dark or not visible, then this triggering is rejected. If a terminator is visible, the terminator flag for this frame is set. If data, while a terminator is visible, is not to be included in attitude calculations, the triggering is rejected. Otherwise, processing continues as for the sunlit case.

4-18

2. As many as two attitudes are computed for this crossing.

3. If no solution is obtained, then there is no possible attitude consistent with the assumption that this triggering resulted from a sunlit horizon crossing on this central body. Therefore, the crossing is rejected.

4. If the central body is fully sunlit, the processing of this crossing is complete. If a terminator is visible, then it must be determined whether this triggering resulted from a terminator crossing.

If a terminator is visible, it must be determined whether the terminator is intersected by the spacecraft sensor scan, i.e., whether a particular triggering of the sensor was in fact a horizon crossing or a terminator crossing. The procedure for this determination is a recursive one. For each attitude computed, the module, through use of the Optical Aspect Data Predictor (see Section 8.2), determines whether a scan of the central body with this attitude would have produced a sunlit horizon crossing for the in or out triggering. If the computed attitude is not consistent with the assumption that this triggering occurred at a sunlit horizon crossing, then this attitude is rejected.

Note that it is possible that this test will fail to reject a terminator crossing. This occurs when the attitude computed from a terminator crossing is so far from the true attitude that a scan with the erroneous attitude would give a sunlit horizon crossing at this triggering. When this occurs, there is one attitude consistent with the assumption that this is a terminator crossing and a second attitude consistent with the assumption that the triggering was a sunlit horizon crossing. Therefore, there is no deterministic procedure for recognizing this problem. However, when the problem occurs, the resulting computed attitude will in general have a large error. Since the error is large, the erroneous attitude is easily recognized and rejected in the block average procedure.

4.4.1.4   Block Averaging Procedure

Once each input telemetry frame has been processed, the best estimate of the attitude must be computed based on the single frame results. Each input telemetry frame results in two output measurement frames, each of which may contain zero, one, or two attitudes. The ambiguities which could not be resolved on a single frame basis can now be eliminated if the block of data is sufficiently large.

In computing the average attitude for a block, several cases must be considered. For each output frame with two attitudes, the attitude to be included in the average must be identified. The procedure is further complicated by the fact that in some frames both attitudes must be rejected as spurious. It should be noted that attitudes are considered independent of the source of the horizon triggering from which they were calculated; i.e., attitudes calculated from moon crossings are given equal weight with those from earth crossings.

The following procedure is used in the most general case, in which every output frame contains two attitudes and no a priori attitude is available: the first attitude from the first output frame is selected as a trial attitude. In each following output frame, the attitude from the pair that is closer to the trial attitude is selected. The average of the selected attitudes is computed and a residual edit procedure performed to compute the final standard deviation.

The trial attitude obtained by this procedure is further refined by the following iterative technique: the trial attitude is used to select one attitude from each pair and an average of the selected attitudes is computed as before. The average attitude is used as a new trial attitude and the sequence

is repeated. The process terminates when the set of attitude selections remains identical for two successive iterations. Convergence normally occurs in two to three iterations.

If an accurate a priori attitude is available, the procedure is greatly simplified. The a priori attitude is used as a trial attitude and the iterative procedure is used immediately.

4.4.1.5   Differential Correction

To further refine the attitude calculations, the OA module has included an option for a least-squares solution on the attitude. This differential correction method utilizes the subroutine GCONES with three types of attitude data: sun angles, nadir angles, and dihedral angles.

After data ambiguities have been resolved and spurious values have been eliminated in the single frame processing, the input arrays with the appropriate telemetry data are initialized for the call to GCONES. For each input telemetry frame with a valid sun angle and sun time, a smoothed value of the sun angle and the sun vector at the sun time are passed to GCONES. Each sun angle passed is assigned a unit weight, unless the user specifies a different weighting factor for sun angles. Following the single frame processing, the selected nadir angle, along with the central body vector at the sensor triggering time, is passed to GCONES. Likewise, the selected dihedral angle is passed to GCONES, along with the central body vector and the sun vector at the triggering time. All nadir and dihedral angles are assigned a unit weight, unless the user specifies a different weighting factor.

Note that GCONES can be used to determine attitude from sun angle data alone, assuming that sun data is available over a sufficiently long period and that the attitude remains constant. This will be the system failure mode in the event of horizon sensor failure.

In addition to the nominal differential correction technique, a second version of GCONES is available to allow for the additional capability of executing a residual edit of the data while processing the differential correction. With this technique, spurious values can be eliminated from the least-squares calculations, whereas, in the original version of GCONES, no capability for data rejection exists.

4.4.2   Module Structure

The Optical Aspect module is called by the executive of the Attitude Determination Subsystem and can be entered through one of four entry points. The function of each entry is as follows:

1.   OPMAIN (IFLAG, IERR) – Read NAMELIST parameters. If IFLAG.LE.0, return. Otherwise, continue.

2.   EPHEM1 (IFLAG, IERR) – Initialize ephemeris routines. If IFLAG.LE.4, return. Otherwise, continue.

3.   QUICKL (IFLAG, IERR) – Perform "Quick Look" attitude determination on requested block(s). If IFLAG.LE.8, return. Otherwise, continue.

    Note: A "Quick Look" can consist of one or more blocks with any number of frames .GE.1. Program flow is the same regardless of block size.

4.   DIFFER (IFLAG, IERR) – Perform differential correction on requested block(s).

As indicated in Figure 4-2, program flow always proceeds from one entry point to the next, in order. Therefore, the choice of an entry point determines the point in the program when execution will begin, and the choice of IFLAG determines the point when the system will return to the monitor.

Input for the OA module consists of the following:

- Card input control parameters and options input through the FORTRAN NAMELIST option

- Spacecraft ephemeris tape – an ORB1 tape containing the orbital position of the satellite

- Lunar ephemeris tape – a tape describing the position of the moon during the time interval being considered

If the spacecraft and/or lunar ephemeris tapes are not available, orbital elements can be substituted.

Output from the module consists of printouts of input data and attitude results from the attitude determination calculation. The output is controlled by an indicator allowing for different levels of output to be printed.

4.5   STAR MODULE

The Star module is designed to yield a precise measurement of spacecraft attitude. The module processes telemetry data from a single on-board star detecting sensor whose optical field of view is swept across the sky by the natural motion of the spacecraft. The instantaneous optical field of view consists of the projection on the celestial sphere of a transparent slit in the otherwise opaque reticle at the focal plane of the optical sensor. Stellar targets are sensed by a photomultiplier behind the slit as the slit pattern is swept over the sphere. In this way, the sensor gathers data from whatever detectable targets come within its view. The Star module's primary input is the telemetry data generated by this sensor. The data is made available in blocks that are specified at execution time. Additional inputs to the Star module consist of an accurate catalog of the celestial positions of the bright stars, an initial spacecraft attitude estimate, and user-selected program parameters and tolerances. Spacecraft attitude is then determined using these

inputs along with a dynamic model describing spacecraft attitude as a function of time. This is accomplished by employing a least-squares technique that makes use of star detections to infer the unknown parameters in the attitude model.

4.5.1   Analytical Techniques

The processed telemetry data consists of center transit times and pulse areas. A center transit time corresponds to the time a detected star is in the center of the instantaneous optical field of view. A pulse area is a measure of the detected star's brightness; however, this is a gross measurement and the Star module makes little use of it. The primary input to the module is thus a block of center transit times.

The attitude determination technique consists of an algorithm that requires four major steps to be performed to arrive at an acceptable answer or to terminate the searching procedure.

The first step is to determine the spacecraft spin period by a correlation technique that calculates the spin period in the presence of noisy data.

The second step is to calculate the mean reduced transit times and determine the catalog stars that are in an augmented field of view. The transit times must first be reduced modulo the calculated spin period, thereby forming clusters of transit times. The initial attitude guess, together with the corresponding error estimate, defines an augmented field of view, assuming the actual field of view is a subset of this augmented field. All catalog stars in this augmented field are then considered as candidates for association with the mean reduced transit times.

The third step involves star-time identification. This entails matching a star triplet with a mean reduced transit time triplet. Once a tentative match occurs, the star triplet is associated with the original transit time data. If star S_j is matched to mean reduced transit time $\bar{t}_K$, then all original transits that formed the cluster which created $\bar{t}_K$ are associated with star S_j. In this manner, stars become associated with the original transit time data.

The fourth step of the algorithm attempts to determine the spacecraft attitude. This information is obtained by inputting into the dynamic model the star-time associations and then using a least-square algorithm to determine the attitude.

If a solution is either not formed or is unacceptable (in terms of the residual error being too large), the algorithm branches back to the third step. A new star-time association is then derived and the fourth step is repeated. This process continues until an acceptable solution is found or until a user-specified limit on the number of trial combinations is exceeded.

4.5.2   Analytical Limitations

The Star module is designed to determine highly accurate attitude information, but the module does have limitations. These limitations are caused by:

1.   Transit time data being contaminated. Noise in the stellar transit times, the presence of spurious pulse type noise, and the presence of systematic type noise all can affect proper execution of the module.

2.   Inaccurate dynamic model input. The Star module has the capability of using any of four different models. The most complex model allows for the existence of a coning angle and a slit-misalignment angle. The selection of an inappropriate dynamic model can adversely affect module execution.

4-25

3. Inaccurate initial attitude estimate input. Perhaps the most critical factor in proper execution of the Star module is the need for an accurate initial attitude estimate. If this attitude guess plus the corresponding error estimate on the guess are in error, proper execution of the module will not occur.

4. Other inputs being in error. Inputs such as bounds on the period estimate and module tolerances can also affect proper execution of the Star module.

There are also other considerations fundamental to proper module execution. If a spacecraft coning angle exists, it must not be large (no greater than a few degrees). The spacecraft angular momentum vector must essentially remain constant.

4.5.3 Module Structure

The Star module consists of 26 FORTRAN routines that can be categorized in four major submodules corresponding to the four steps of the attitude determination algorithm. The input for the module consists of the following:

- Preprocessed telemetry data – transit times, amplitude, and pulse duration

- Card input – star catalog, user selected parameters and tolerances

- Orbit tape – used in determining earth blocking

The primary output from the Star module is the attitude solution. This solution is printed out by the module and, when executed in conjunction with the Attitude Determination Subsystem in the interactive graphics mode, displayed on the IBM 2250 Display Unit. Intermediate calculations are available for output upon user request. In the interactive graphics mode, input parameters are displayed on the IBM 2250 and therefore available for viewing and alteration.

SECTION 5

MSAP/SSS-A SUBSYSTEM

5.1   SUBSYSTEM OVERVIEW

The purpose of the Multi-Satellite Attitude Prediction (MSAP/ SSS-A) Subsystem for the SSS-A satellite is to generate a prediction of spacecraft attitude for specified time intervals and to aid in the creation of attitude control commands for the satellite, based upon mission constraints.

The attitude prediction feature of the MSAP/SSS-A Subsystem has the capability of calculating spacecraft attitude, based upon a given initial attitude and orbit description. The subsystem summarizes spacecraft attitude and spin rate as a function of time for any requested interval. The prediction algorithm only assumes that the satellite's angular momentum vector is coincident with the spacecraft spin axis, which is a condition that results from a spin-stabilized satellite. The prediction capability is further refined with the addition of a direct search optimization algorithm (DSOAP) that optimizes questionable parameters in the calculation to fit an attitude prediction to empirical data.

The MSAP/SSS-A Subsystem aids in generating control recommendations by predicting the attitude motion resulting from the implementation of magnetic control commands. Although there are no automatic recommendations by the subsystem, an analyst can interpret the prediction results to select the appropriate command to accomplish the desired attitude maneuver.

5.2   ANALYTICAL TECHNIQUES

To simulate attitude motion, the MSAP/SSS-A Subsystem must model the torques acting on the spacecraft and determine how these will affect the satellite's attitude. This requires a knowledge of the physical description of the satellite, the environmental conditions, and the dynamic characteristics of the mission. These factors are then combined to determine the essential features required of an attitude prediction and control program.

5.2.1   Attitude Prediction

The attitude prediction algorithm consists of calculating the torques acting upon the satellite and, from this information, determining the nature of attitude drift. The disturbance torques considered for the SSS-A satellite are gravity gradient, magnetic, and aerodynamic. Of these, the aerodynamic torque is the most significant, causing attitude drift when the satellite is not being maneuvered by control coils. Two methods are available for calculating the aerodynamic disturbance. One is a rigorous calculation utilizing a satellite decomposition model consisting of plates and spheres. The second is faster, although less rigorous, and utilizes a satellite decomposition model consisting of plates, spheres, and cylinders.

To increase the algorithm's efficiency, the MSAP/SSS-A prediction technique includes various options to control the quantity of required calculations. One option is an altitude cutoff for torque computations. This allows for the bypassing of torque calculations above altitudes at which the torque is no longer active in causing attitude drift. Several prediction time parameters used in the calculations can also be controlled by the user and therefore optimized for the prediction desired.

The attitude prediction algorithm utilizes orbital information in determining attitude drift. This requirement necessitates the existence of an orbit generator to predict orbital position during the interval being investigated. Due to the highly eccentric nature of the SSS-A orbit, it is necessary to simulate the variation in perigee altitude during an attitude prediction. The highly eccentric orbit has also created a need for information describing conditions at perigee. The MSAP/SSS-A Subsystem will supply perigee velocity vector, control coil triggering, and sun angle data for each perigee pass in a prediction.

5.2.2   Attitude Control

Although MSAP/SSS-A will not generate attitude control commands, it will be used extensively in verifying final attitudes and drift rates based upon manually generated commands. This section describes the control devices on the satellite and the method used to determine the appropriate control recommendations.

SSS-A is equipped with a non-pulsing, 9230 pole-cm coil aligned with the spacecraft spin (z) axis. This coil will be used to implement any attitude change necessary to meet declination or sun angle constraints. An alternately pulsating, 2654 pole-cm coil, mounted along the spacecraft's x-axis, serves for spin rate control. To conserve spacecraft power levels at altitudes where spin axis motion due to the control coils is negligible, an automatic system controlling coil on and off times has been installed. This system consists of a magnetometer mounted along the y-axis and a threshold detector such that the coils cannot be activated unless the external magnetic field strength perpendicular to the spin axis is at least 75 milligauss. There is, however, an override capability that allows the coils to be turned off even though the sensed magnetic field strength is greater than 75 milligauss.

Spin axis reorientations and attitude maintenance will be accomplished manually. Several aids will be available to assist the control analyst in arriving at the necessary maneuvers to satisfy mission requirements. An initial estimate of desired attitude will be selected based upon tabulated output of support programs. Knowing both current and desired attitude, coil settings and times can be selected and input to the MSAP/SSS-A Subsystem. The control times will then be refined through the interactive graphics capabilities of MSAP/SSS-A.

5.2.3   Attitude Prediction Optimization

The attitude prediction capabilities of the MSAP/SSS-A Subsystem have been extended by the addition of an optimization capability. The optimization procedure will serve two functions:

1.   Estimating non-measurable parameters that affect spacecraft attitude (i.e, magnetic basis, drag coefficients)

2.   Generating weekly attitude summaries used for definitive processing

The technique used by the subsystem is a direct search optimization algorithm (DSOAP). The advantage of using DSOAP is inherent in the nature of the direct search procedure, namely, that expressions for the partial derivatives of the function being optimized are not required for a solution. The DSOAP algorithm consists of four steps,

1.   For $r = 1, 2, \ldots, n$, calculate S_r so that $f\,(\tilde{P}_{r-1} + S_r \tilde{D}_r)$ is a minimum, and define $\tilde{P}_r = \tilde{P}_{r-1} + S_r \tilde{D}_r$. Note that the function f is to be minimized here with respect to an n-dimensional vector $\tilde{P}$. $\tilde{D}$ is a one-dimension directional vector for optimum search.

2. For $r = 1, 2, \ldots, n-1$, replace $\tilde{D}_r$ by $\tilde{D}_{r+1}$.

3. Replace $\tilde{D}_n$ by $(\tilde{P}_n - \tilde{P}_o)$.

4. Choose S so that $f\left[\tilde{P}_n + S\,(\tilde{P}_n - \tilde{P}_o)\right]$ is a minimum and replace $\tilde{P}_o$ by $\tilde{P}_n + S\,(\tilde{P}_n - \tilde{P}_o)$.

The convergence of the algorithm will take place in a finite number of steps. The maximum number of iterations is m·n(n+1) where n is the number of parameters being optimized and m is the number of function evaluations (MSAP predictions) per linear search. The accuracy of the results are dependent upon the initial accuracy of the parameters and the search step size. However, as the search step size decreases, the number of function evaluations increases. Random noise in the observed attitude points used in the evaluation has no effect on the accuracy of the results or the speed of the convergence.

5.3 SYSTEM STRUCTURE

The data flow for the MSAP/SSS-A subsystem is given in Figure 5-1. The initial attitude point used in the prediction may be supplied by the Attitude Determination Subsystem or by a previous MSAP prediction.

All input data to the subsystem is read from FORTRAN NAMELISTs. Parameters characteristic of the general MSAP system comprise a separate NAMELIST, since the system has been designed to support various satellite missions. These parameters include the simulation time; the initial attitude parameters: right ascension, declination, and spin rate; data set reference numbers used for input and output purposes; time parameters from which both program efficiency and predictor accuracy can be controlled; and the orbital elements required by the orbit generator.
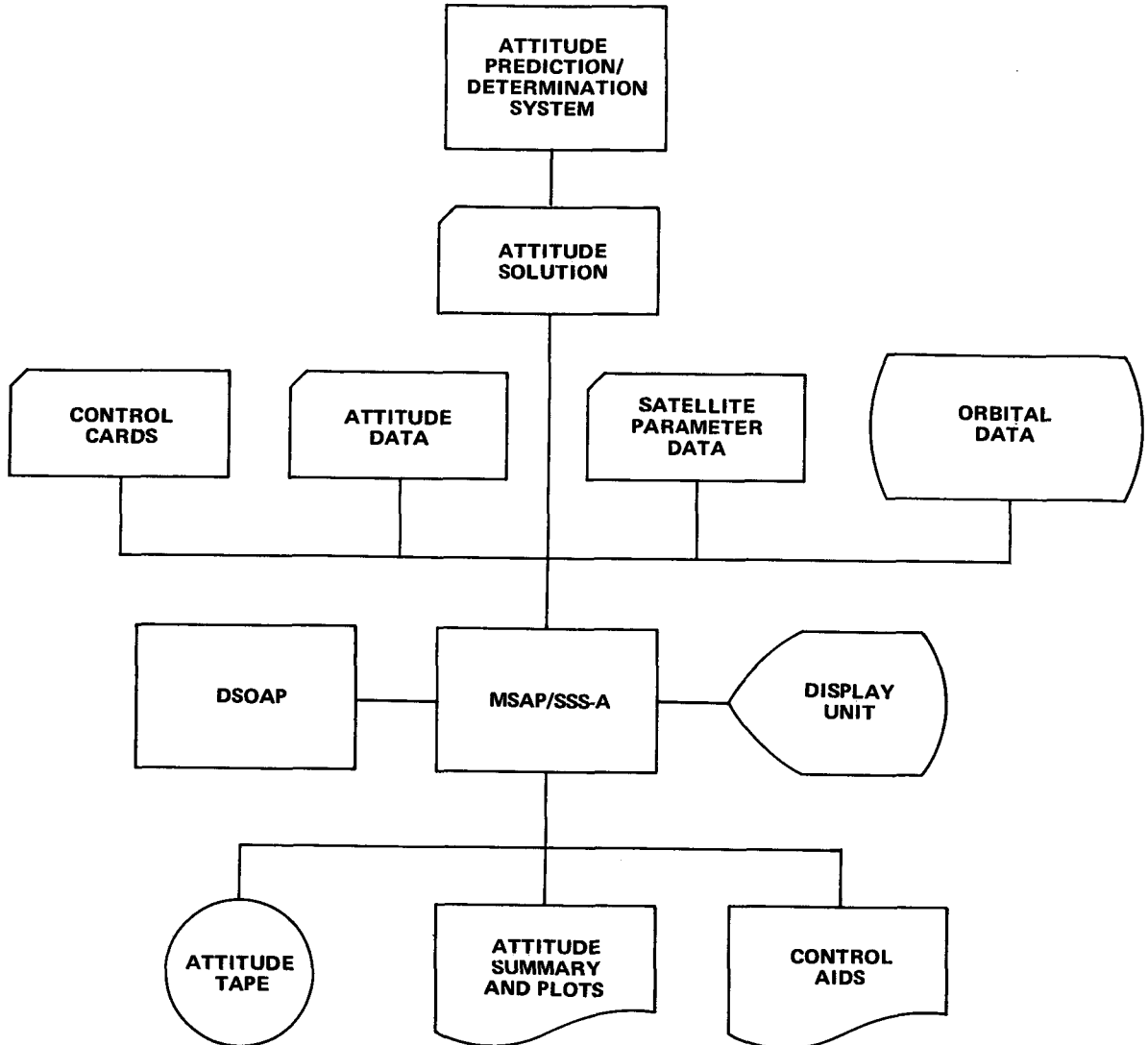
Figure 5-1. MSAP/SSS-A Subsystem Data Flow

Satellite-related parameters, specifically the satellite physical data and attitude control coil settings, are read in separate NAMELISTs. The coil can be activated in one of two ways:

1. Automatic mode. The coil is turned on when the external magnetic field perpendicular to the spin axis becomes greater than 75 milligauss and turned off when the same field becomes less than 75 milligauss.

2. Manual mode. The coil is turned on and off at user specified times regardless of the external magnetic field.

System output consists of a formatted listing of input data, an attitude parameter output, control data output, intermediate data output, and error messages. The attitude parameters, in the form of listings and plots, and the input data comprise the standard output units. All other data is printed out on option according to user requirements.

In addition to the standard attitude parameters (right ascension, declination, and spin rate), three other parameters (zeta, lambda, and gamma) are included in the summaries and plots. Zeta is the angle between the current spin axis and the perigee velocity vector, lambda is the azimuth angle of the spin axis relative to the perigee velocity vector, and gamma is the sun angle.

To aid in the manual determination of control, the following information will be printed for each perigee pass:

- Time of perigee
- 75 milligauss on-time
- Control on-time
- 75 milligauss off-time

- Control off-time

- Sub-satellite latitude-longitude at perigee (earth fixed frame)

- Inertial right ascension and declination of sub-satellite point at perigee

- Inertial right ascension and declination of the perigee velocity vector

SECTION 6

MERGE SUBSYSTEM

The Merge Subsystem is designed to generate definitive orbit attitude tapes required for experimenter data processing. The subsystem consists of two programs, a MERGE program and a CHECK program.

The MERGE program merges definitive attitude data supplied by the MSAP Subsystem, definitive attitude results from the Optical Aspect module, and definitive orbit data from an ORB3A tape. The program creates the orbit attitude tape by inserting attitude data into an existing ORB3A data set record and then writing the modified record into an output data set. In addition, the errors in right ascension and declination and the angle between the spin axis and the magnetic field vector are inserted at times when optical aspect data is available. These errors are calculated by comparing the attitude results of the MSAP Subsystem and the Optical Aspect module.

The merging process is based on the time intervals of both the attitude and orbit input data sets. Nominally, the merge interval coincides in time with the start and stop time interval of the ORB3A data set. However, if this is not the case, an option is provided to select a particular section of the attitude data set by specifying the beginning and ending times of the merge interval. A description of the orbit attitude tape is given in Appendix D.

The CHECK program performs quality checks on the final orbit attitude tape by reading the tape and printing data records or sections of data records for analysis.

An overview of the Merge Subsystem is given in Figure 6-1.
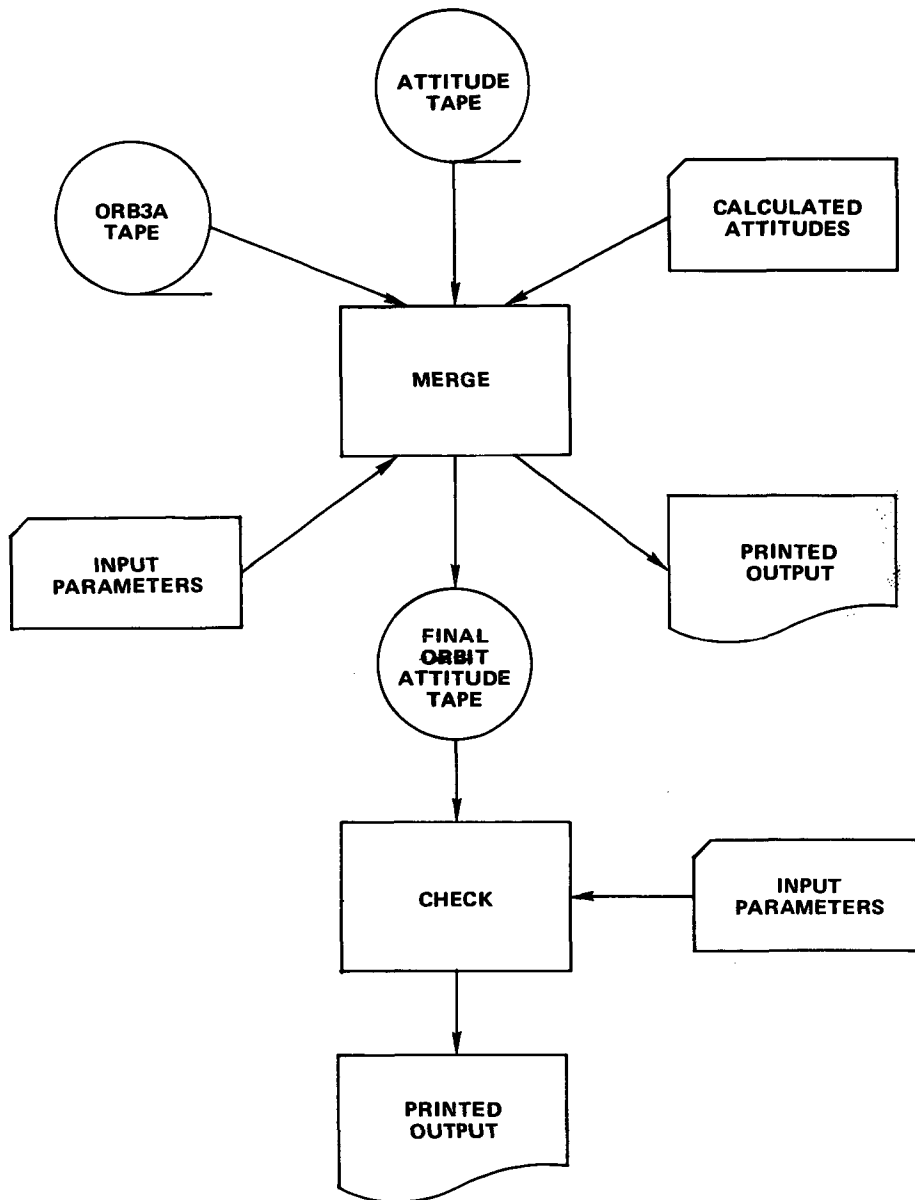
Figure 6-1. MERGE Subsystem Overview

SECTION 7

OPERATIONS PLAN

7.1   ATTITUDE SUPPORT PLAN

In support of the SSS-A mission, the Attitude Determination Office (ADO) is responsible for the determination and control of spacecraft attitude for the entire SSS-A mission. Due to hardware and experimenter requirements, the following attitude constraints have been specified for the SSS-A satellite:

1.   Maintain the spin axis between ± 10 degrees declination

2.   Maintain the angle between the spin axis and the sun line between 30 and 70 degrees

To achieve the ADO objectives, a software Attitude Support System has been developed. This system is expected to be operated on a daily basis with 24-hour response; however, it is capable of operating in a real-time environment if data is available and the need exists.

The attitude support operations can be divided into three categories:

1.   Attitude control and related attitude processing

2.   Star sensor evaluation

3.   Definitive attitude processing

A description of each process is given in the following sections.

7.2   ATTITUDE CONTROL AND RELATED ATTITUDE PROCESSING

To satisfy the attitude constraints imposed by mission requirements, the SSS-A satellite has been equipped with an Optical Aspect (OA) attitude determination system and an attitude and spin control system (for a complete description of hardware, reference Section 1.4). The function of the Attitude Support System is to process the OA telemetry data and obtain an attitude solution to be used in determining the attitude control commands necessary to satisfy mission objectives. The OA data is processed by the Attitude Determination Subsystem, which contains an OA attitude determination module (see Section 4.4) similar to the attitude determination program used on the IMP-I satellite. For attitude control purposes, an attitude calculation will be made on a daily basis on telemetry data received from MSOCC via a data link. This attitude will be used as input to the attitude prediction and control program (MSAP/SSS Subsystem, Section 5), which generates attitude predictions for a future portion of the mission and produces control command recommendations based upon the predicted attitudes.

The attitude prediction results from the MSAP/SSS Subsystem will also be used as input to an OA Data Availability Program (Section 8.2) to determine the time intervals when useful OA data will be available. These times are then used to formulate a request to MSOCC to make available telemetry data for the appropriate time intervals for attitude processing.

In support of the control activities required by the SSS-A satellite the following items will be generated by the Attitude Support System:

1.   Daily attitude results. Attitude solutions will be generated by the Attitude Determination Subsystem through the processing of real-time telemetry data transmitted from MSOCC via a direct data link.

2. Weekly attitude history. A summary of daily attitude results will be supplied weekly.

3. 30-day attitude prediction, updated weekly. The MSAP/SSS Subsystem will be used to predict attitude variations over a one-month period. Each week the prediction will be reproduced, using the most recent attitude solutions available.

4. Attitude control recommendations. The recommended magnetic control commands generated by the MSAP/SSS Subsystem will be supplied to MSOCC.

5. OA data availability with recommended data transmission schedule. A summary will be generated listing the times when useful OA data should be available from the on-board attitude system.

As can be seen from the mission simulation for the Launch Window Study, the amount of control maneuvers required to maintain the attitude constraints will vary during the mission. As a result, the effort required to produce these commands will vary according to control needs.

7.3 STAR SENSOR EVALUATION

The Attitude Determination Office has the additional responsibility to evaluate the performance of the SSS-A star sensor (described in Section 1.4). This evaluation will be accomplished through the use of two Attitude Support System programs: the Attitude Determination Subsystem and the Star Sensor Gain Selection program. The specific requirements are to provide support for the SCADS engineering experiment and to ensure that sufficient stars are available for definitive attitude processing.

The Attitude Determination Subsystem (ADS) will be used to determine attitude from the star sensor data. It is felt that the best method to evaluate and monitor the performance of SCADS is to determine attitude from the device. The ADS contains a Star module to calculate attitude from SCADS

data. The initial attitude estimate used in the calculation will be attitude results from Optical Aspect data.

The Star Sensor Gain Selection program will be used to establish the gain setting which will provide a proper mix of stars to ensure the success of the sensor for definitive data processing. The program will likewise predict the times during which SCADS can be operated without the sensor "seeing" the sun or a sunlit earth. It is anticipated that the sensor will be capable of operation during spacecraft day.

The following items will be generated by the Attitude Support System:

1. SCADS gain settings. According to the variation in star data availability, recommendations will be supplied for the alteration of the star sensor's gain setting when it appears that insufficient star data will be available at a current setting.

2. SCADS operations schedule. A listing of time intervals will be supplied summarizing when useful SCADS data should be available. This schedule will be used by MSOCC to determine when to transmit data.

3. Attitude results from star calculations. The attitude solutions from the Attitude Determination Subsystem that utilizes SCADS data will be supplied for analysis of star sensor performance.

7.4 DEFINITIVE ATTITUDE PROCESSING

The Attitude Support System will be used to provide definitive spin axis attitude results. The results will be obtained from the OA data used in attitude control processing, except that the attitude determination calculation will be repeated using definitive orbit data. The attitude solutions from this processing will be smoothed by the MSAP/SSS Subsystem to produce

an attitude tape containing the spin axis vector at one-minute increments for the specified time interval. The data from this tape is then merged with definitive orbit data contained on an ORB3A tape. The result of this merging process is an orbit attitude tape that covers a time interval of approximately one week. The final tape will be delivered to the Information Processing Division for further processing.

SECTION 8

SYSTEM SUPPORT PROGRAMS

8.1 INTRODUCTION

Utility programs have been developed to aid in the support of the operational requirements for attitude determination, prediction, and control. These programs are briefly described in the following sections.

8.2 OPTICAL ASPECT DATA PREDICTION PROGRAM

The Optical Aspect Data Prediction Program predicts the time interval during which the Optical Aspect System on-board the satellite will provide useful data and predicts the quality of that data.

The program accepts as input an attitude tape produced by the MSAP Subsystem. This tape contains a set of records, each giving the components of the spin vector and the time. Additional input consists of ephemeris tapes that give the spacecraft ephemeris and lunar epehemeris during the period of interest. Control parameters are read from cards.

For each input record, the program produces printed output describing the availability of solar aspect, lunar aspect, and earth aspect data at the specified time.

Various options are available to alter the specifications given above; e.g., ephemerides may be generated internally from the orbital elements; the moon may be ignored; a fixed attitude may be read from cards so that no attitude tape is required; and printout may be suppressed, depending on the optical aspect data conditions at each point.

8.3 SSS GAIN SELECTION PROGRAM

The star sensor output must exceed a commandable (eight-level) threshold voltage in order for the detection circuitry to indicate a star presence. The SSS Gain Selection Program will be used to determine the threshold level setting which will give the best mix of stars to ensure successful attitude determination.

The Gain Selection Program will provide compact, easily interpreted, star data availability printout. This printout will include the identification of all stars in the field of view, a listing of those stars that are blocked by the earth, and a listing of any double stars that may exist. The data will be a function of spacecraft attitude, spacecraft position, and threshold setting. Spacecraft attitude can be obtained from input cards or via an attitude tape. Spacecraft position can be obtained from spacecraft orbital elements or via an ephemeris tape.

8.4 PERIGEE HISTORY PROGRAM

In order to successfully meet the mission contraints on spacecraft attitude and sun angle, it is necessary to know several parameters that are related to a perigee pass. The Perigee History Program provides this information. The program requires as input the start and stop time of the desired history interval and orbital information.

The program generates the times of each perigee pass in the requested interval. For each pass, a listing is generated of the orientation in geocentric inertial coordinates of the perigee positional vector, the perigee velocity vector, and the sun. The listing also gives the latitude,

longitude, and altitude of the perigee pass. In addition, the program prints out the ratio of the atmospheric density at perigee to a reference density and the angle between the sun line and the perigee velocity vector.

8.5   MAGNETIC CONTROL PROGRAM

In the course of planning a control maneuver, it is often necessary to know the direction of the declination motion that would occur if the magnetic control coil were energized on a specific perigee pass. In cases where the spin axis is near to violating a mission constraint, it is necessary to know the final attitude to a fraction of a degree.

The Magnetic Control Program is designed to be run in parallel with an MSAP drift prediction. The program requires as input an attitude grid that includes the attitudes expected from the drift run. The grid can be made large enough to include the possibility that the solution to an attitude problem uncovered in the drift run may require several torques. The grid can be fairly coarse and still permit accurate estimates of the motion. Given a start time, a stop time, and orbital information, the program computes the resultant attitude and sun angle for every initial attitude in the grid at every perigee pass in the start-stop interval.

Once a perigee pass or series of passes have been selected to make up a control maneuver, the maneuver can be implemented in another MSAP run to check the details of the maneuver and the subsequent drift period.

8.6   QUICK-LOOK UTILITY PROGRAM

The functions of the Quick-Look Utility Program are to assist in the analysis of raw telemetry data which is input to the Attitude Determination Subsystem and to archive specified telemetry records on an

independent data set for use during definitive attitude data processing. The program can be operated in either a non-interactive or an interactive graphics mode, the latter utilizing an IBM 2260 Display Unit.

In support of the analysis of telemetry data, the Quick-Look Program prints out a hexadecimal and/or binary representation of all records contained within a specified time or record interval. In the interactive graphics mode, each record is analyzed for the availability of OA and SCADS data and the results of this analysis are displayed on an IBM 2260 Display Unit. In addition, in the interactive mode, a hexadecimal display of any record is available for viewing. The purpose of both the displays and the program output is to assist the user in determining the times and quality of the telemetry data used in attitude processing.

The archiving of telemetry records is accomplished by copying specific records from an input telemetry data set to an output data set that contains records with useful attitude data. In the interactive graphics mode, the user can archive records from a 2260 display and therefore be assured of the quality of the attitude data.

Input to the program consists of a telemetry data set either from disk or tape. The latter can contain multiple files. The control parameters are specified through the FORTRAN NAMELIST feature. Output consists of hard copy printout and, optionally, a tape or disk data set containing archived records.

8.7   TELEMETRY DATA SIMULATOR

The purpose of the Telemetry Data Simulator is to create a data set containing valid SSS telemetry data. The Simulator utilizes the Optical Aspect and Star data simulators to generate attitude data, which is

then converted into telemetry counts and inserted into simulated telemetry records. A complete description of a telemetry record is contained in Appendix D. In order to simulate all possible formats of telemetry data, the Simulator is divided into three subsystems: Primary, Backup, and SCADS, which coincide to primary mode transmission of Optical Aspect (OA) data, backup mode transmission of OA data, and primary mode SCADS data, respectively. In addition, a Data Modification Program exists that generates degraded telemetry data for use during system testing. The output of the program consists of a tape or disk data set of telemetry records in a format that can be input to the Attitude Determination Subsystem.

APPENDIX A

MISSION SIMULATION FOR A LAUNCH DATE OF JULY 15, 1971

ASSUMPTIONS

The simulation assumed a launch date of July 15, 1971, at 7:00 U.T. The following orbital elements were used initially:

$$a = 23058.23 \text{ (km)}$$
$$e = 0.713750$$
$$i = 2.92^{\circ}$$
$$M = 0.0^{\circ}$$
$$\omega = 289.96^{\circ}$$
$$\Omega = 165.30^{\circ}$$

These elements were updated at three-day intervals using orbital elements derived from a launch window program output. The MSAP atmospheric tables were updated periodically to reflect changes in the atmospheric density due to the slow regression of perigee away from the diurnal bulge. The decomposition of the satellite into flat plates, spheres, and cylinders was modified to include changes in the satellite configuration as of March 2, 1971. Detailed sketches of the decomposition are given in Appendix B.

The satellite was controlled to maintain the declination of the spin axis within $\pm 10^{\circ}$. Many of the maneuvers, however, were necessary to avoid violating the spin axis sun angle constraints of 30°-70° early in the mission when the shadow time was large and 20°-70° later when the shadow time ceased to be a problem. The strength of the control coil was taken as 9230.0 p-cm.

CONCLUSIONS

The control coil was adequate for maintaining the spin axis within the assumed mission constraints. Many of the techniques used in this simulation are applicable to a November launch if the launch occurs early enough so that the sun catches the spin axis at the winter solstice. However, if power requirements are revised so that the .30° constraint is changed to 35° or 40°, a different approach will have to be investigated.

SIMULATION DESCRIPTION

The path of the spin axis in inertial coordinates over the course of the simulation is presented in Figures A-1 to A-10 at the end of this appendix. The points represent the position of the spin axis at four-day intervals. The lines connecting points represent the motion due to magnetic control torques. The number on the line is the perigee pass during which the torque was accomplished. In many cases, the points extend beyond a torque. These points are plotted to show the resulting drift if the torque had not been done. Numbers near points represent the perigee associated with that point. The small x's represent the position of the perigee velocity vector corresponding to that perigee pass. Note the change of scale from Figure A-6 to A-7 and from A-7 to A-8. The altitude, date, and sun position corresponding to selected perigee passes are given in tables in the figures. The approximate time span for the figure is given at the bottom.

The first control was necessary to avoid violating the $+10^{\circ}$ constraint on the declination. (See Figure A-1.) Due to the low perigee altitude in this early phase, the aerodynamic torque caused a strong positive declination drift as the spin axis fell behind the perigee velocity vector in right ascension. The declination would have reached about 10°

in 28 days from launch. Therefore, it was necessary to get well ahead of the perigee velocity vector on the first maneuver. Then a large negative declination drift could be expected to assist in a recovery from the $+7^{\circ}$ declination. (See Figure A-2.)

The next phase consisted of five torques to stay ahead of the sun by at least 30° and to maintain the spin axis at a high declination as the sun approached the winter solstice and a declination of -23°. (See Figures A-2 to A-4.) At that time the spin axis was allowed to drift for a period of 56 days while the sun passed underneath it. (See Figure A-4, pass 363.) The sun angle reached a minimum of 29°. Drift due to aerodynamic torque was not a problem due to the high altitude of perigee at this time. However, the spin axis was kept in the vicinity of the perigee velocity vector to minimize the drift. Note that the declination drift ceases when the spin axis is at the same right ascension as the perigee velocity vector. (See, e.g., Figures A-2 and A-3.)

The phase following the initial encounter consisted of six torques which were necessary to catch up with the sun. (See Figures A-4 to A-7.) Due to the decreasing altitude of perigee during this time, it was necessary to keep the spin axis close to the perigee velocity vector to minimize drift due to aerodynamic torque. For about three months, it was possible to track both the sun and the perigee velocity vector.

About April 18, the inversion phase was begun because it was no longer possible to simultaneously track the perigee velocity vector and maintain the 70° sun angle constraint. (See Figure A-7.) The inversion was accomplished in several steps. The first was to move the spin axis to a right ascension of 90° relative to the perigee velocity vector. At this angle of attack, the aerodynamic torque nearly vanishes. Thus, it

should be possible to keep the spin axis there until the sun reaches a right ascension of 110° relative to the perigee velocity vector. The spin axis could then be precessed to 180° relative to the perigee velocity vector and a sun angle of 70°. The spin axis would track the negative perigee velocity vector as well as the positive.

A direct move to 90° relative right ascension, however, encounters a violation of the 20° sun constraint on pass 698. (See Figure A-8. Note also the position of the sun on pass 699.) To avoid this problem, the maneuver was halted after six torques when the right ascension of the spin axis was about 50° ahead of the perigee velocity vector. At this angle of attack, aerodynamic torque causes a rapid drift to a negative declination. When the declination reached -9° on pass 716, the move to 90° relative right ascension was completed with five torques, while easily fulfilling the 20° sun constraint.

Two corrective torques were necessary to keep the spin axis at this altitude for about 46 days as the sun passed overhead approaching the summer solstice. The perigee velocity vector is advancing in right ascension at $\frac{1}{2}$° per day. Thus the spin axis had to be maneuvered to maintain 90° relative right ascension. By perigee pass 877, the sun had reached 115° right ascension relative to the perigee velocity vector. Therefore an attempt was made to precess the spin axis to the negative perigee velocity vector by torquing on every pass. (See Figures A-9 and A-10, bottom curve.) A violation of the -10° declination constraint was encountered on pass 885. (See Figure A-10, bottom curve.) This was due to the fact that at this right ascension, most of the magnetic torques produced negative declination motion in addition to that caused by aerodynamic torque.

In order to reduce this problem, a torque was done on pass 840 to stay at 90° relative to the perigee velocity vector. In this way, the declination of the spin axis was increased to about 0° by pass 875. (See Figure A-9.) The maneuver to 180° relative to the perigee velocity vector was begun on pass 875. Only those passes during which a magnetic torque produced little or no negative declination motion were selected for torquing.

This technique worked until about pass 892, where the aerodynamic torque became so strong that it was impractical to let the spin axis drift on a pass where a magnetic torque would have caused a strong negative declination motion. (See Figure A-10.) Therefore, the sense of the coil was reversed. The resulting torque produced a positive declination drift. (See Figure A-10, pass 892, top curve.) This type of maneuver had to be repeated several times before the spin axis reached 186° right ascension relative to the perigee velocity vector. (See Figure A-10, pass 911.) At this point the spin axis was allowed to drift with no foreseeable problems until the sun eventually caught up to the near 180° right ascension relative to the perigee velocity vector.
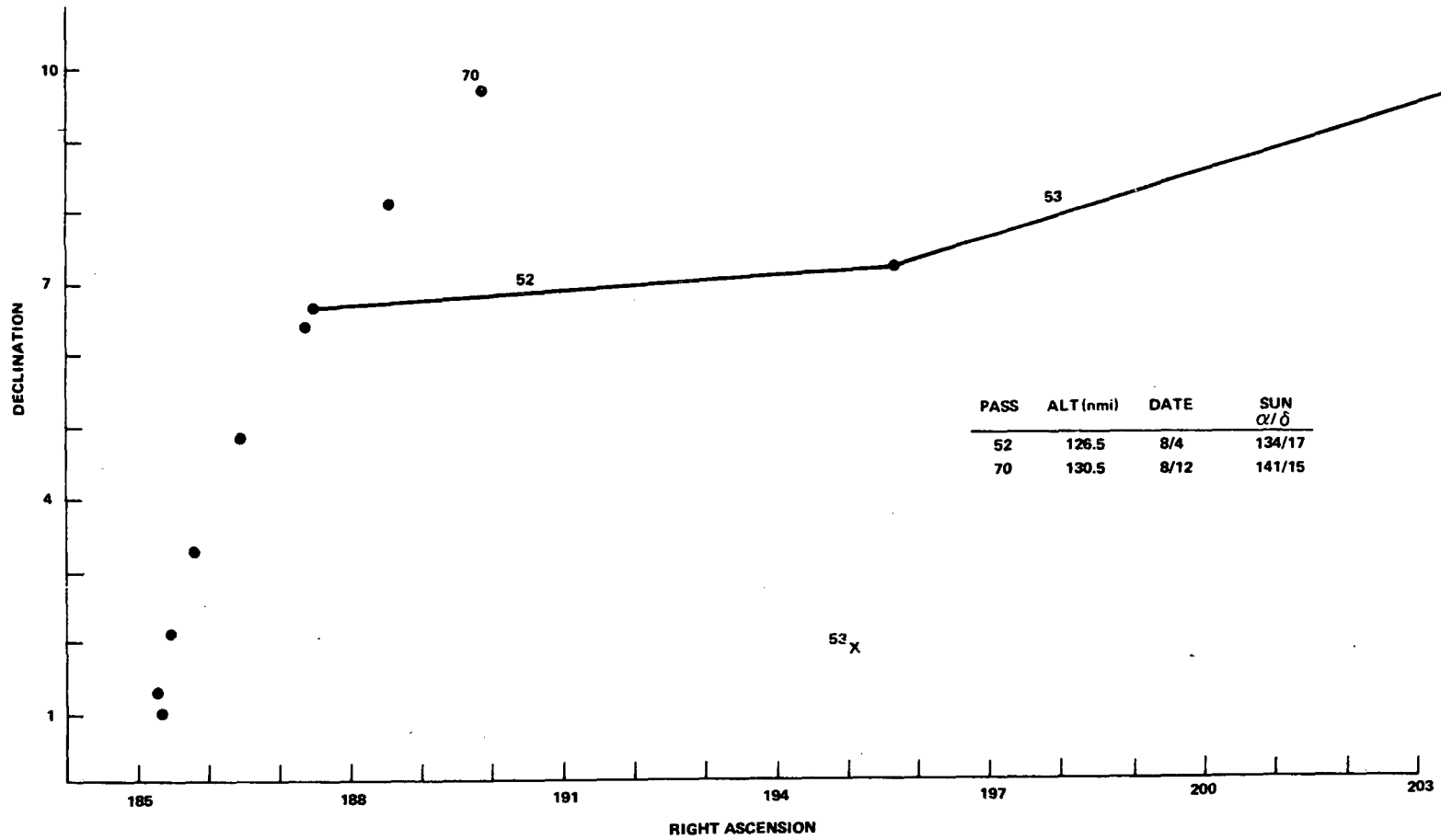
Figure A-1.   July 15 to August 12.   4 days/point

PASS	ALT(nmi)	DATE	SUN α/δ
113	140	8/29	157/9.5
123	141.5	9/2	161/8
168	151.5	9/20	177/1.2
193	156	9/30	186/-2.7
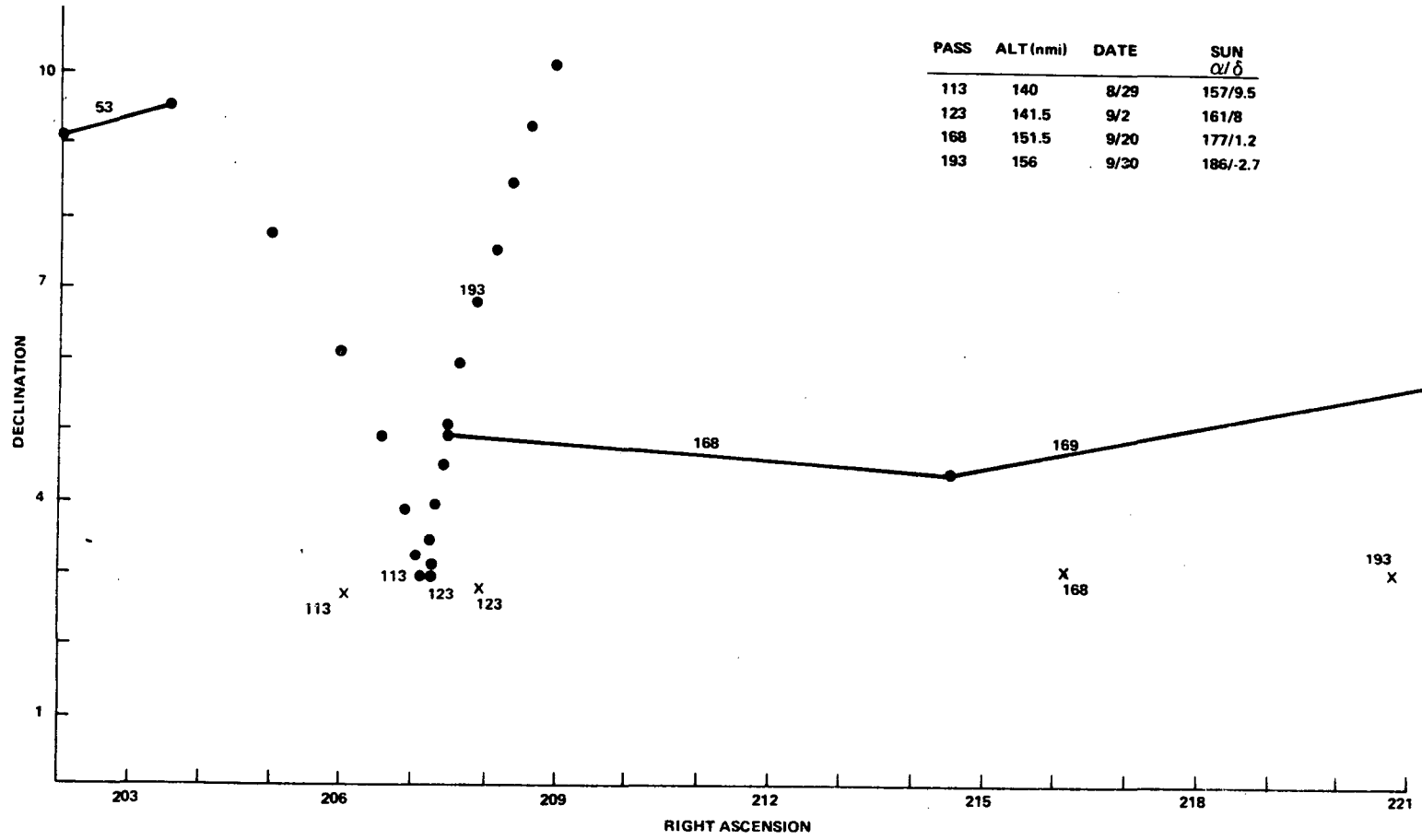
Figure A-2. August 4 to October 20. 4 days/point

PASS	ALT (nmi)	DATE	SUN α/δ
169	151.5	9/21	177.6/1
209	161	10/7	192/-5
221	162.5	10/11	196.6/-7
251	168	10/24	208/-11.5
291	174	11/9	224/-17
309	175	11/16	231/-18.6

(TO AVOID γ<30°)

DECLINATION

RIGHT ASCENSION
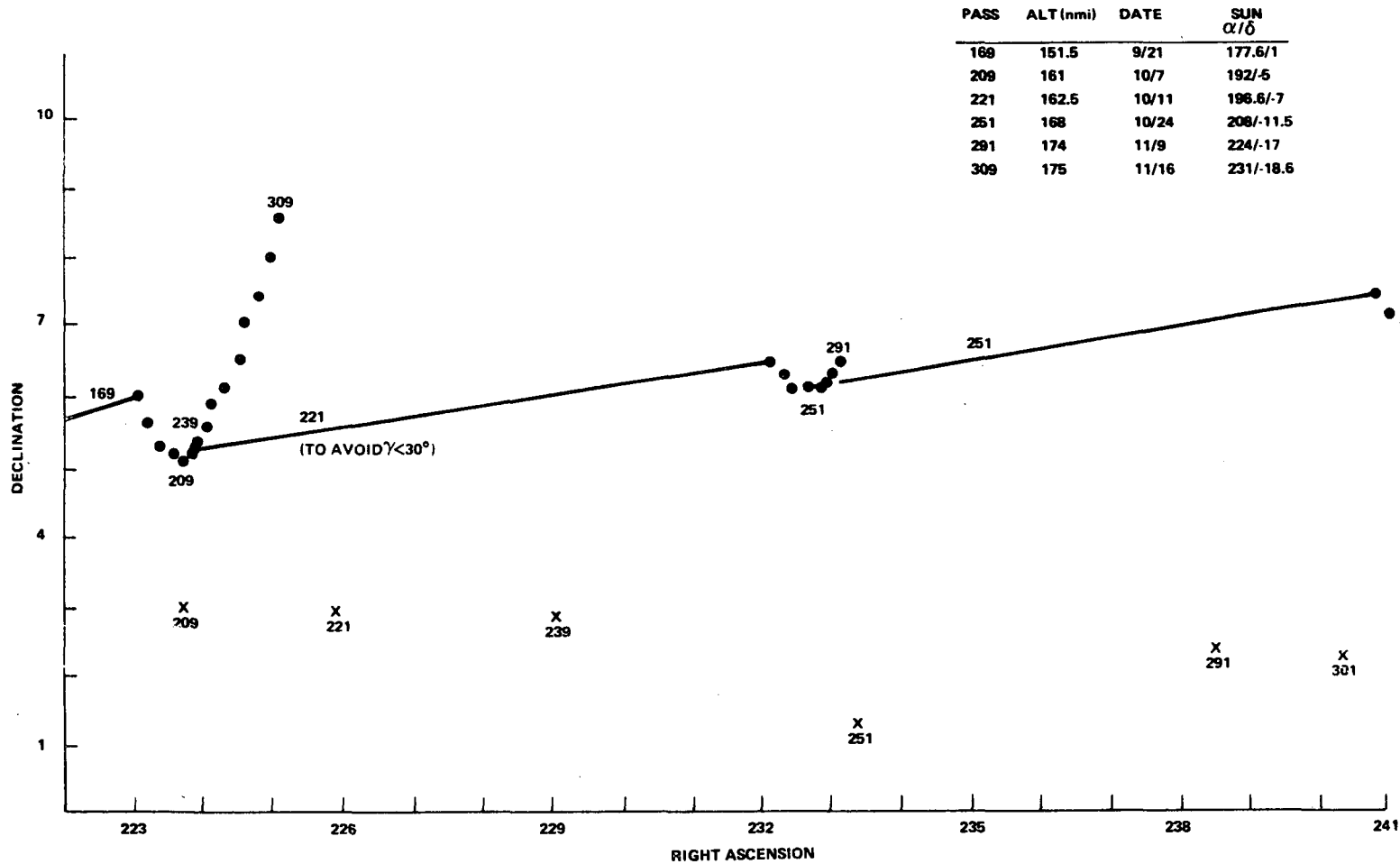
Figure A-3.   September 20 to November 24.   4 days/point
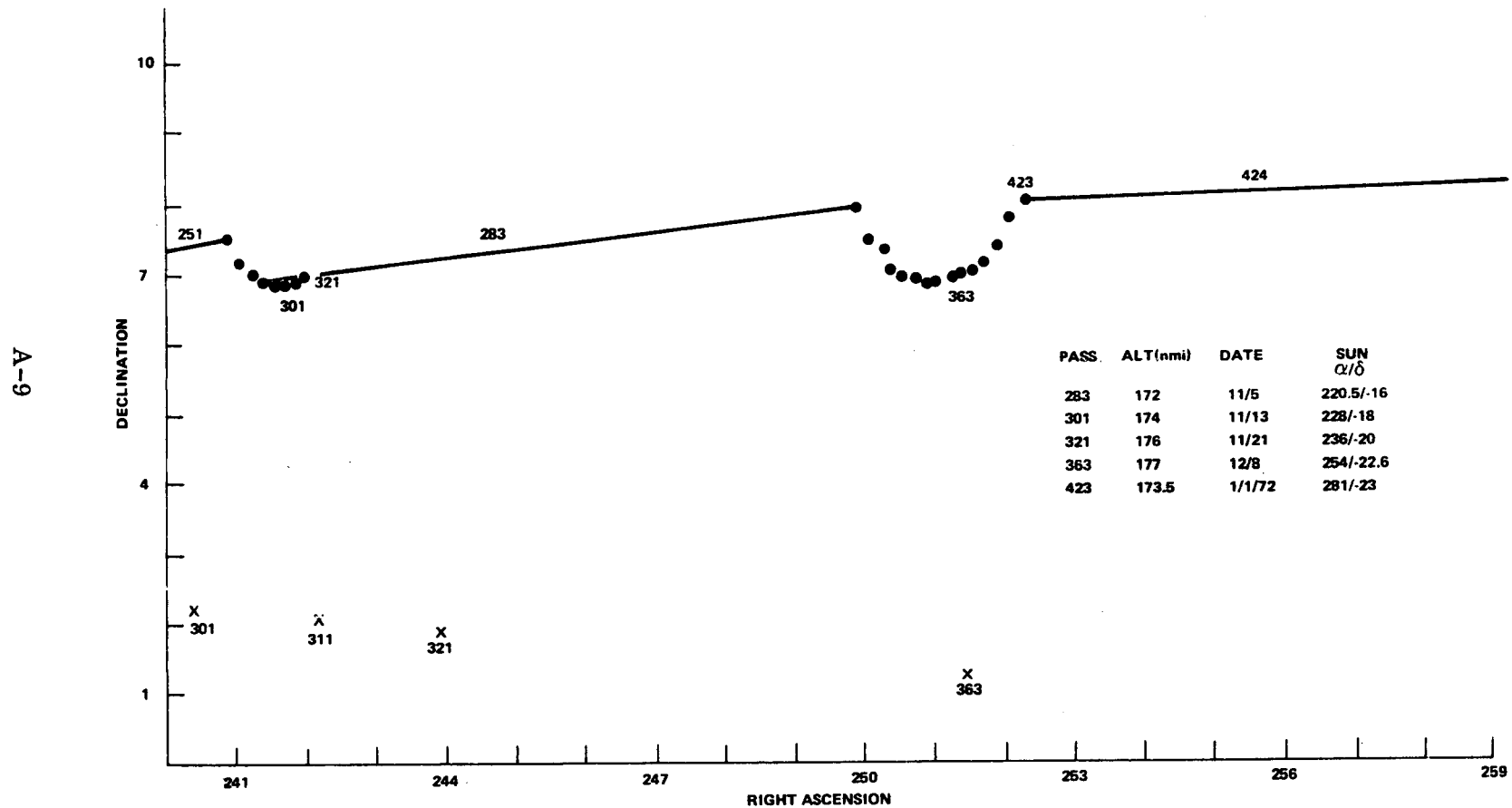
Figure A-4. October 24 to January 1. 4 days/point

PASS	ALT(nmi)	DATE	SUN α/δ
425	173	1/2/72	282/-23
445	171	1/10	291/-22
475	166	1/22	304/-20
497	162.5	1/31	313/-18
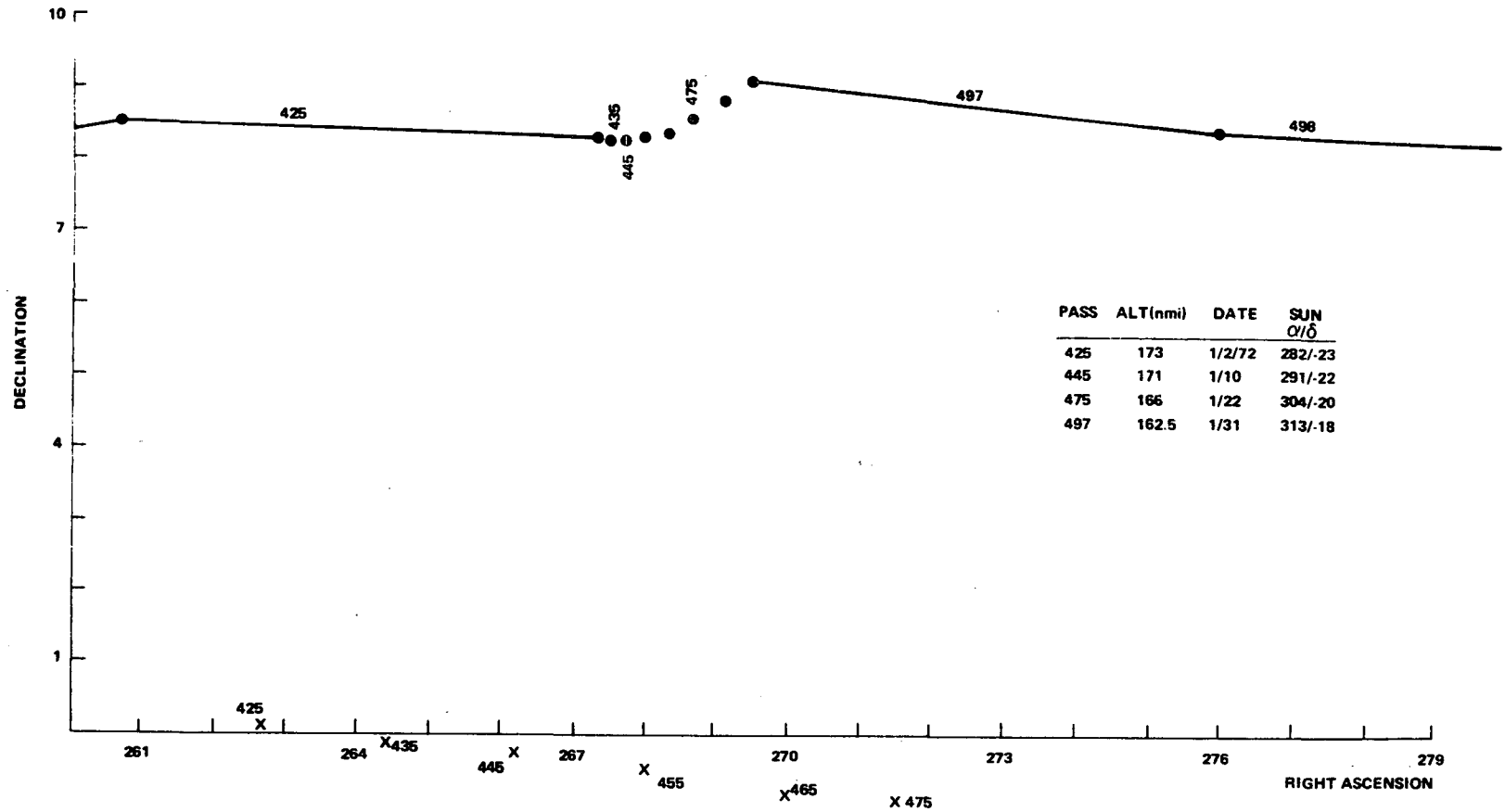
Figure A-5. January 1 to January 31. 4 days/point
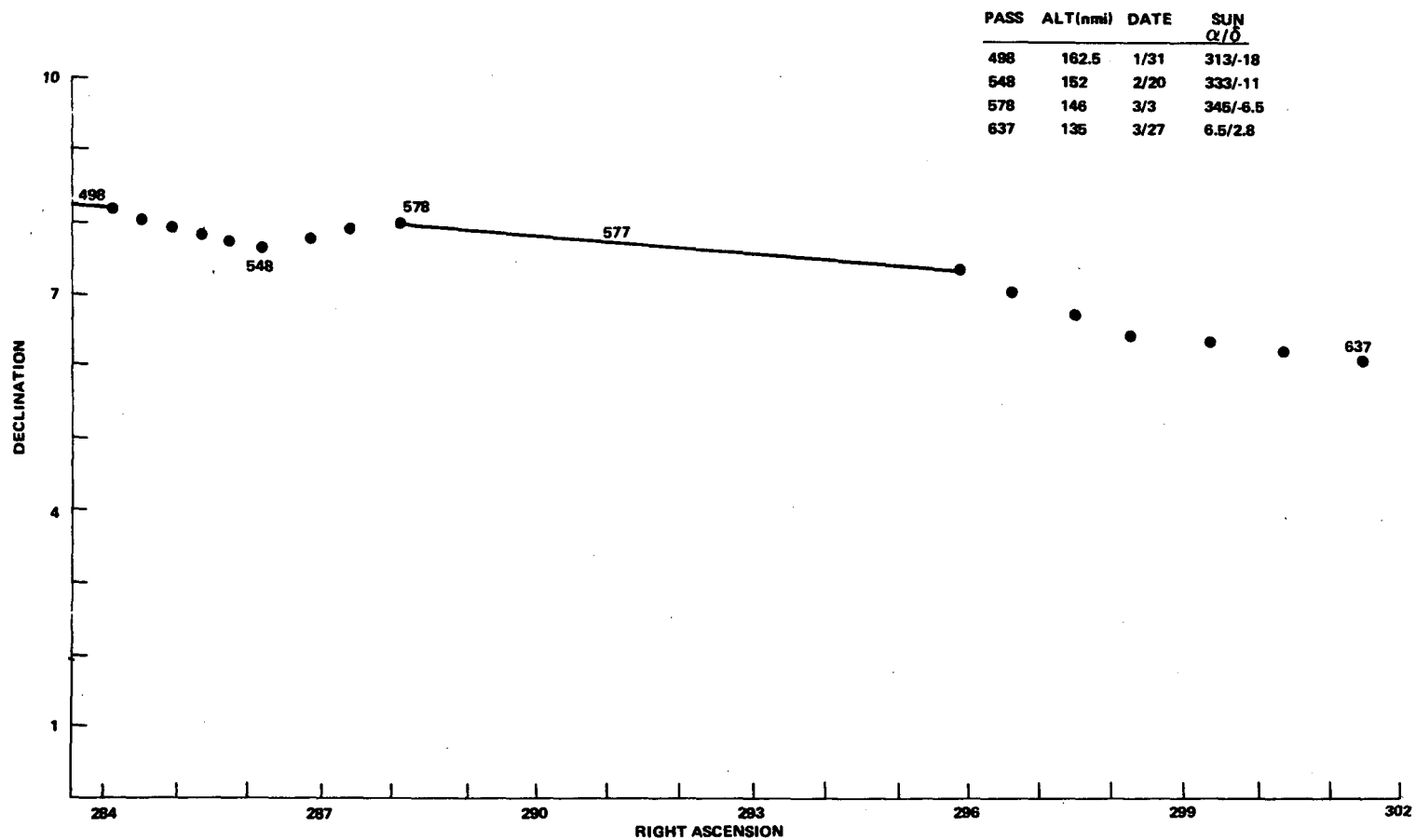
PASS	ALT(nmi)	DATE	SUN α/δ
498	162.5	1/31	313/-18
548	152	2/20	333/-11
578	146	3/3	345/-6.5
637	135	3/27	6.5/2.8

Figure A-6.   January 31 to March 31.   4 days/point

PASS	ALT(nmi)	DATE	SUN α/δ
647	133.5	3/31	10/4.4
691	127	4/18	26.5/11
717	124	4/28	36/14.5
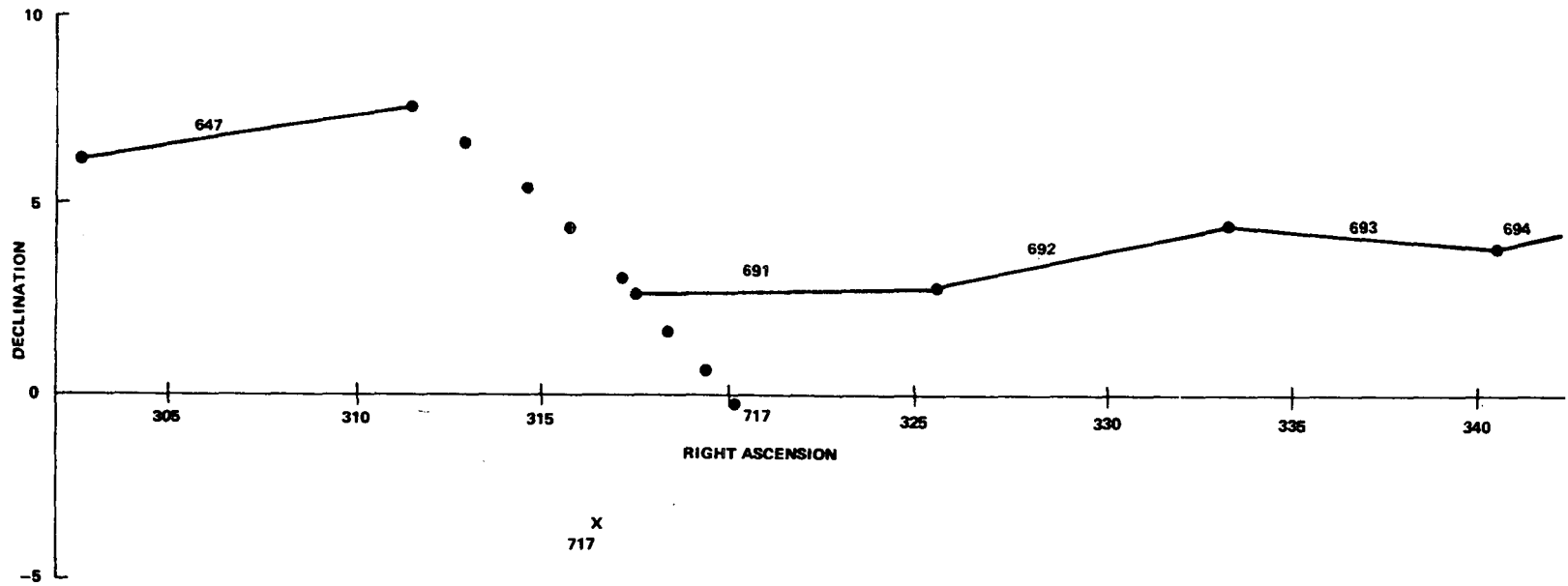
Figure A-7.   March 31 to April 28.   4 days/point

PASS	ALT(nmi)	DATE	SUN	PERIGEE VELOCITY (α/δ)
694	126	4/19	28/11.4	312/-3.4
716	124	4/28	33/14	316/-3.3
722	124	4/30	38/16	317/-3.25
773	122	5/21	58.5/20	327/-2.8
803	122	6/2	71/22	332/-2.4
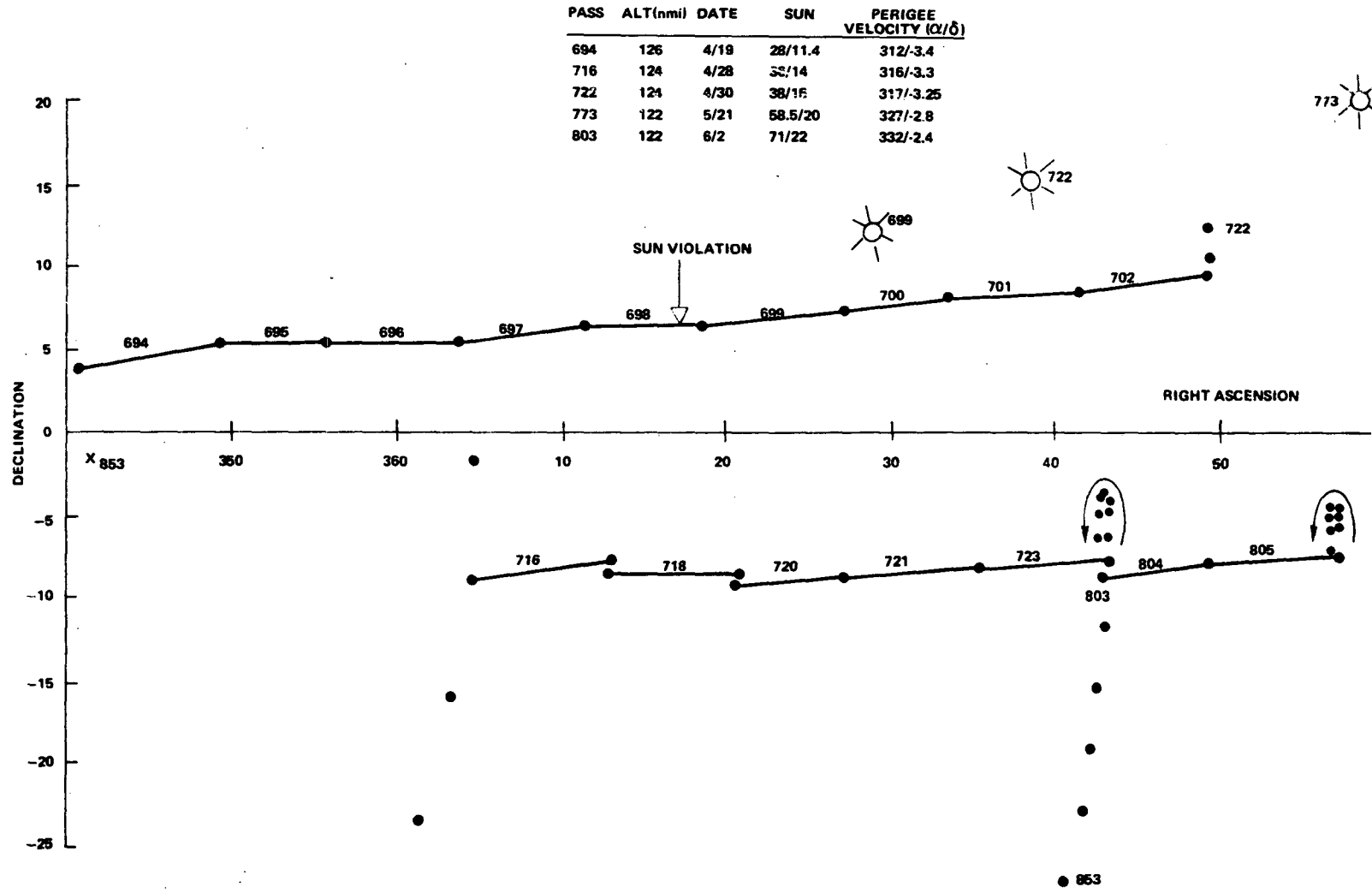
Figure A-8. April 19 to July 1. 4 days/point
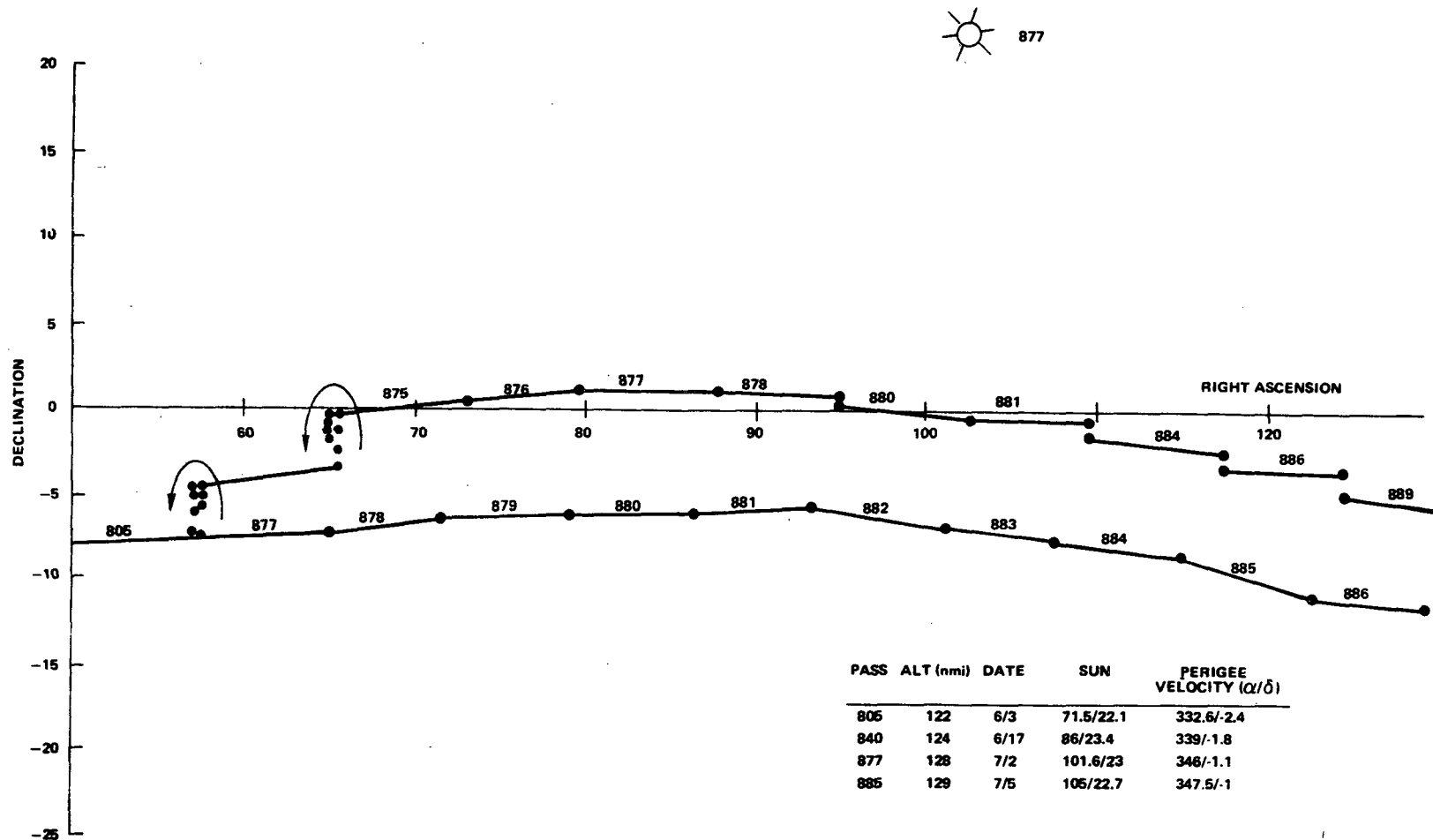
Figure A-9.   June 3 to July 7.   4 days/point

PASS	ALT(nmi)	DATE	SUN	PERIGEE VELOCITY (α/δ)
886	129.5	7/6	105/22.7	347.6/-1
893	129.5	7/8	108/22	349/-1
911	132	7/18	116/21	352.5/-0.3
971	132	8/9	139/16	3.6/1
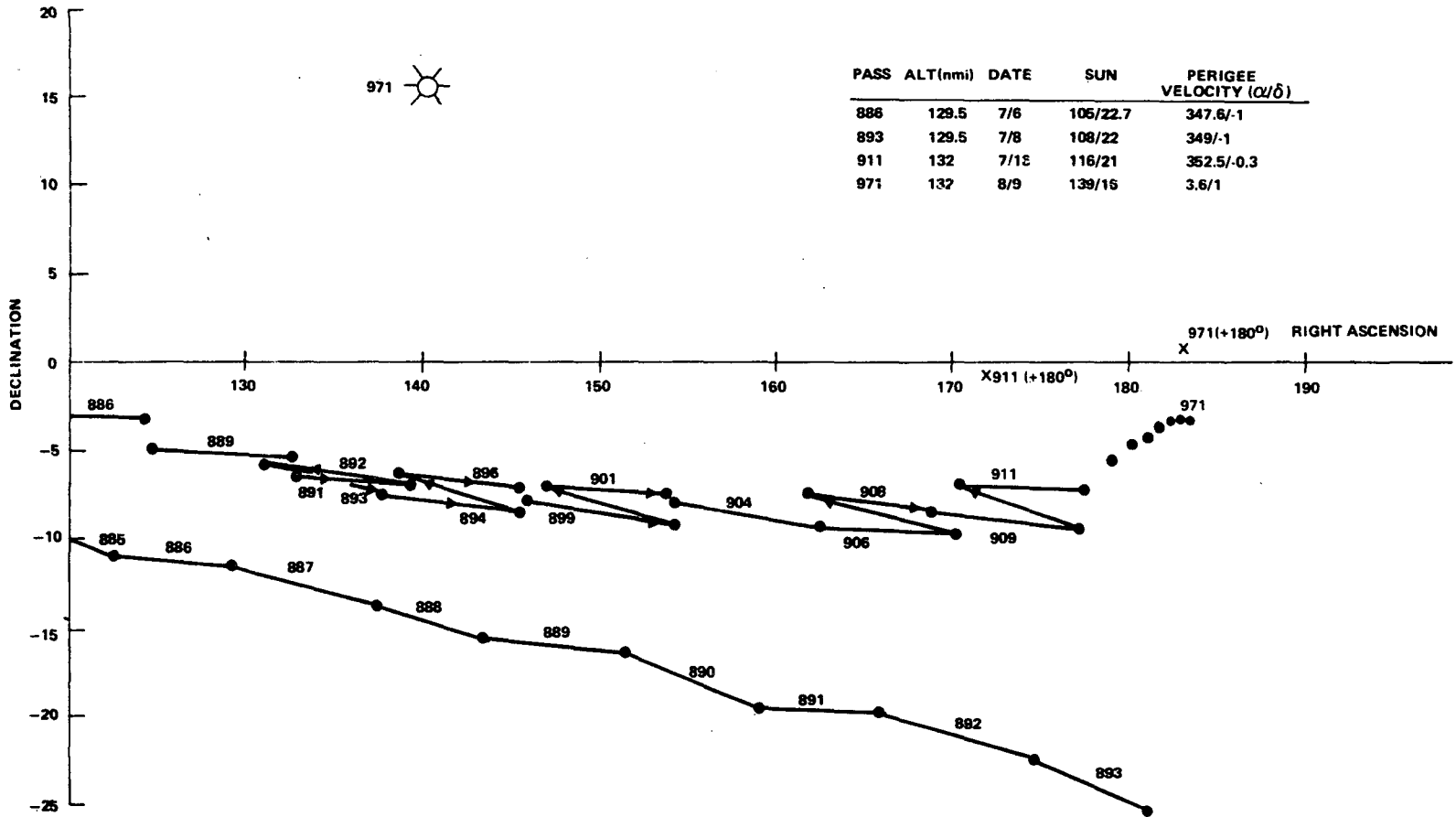
Figure A-10.   July 6 to August 13.   4 days/point

APPENDIX B

SPACECRAFT DECOMPOSITION

Figures B-1, B-2, and B-3 indicate the dimensions used in breaking the satellite down into plates, spheres, and cylinders. Three views are given: (1) as viewed from the y axis, (2) as viewed from the x axis, and (3) as viewed from the top. The dimensions are given in centimeters. The drawings are nearly to scale. The approximate scale is given on each sketch and is different for all three. The small numbers in circles are the numbers assigned to the particular components. Note the revision dated 3/2/71, which reflects a revision in the distance of the center of mass from the separation plane.

VIEW FROM Y AXIS
SCALE ~ |___20 cm___|
REV: 3/2/71
 ADD 1.8 cm TO ALL Z MEAS.
 CENTER OF MASS NOW 36.3 cm

9.84

73.22

156.79

72.2

35.63

33.2

20.4

43.5°

21.58

12.8

73.7

18.85

11.9

CM

49.0

50.75

1.9

254.0

140.8

38.1

1.9 CM

SEP. PLANE

65.9
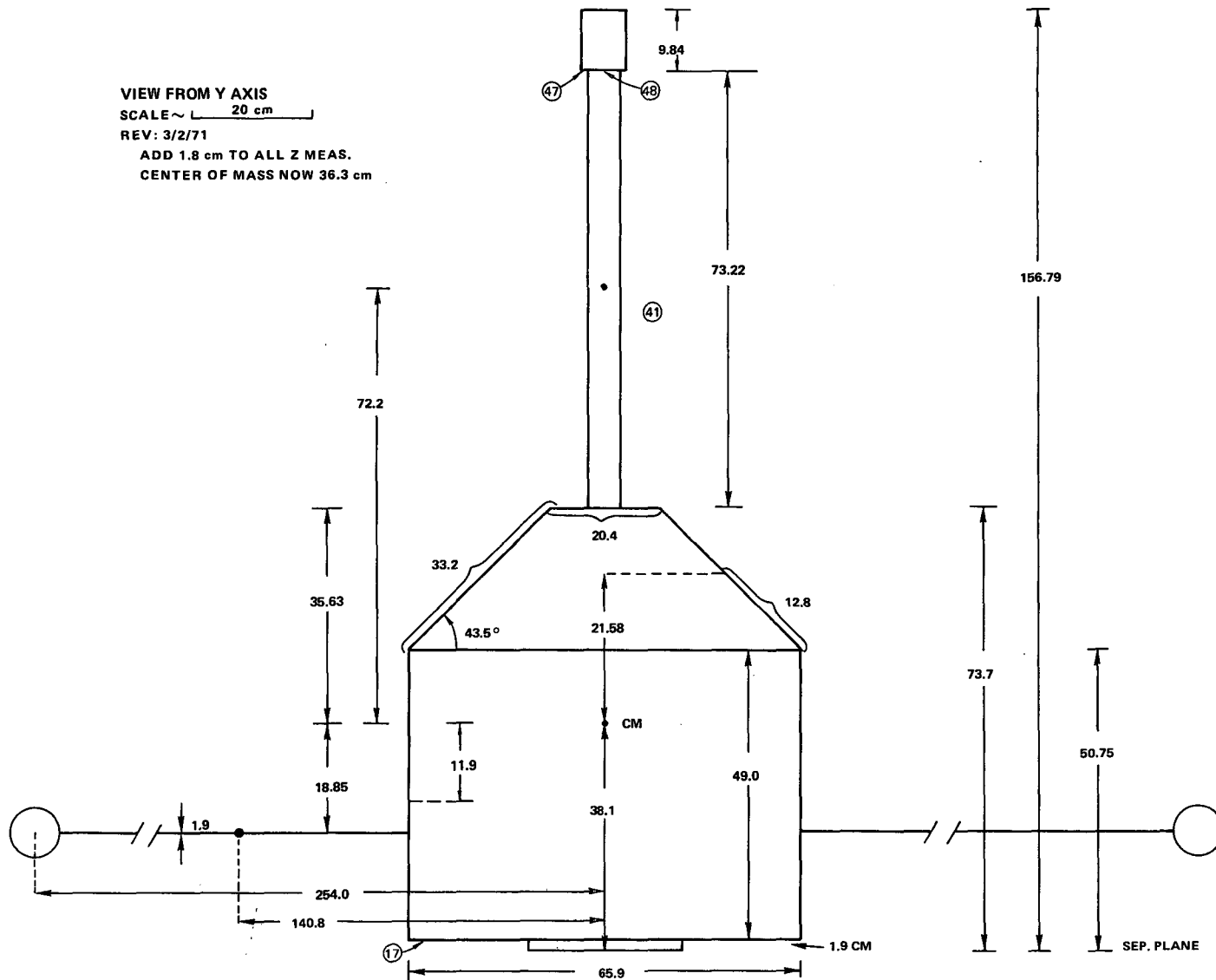
Figure B-1. View from Y Axis

VIEW FROM X AXIS
SCALE ~ |——28 cm——|
REV: 3/2/71
   ADD 1.8 cm TO ALL Z MEAS.
   CENTER OF MASS NOW 36.3 cm

B-3
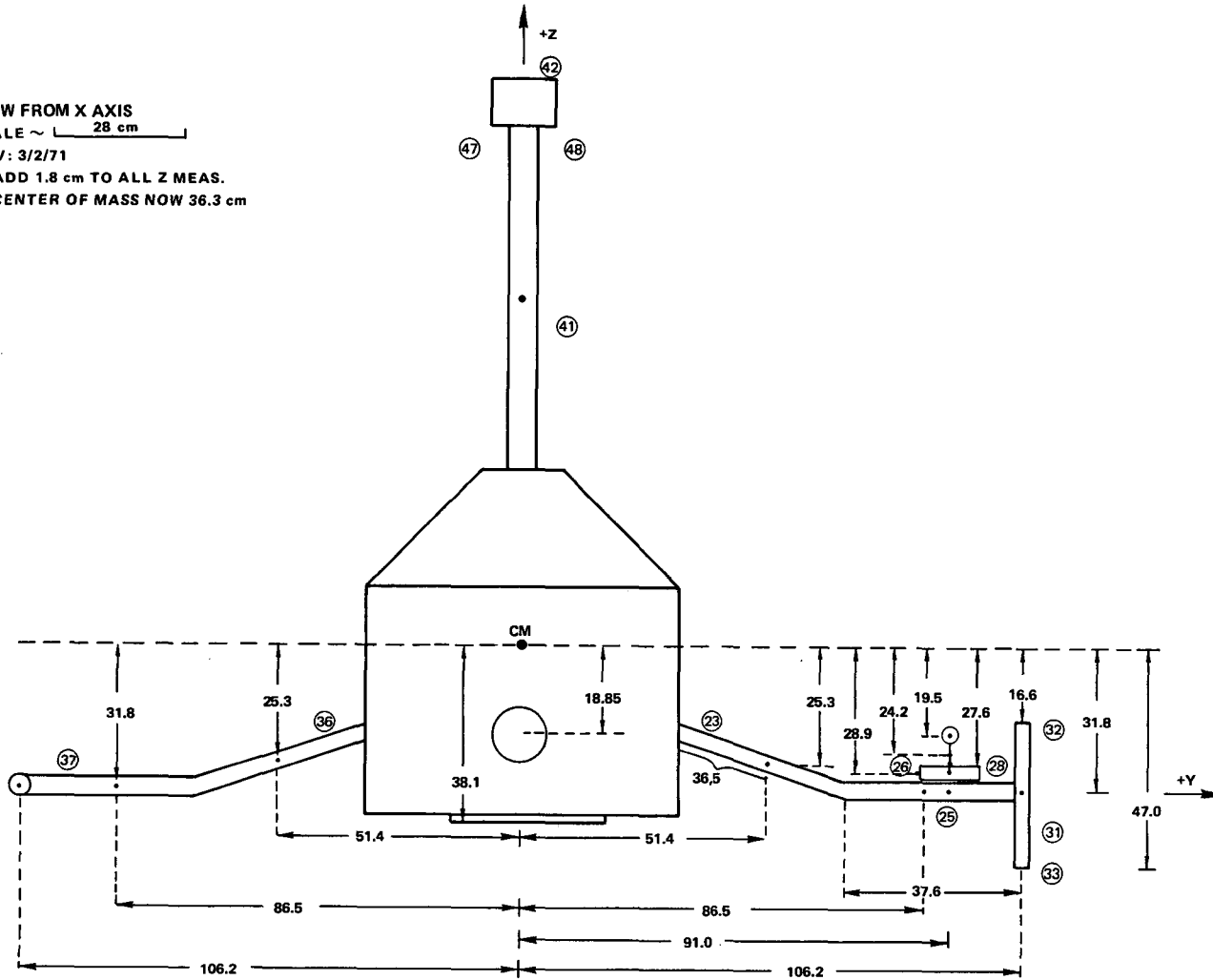
Figure B-2.   View from X Axis
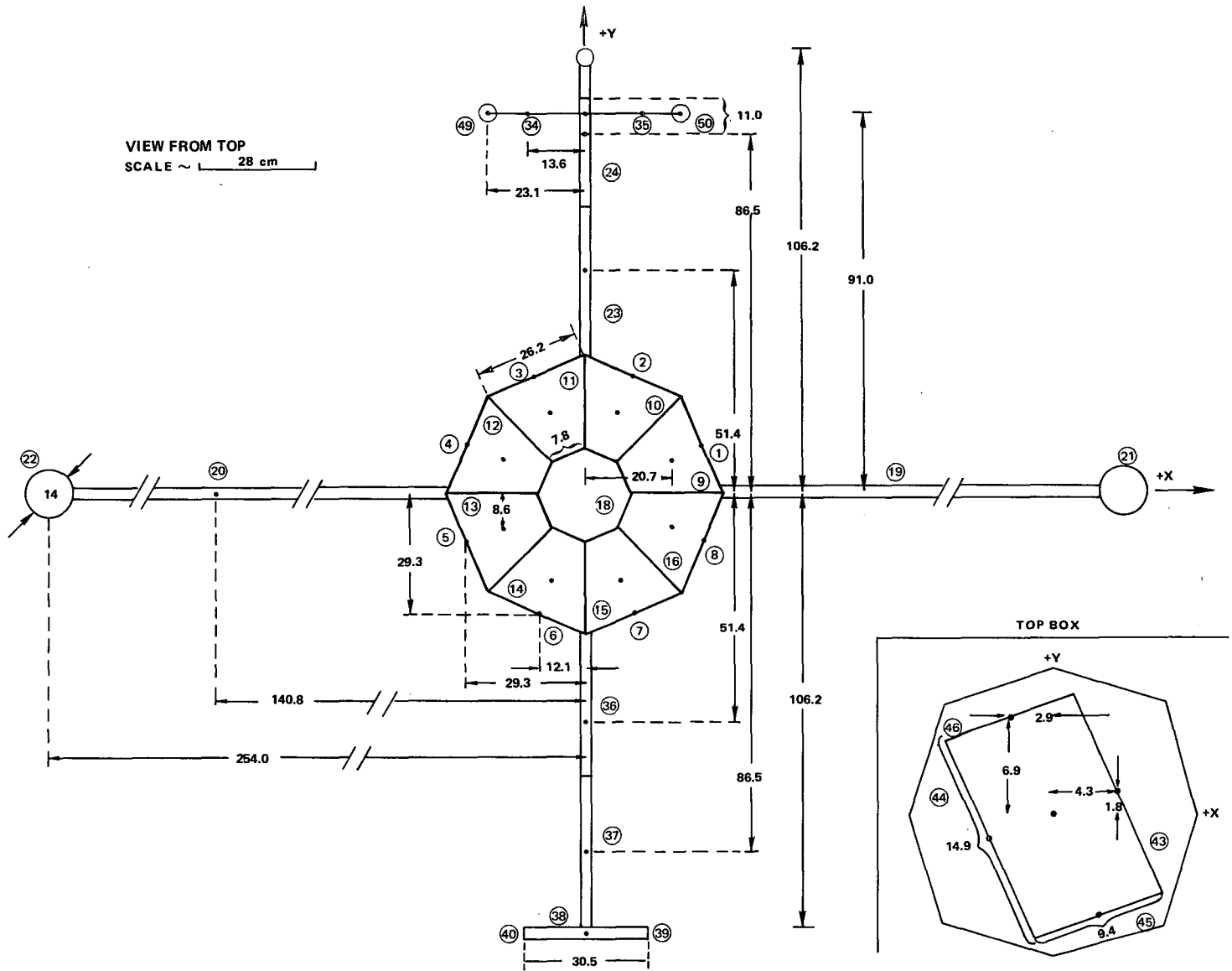
Figure B-3. View from Top

APPENDIX C

PLOTTED RESULTS OF THE SENSOR MOUNTING ANGLE STUDY

Figures C-1 through C-8 show minutes of useful data plotted versus the right ascension of the spin axis. Each graph includes results for a single fixed orbit, that is, argument of perigee, and each curve includes data for a single declination of the spin axis. The following points are helpful in interpreting the results. For the simulation time of July 1, 1971, the right ascension of the sun is approximately 100 degrees. Since the right ascension of the ascending node is zero, the argument of perigee is approximately the right ascension of perigee. Therefore, an argument of perigee of 100 degrees corresponds to perigee at noon, and an argument of perigee of 280 degrees corresponds to perigee at midnight. If perigee occurs at noon, data is obtained only during a short interval, but the data is of high quality. If perigee occurs at midnight, data is obtained over a longer interval, but most of the data includes terminator crossings.
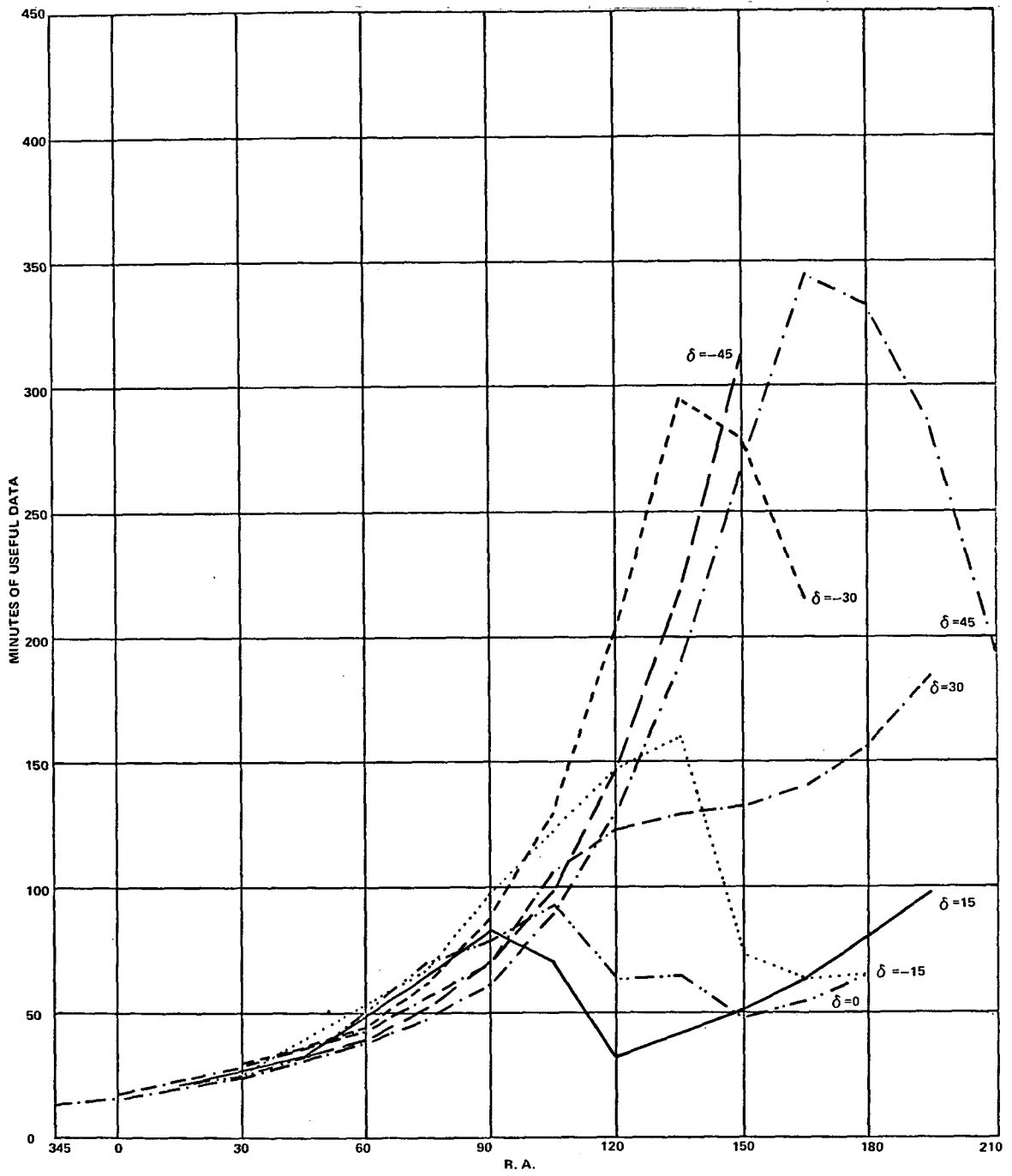
Figure C-1. Argument of Perigee = 0°
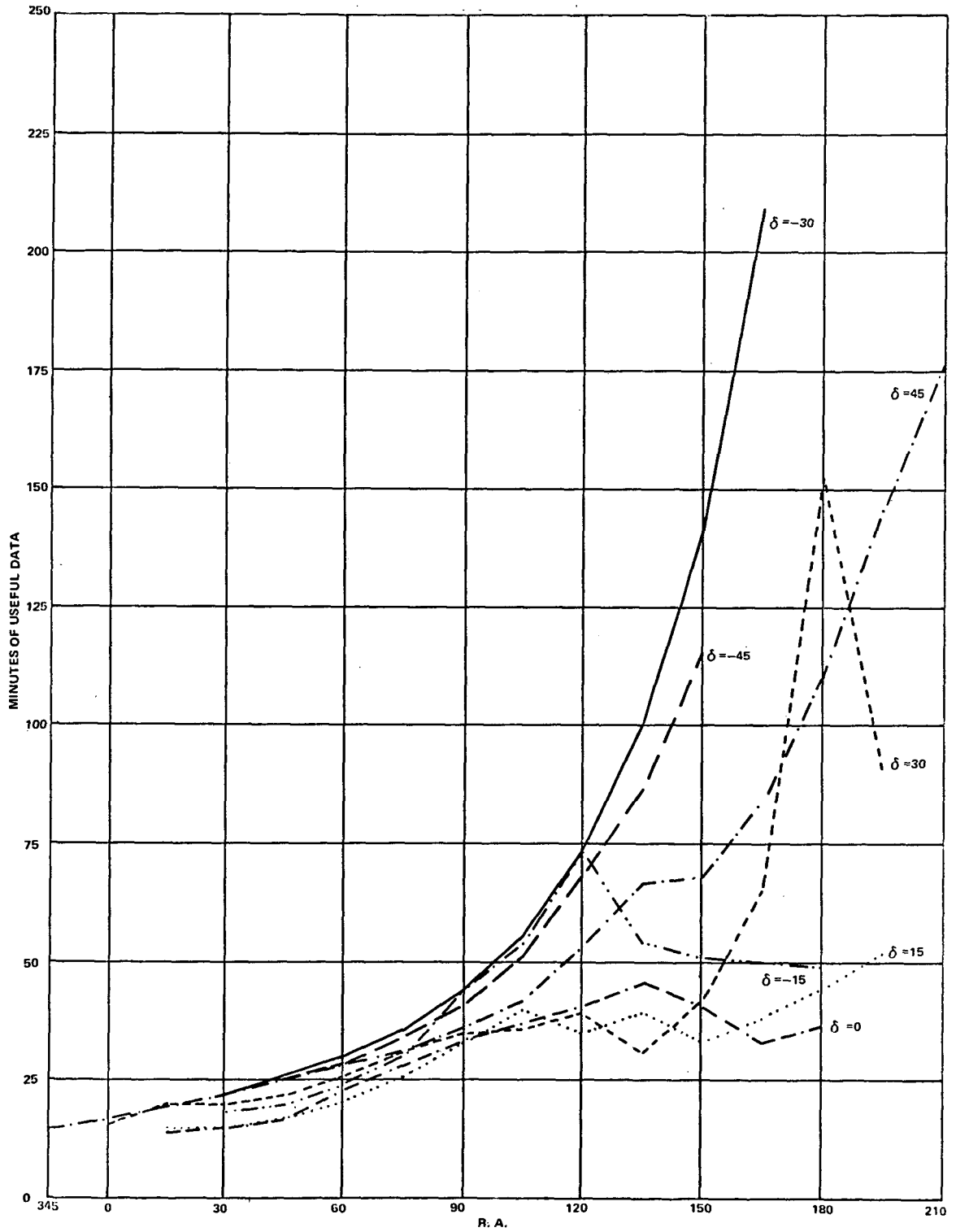
Figure C-2. Argument of Perigee = 45°
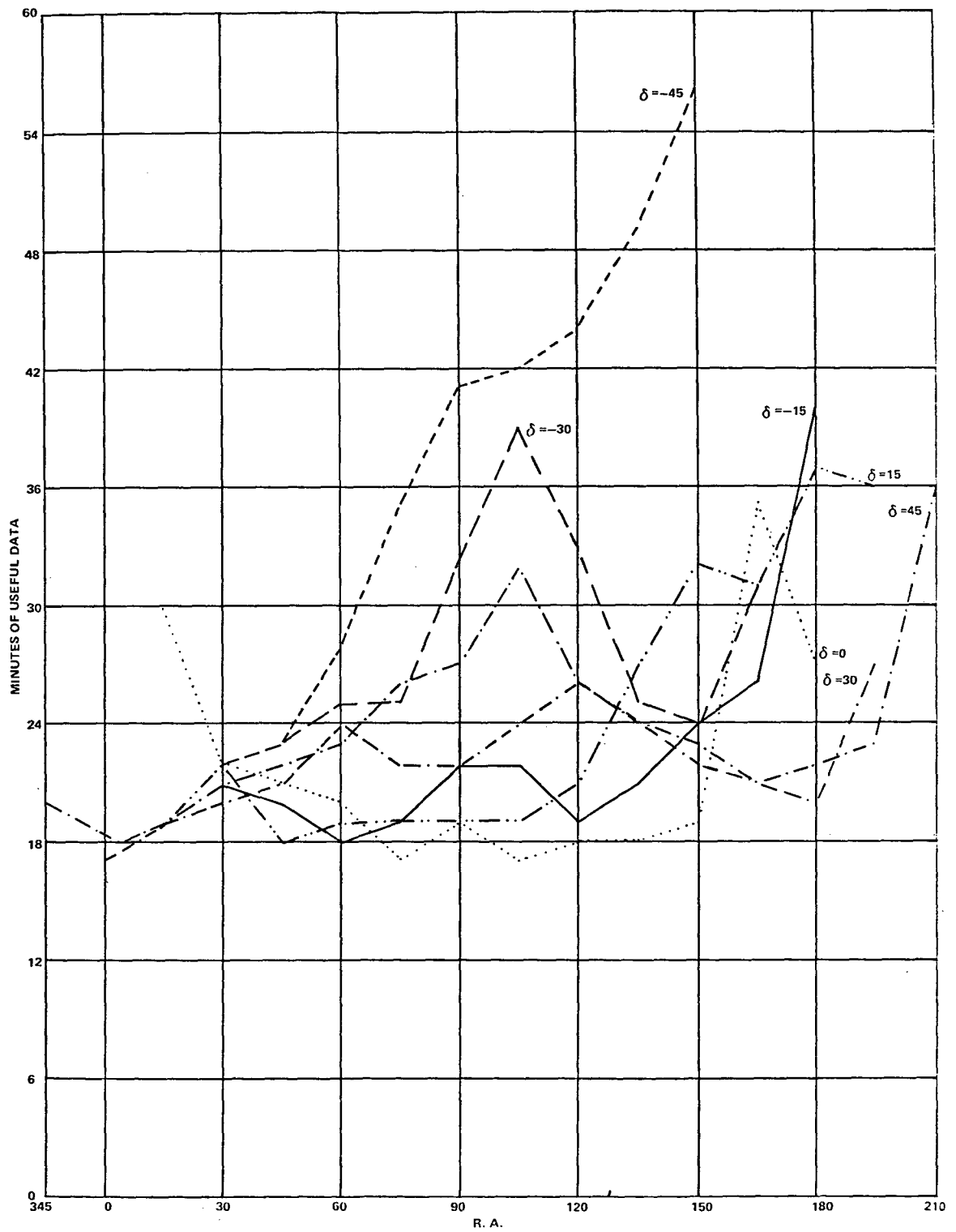
Figure C-3. Argument of Perigee = 90°
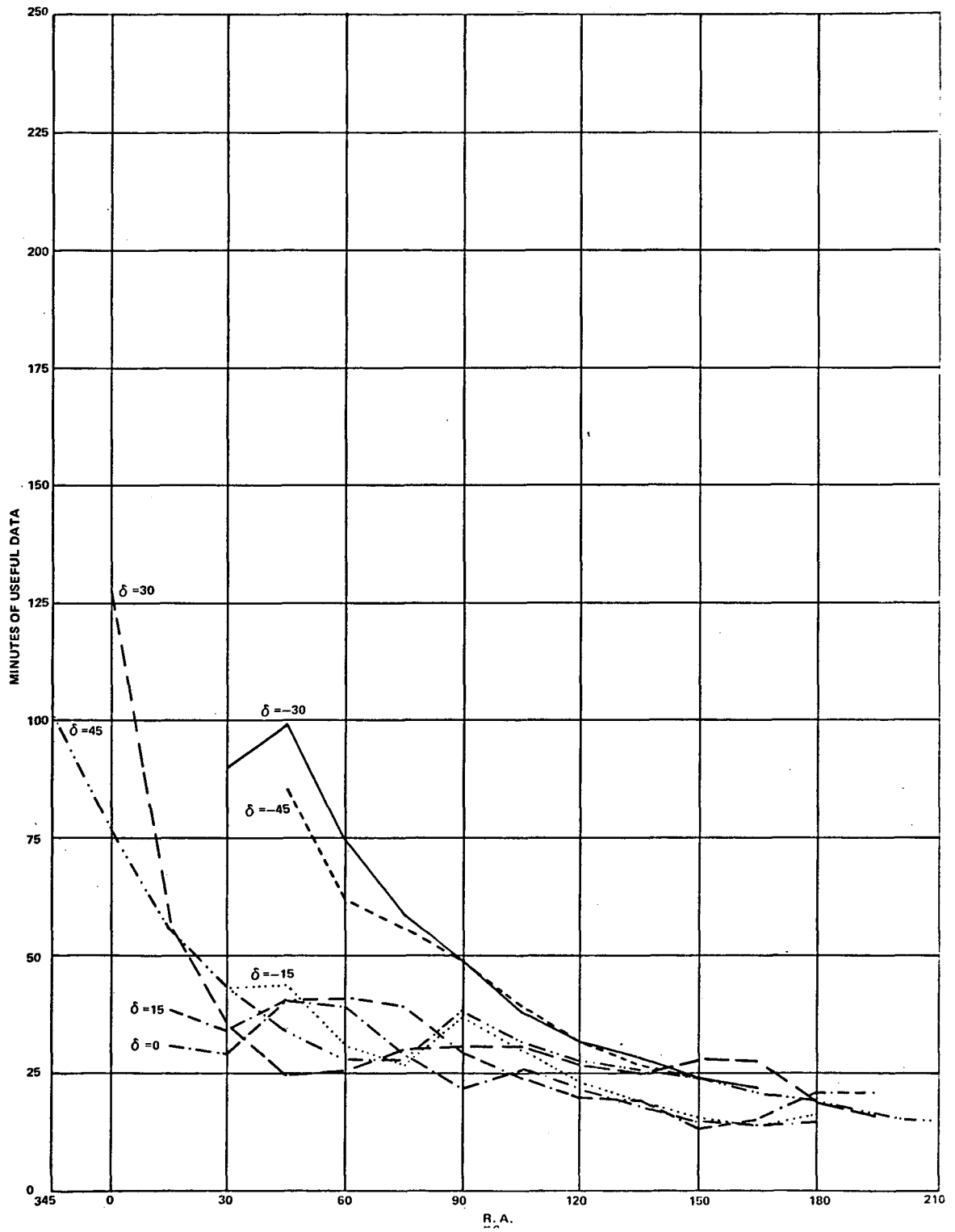
Figure C-4. Argument of Perigee = 135°
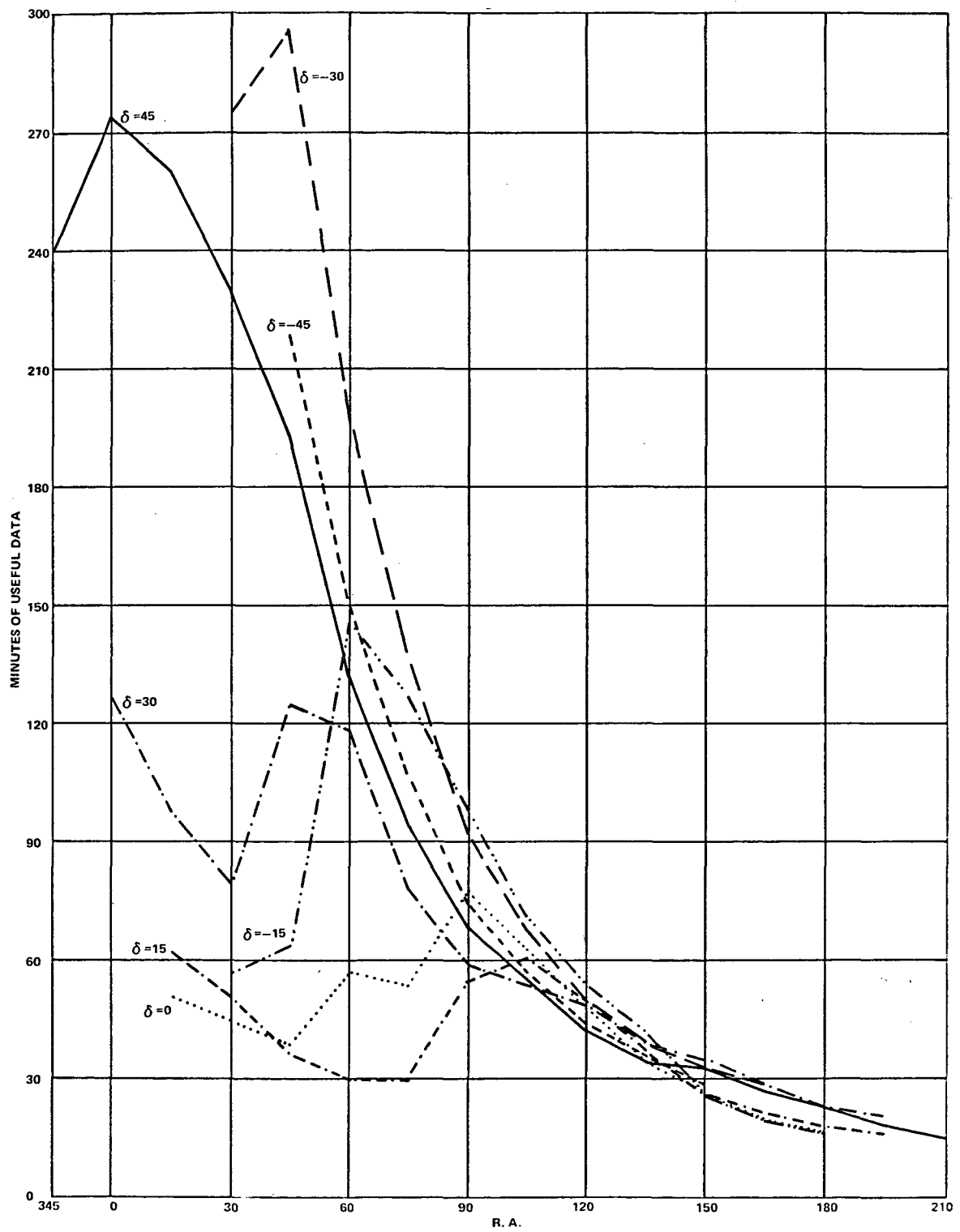
Figure C-5. Argument of Perigee = 180°
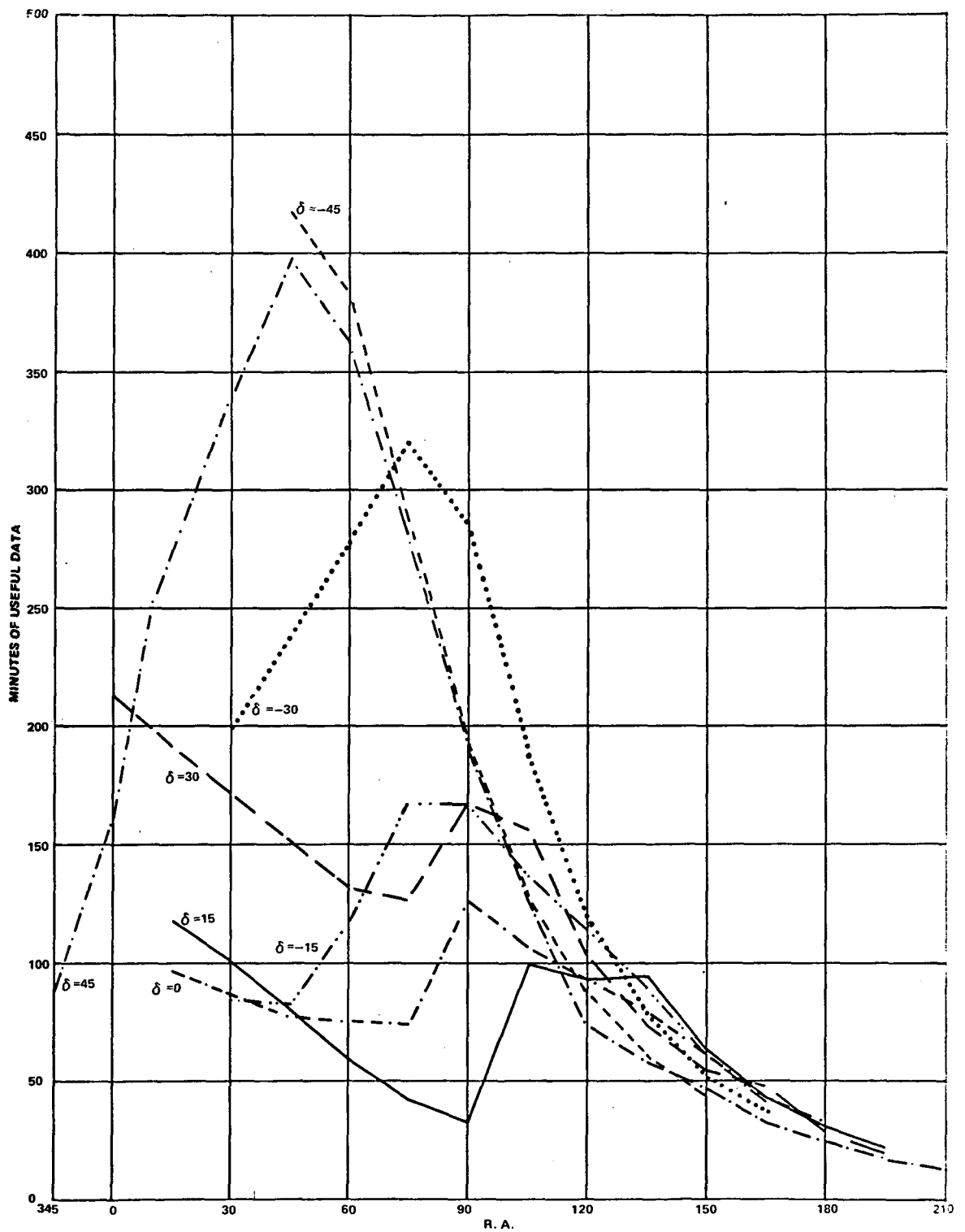
Figure C-6. Argument of Perigee = 225°

C-7
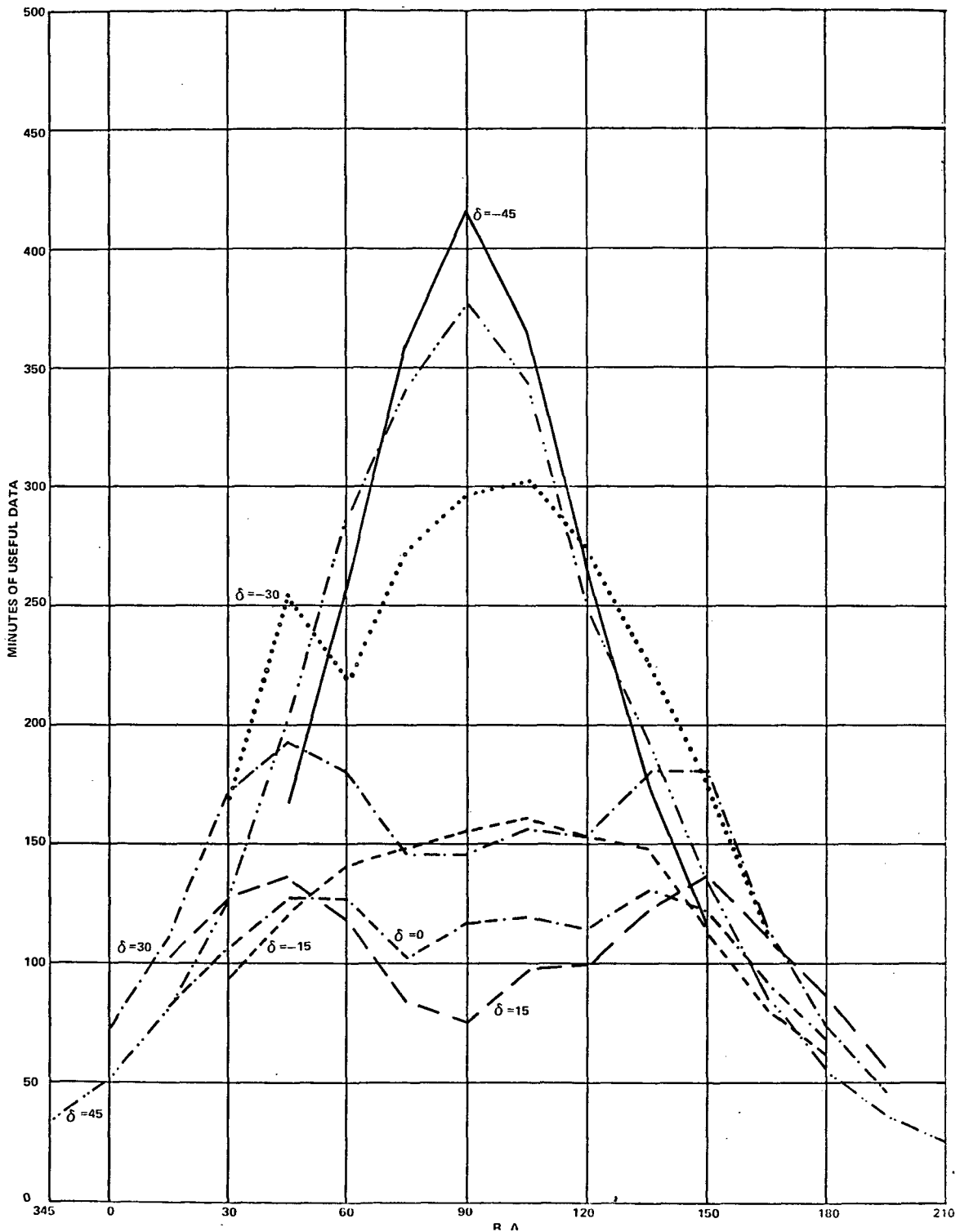
Figure C-7. Argument of Perigee = 270°
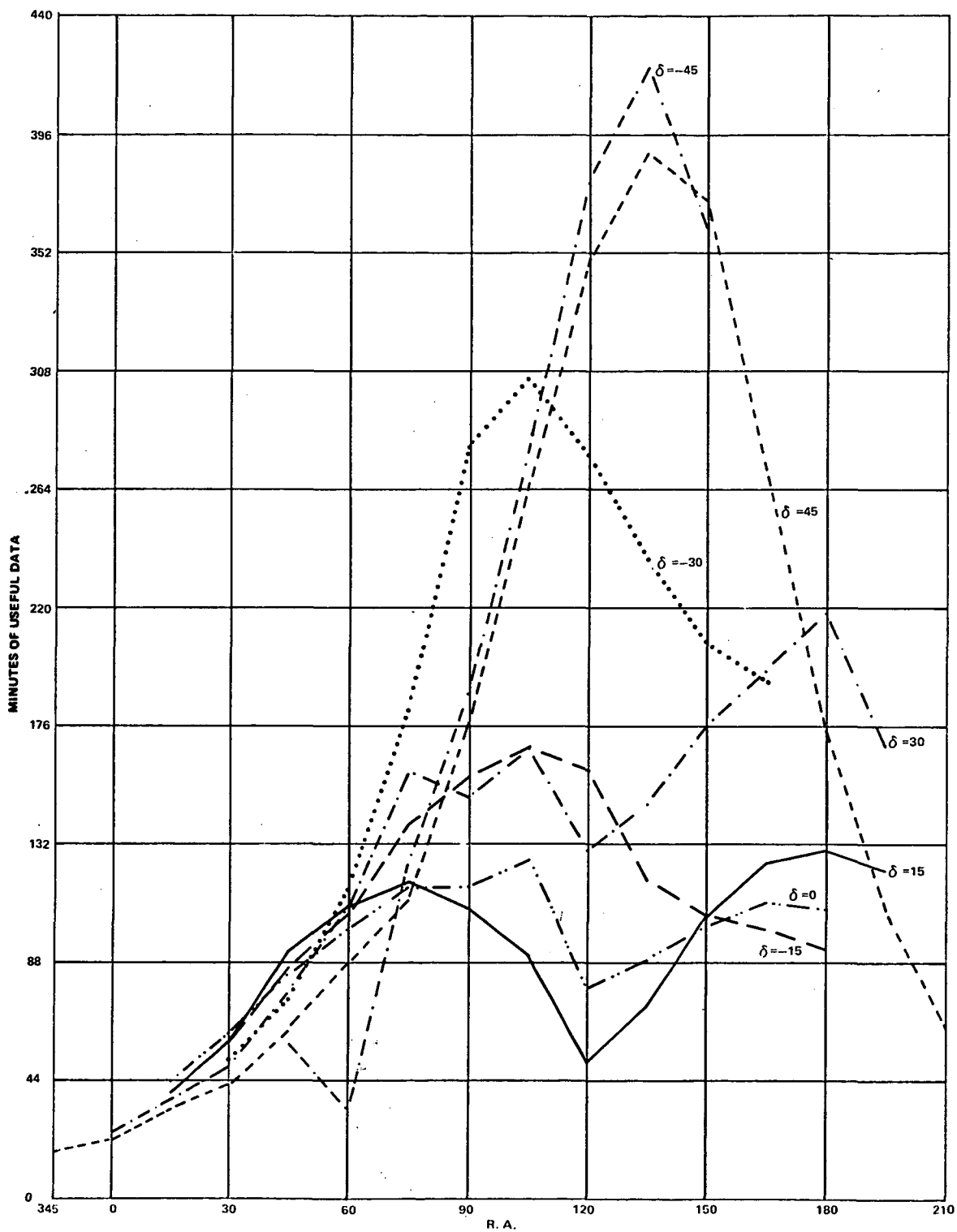
Figure C-8. Argument of Perigee = 315°

APPENDIX D

DATA SETS

RAW TELEMETRY DATA SET

The raw telemetry data set input to the Telemetry Processor resides either on a satellite-dependent disk file or on a magnetic tape. The tape is 7-track, odd-parity, with 556 bpi density. For either tape or disk, each record consists of 312 8-bit characters or 104 24-bit words.

A single end-of-file is written on tape after the last record of a pass, and multiple passes may be stacked on a single tape. Multiple end-of-files follow the last record of the last file. The disk data set does not have end-of-files between passes and has only one end-of-file at the end of the data.

Figure D-1 illustrates the format of the telemetry data record. Each record contains 24 bytes of header information, eight frames of attitude data, and 112 bytes of zero fill. Each frame begins with four bits of zeros, followed by a 36-bit time value for the frame in GMT milliseconds of year. This time value is obtained either from one of the DTSs at the receiving ground station or from the wall clock of MSOCC.

Following the time value is a quality byte containing a "1" if the frame sync and parity are good, or a "0" if either is bad. Data from the fixed portion of the telemetry follows. The 16-bit SCADS data is inserted next if present in this main frame; otherwise, the 16 bits are set to "0011001100110011", which is not a legal SCADS pattern. Figure D-2 illustrates the SCADS data format.

LABEL	BYTES	CONTENTS
HEADER		
SPACECRAFT ID	2	1011000000000000
DATA TYPE INDICATOR	1	FIXED POINT BINARY
PASS RECORD NUMBER	3	FIXED POINT BINARY
STATION NAME	6	SSSSSSbb
ORBIT NUMBER	3	FIXED POINT BINARY
DATE OF PASS	6	YY/MM/DD
TIME OF PASS	3	HHMM
DATA		
GMT TIME OF FRAME 1	5	FOUR LEADING ZEROS FOLLOWED BY 36 BITS REPRESENTING MILLI-SECONDS OF YEAR (ZERO FILL IF PADDING FRAME)
QUALITY OF FRAME 1	1	0000000X; X = 1 (GOOD) OR 0 (BAD)
FN (T/L WORD 0)	1	0000XXXX
STAT A	1	0000XXXX (BUILT FROM PROMPTS)
FRAME COUNT (WORDS 122-123)	1	XXXXXXXX
SUB COM A (WORDS 124-125)	1	XXXXXXXX
SUB COM B (WORDS 126-127)	1	XXXXXXXX
STAT B (WORDS 128-129)	1	XXXXXXXX
SCADS 1	2	
OA 1	2	
OA 2 OR SCADS 2	2	
OA 3 OR SCADS 3	2	
OA 4 OR SCADS 4	2	
GMT TIME OF FRAME 2	5	SAME FORMAT AS ABOVE
. . .		
. . .		
. . .		
OA 4 OR SCADS 4	2	
GMT TIME OF FRAME 3	5	SAME FORMAT AS ABOVE
. . .		
. . .		
GMT TIME OF FRAME 8	5	SAME FORMAT AS ABOVE
. . .		
. . .		
OA 4 OR SCADS 4	2	
ZERO FILL	112	00000000

Figure D-1. Attitude Record Format for SSS-A
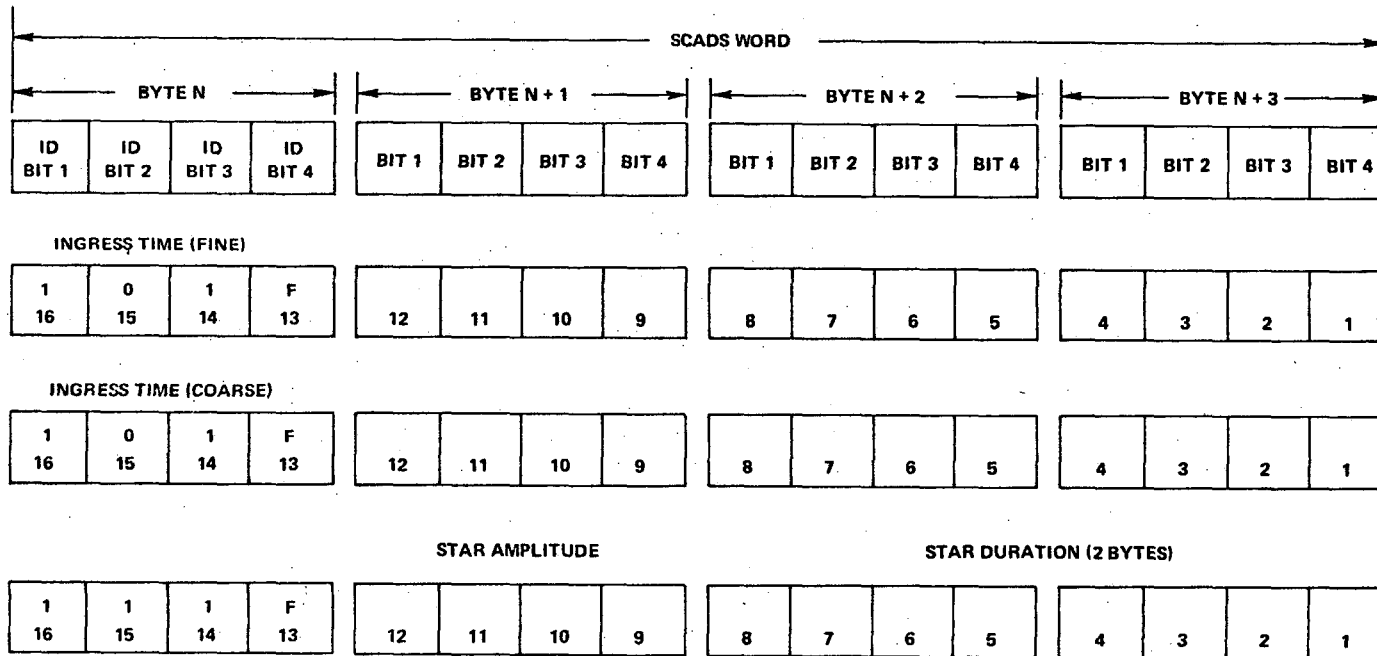
Figure D-2. SCADS Time/Star Data Sequence

Following the 16-bit SCADS data is a 16-bit OA data word. (The formats for an OA data word in both primary and backup modes are shown in Figure D-3 and D-4 respectively.) Next are three 16-bit data words containing either SCADS or OA data, according to the data mode being used. In primary mode, there is only one OA word per frame and the three additional data words may optionally be used for SCADS data. Thus the sequence of five attitude data words is: SCADS1, OA1, SCADS2, SCADS3, SCADS4, where the last three SCADS words are optional.

In backup mode, no SCADS data is available and the three additional data words are used for OA data. Thus there may be up to four OA words per frame. The first SCADS word has the fill pattern "0011001100110011" to indicate the absence of SCADS data. The OA data words in backup use only 12 bits; therefore the leftmost four bits of each OA word are set to the pattern "0011".

In both primary and backup modes, when any of the five available attitude words are not being used for either SCADS or OA data, they are set to the pattern "0011001100110011".

Data dropout may cause the insertion of frames of padding within a record. Such frames will have non-zero values in only the ID and record number. The presence of a "0" in the quality byte indicates that the frame does not contain good data.

ORBIT ATTITUDE TAPE

The orbit attitude tape is generated on the IBM 360. Physical specifications are 7-track, 556 bpi, and odd parity. The tape consists of a file header record followed by a series of file data records. Each data record contains 11 data items of 27 words each. After the last valid data item, the remaining items in the record contain 999999.0 in

PRIMARY MODE (P1 = 0)

OPTICAL ASPECT WORD

BYTE N | BYTE N + 1 | BYTE N + 2 | BYTE N + 3

| IC-11 CODE BIT 1 | IC-12 CODE BIT 2 | DATA DATA — "1" NO DATA "0" | TABLE TABLE A "0" TABLE B "1" | BIT - 1 | BIT - 2 | BIT - 3 | BIT - 4 | BIT - 1 | BIT - 2 | BIT - 3 | BIT - 4 | BIT - 1 | BIT - 2 | BIT - 3 | BIT - 4 |

SUN ANGLE DATA

| 1 | 0 | 1 | | SUN BIT 1 | SUN BIT 2 | SUN BIT 3 | SUN BIT 4 | SUN BIT 5 | SUN BIT 6 | SUN BIT 7 | SUN BIT 8 | SUN BIT 9 | 0 | SEL. SUN I.O. NO EARTH "1" EARTH "0" | PSEUDO I.O. TRUE SIGHT PSEUDO "0" |

SUN TIME FINE (SCTF)

| 1 | 0 | 1 | | 2^9 BIT RATE | 2^8 BIT RATE | 2^7 BIT RATE | 2^6 BIT RATE | 2^5 BIT RATE | 2^4 BIT RATE | 2^3 BIT RATE | 2^2 BIT RATE | 2^1 BIT RATE | 2^0 BIT RATE | 2^{-1} BIT RATE | 2^{-2} BIT RATE |

SUN TIME COARSE (SCTC)

| 1 | 0 | 1 | | 2^{18} BIT RATE | 2^{17} BIT RATE | 2^{16} BIT RATE | 2^{15} BIT RATE | 2^{14} BIT RATE | 2^{13} BIT RATE | 2^{12} BIT RATE | 2^{11} BIT RATE | 2^{10} BIT RATE | 2^9 BIT RATE | 2^8 BIT RATE | 2^7 BIT RATE |

EARTH "IN" TIME FINE (SCTF)

| 0 | 1 | 1 | | 2^9 BIT RATE | 2^8 BIT RATE | 2^7 BIT RATE | 2^6 BIT RATE | 2^5 BIT RATE | 2^4 BIT RATE | 2^3 BIT RATE | 2^2 BIT RATE | 2^1 BIT RATE | 2^0 BIT RATE | 2^{-1} BIT RATE | 2^{-2} BIT RATE |

EARTH "IN" TIME COARSE (SCTC)

| 0 | 1 | 1 | | 2^{18} BIT RATE | 2^{17} BIT RATE | 2^{16} BIT RATE | 2^{15} BIT RATE | 2^{14} BIT RATE | 2^{13} BIT RATE | 2^{12} BIT RATE | 2^{11} BIT RATE | 2^{10} BIT RATE | 2^9 BIT RATE | 2^8 BIT RATE | 2^7 BIT RATE |

EARTH "OUT" TIME FINE (SCTF)

| 1 | 1 | 1 | | 2^9 BIT RATE | 2^8 BIT RATE | 2^7 BIT RATE | 2^6 BIT RATE | 2^5 BIT RATE | 2^4 BIT RATE | 2^3 BIT RATE | 2^2 BIT RATE | 2^1 BIT RATE | 2^0 BIT RATE | 2^{-1} BIT RATE | 2^{-2} BIT RATE |

EARTH "OUT" TIME COARSE (SCTC)

| 1 | 1 | 1 | | 2^{18} BIT RATE | 2^{17} BIT RATE | 2^{16} BIT RATE | 2^{15} BIT RATE | 2^{14} BIT RATE | 2^{13} BIT RATE | 2^{12} BIT RATE | 2^{11} BIT RATE | 2^{10} BIT RATE | 2^9 BIT RATE | 2^8 BIT RATE | 2^7 BIT RATE |

Figure D-3. Optical Aspect Word Format (Primary Mode)

D-5

BACKUP MODE (P1 = 1)

SUN ANGLE DATA	SUN BIT 1	SUN BIT 2	SUN BIT 3	SUN BIT 4	SUN BIT 5	SUN BIT 6	SUN BIT 7	SUN BIT 8	SUN BIT 9	0	SEL. SUN I.Q.	PSEUDO I.Q.
SUN-FRAME END INTERVAL TIME	$\frac{2^0}{\text{BIT RATE}}$	$\frac{2^1}{\text{BIT RATE}}$	$\frac{2^2}{\text{BIT RATE}}$	$\frac{2^3}{\text{BIT RATE}}$	$\frac{2^4}{\text{BIT RATE}}$	$\frac{2^5}{\text{BIT RATE}}$	$\frac{2^6}{\text{BIT RATE}}$	$\frac{2^7}{\text{BIT RATE}}$	$\frac{2^8}{\text{BIT RATE}}$	$\frac{2^9}{\text{BIT RATE}}$	0	1
EARTH "IN" - FRAME END INTERVAL TIME	$\frac{2^0}{\text{BIT RATE}}$	$\frac{2^1}{\text{BIT RATE}}$	$\frac{2^2}{\text{BIT RATE}}$	$\frac{2^3}{\text{BIT RATE}}$	$\frac{2^4}{\text{BIT RATE}}$	$\frac{2^5}{\text{BIT RATE}}$	$\frac{2^6}{\text{BIT RATE}}$	$\frac{2^7}{\text{BIT RATE}}$	$\frac{2^8}{\text{BIT RATE}}$	$\frac{2^9}{\text{BIT RATE}}$	1	0
EARTH "OUT" FRAME END INTERVAL TIME	$\frac{2^0}{\text{BIT RATE}}$	$\frac{2^1}{\text{BIT RATE}}$	$\frac{2^2}{\text{BIT RATE}}$	$\frac{2^3}{\text{BIT RATE}}$	$\frac{2^4}{\text{BIT RATE}}$	$\frac{2^5}{\text{BIT RATE}}$	$\frac{2^6}{\text{BIT RATE}}$	$\frac{2^7}{\text{BIT RATE}}$	$\frac{2^8}{\text{BIT RATE}}$	$\frac{2^9}{\text{BIT RATE}}$	0	1

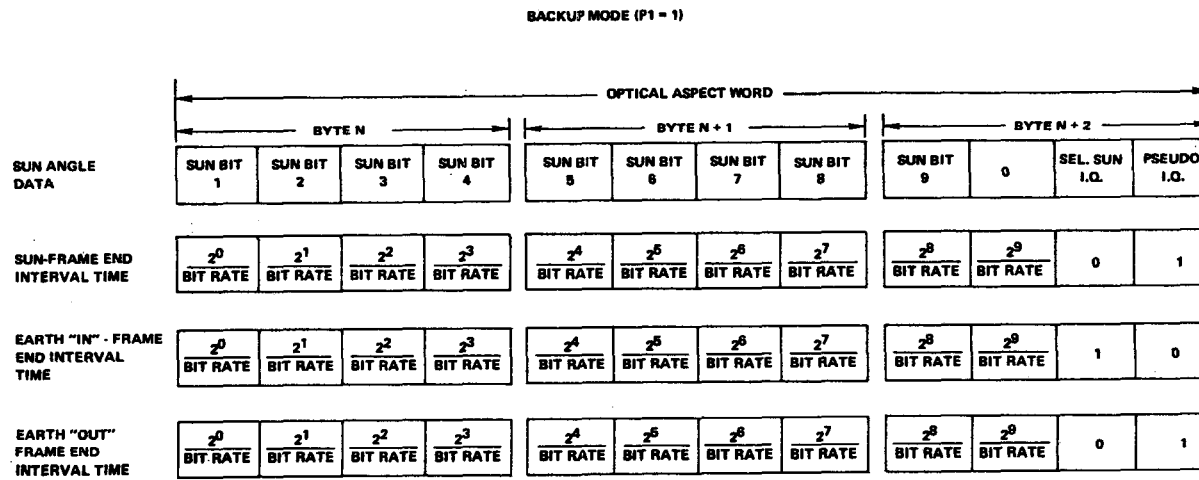OPTICAL ASPECT WORD — BYTE N — BYTE N + 1 — BYTE N + 2

Figure D-4. Optical Aspect Word Format (Backup Mode)

Word 2 (the date word) of each data item. If the last valid data item fills a record, another full record appears with 999999.0 in Word 2 of each of the 11 data items. The value 999999.0 is used as a fill word for words in incomplete data items. Two end-of-file marks end the tape. The tape is compatible with a tape written on the IBM 7094 computer. Format of the header and data records is shown below.

<u>HEADER RECORD</u>

<u>Word</u>	<u>Description</u>
0	FORTRAN data record size indicator
1	Spare
2-3	7-digit satellite identification
4	Date, UT start time of satellite data
5	Day count of year, UT start time of satellite data
6	Seconds of day, UT start time of satellite data
7	Date, UT end time of satellite data
8	Day count of year, UT end time of satellite data
9	Seconds of day, UT end time of satellite data
10	$= \Delta t$, if tape has equal intervals (seconds) $= 0$, if tape has unequal intervals
11	Number of data items in data record $= 12$, (includes a special type of item as item no. 12)
12	Number of words per data item, $= 27$
13	Number of words per data item that are a function of time (those words follow the time words consecutively), $= 22$

Word	Description
14	Number of words in data record, = 301
15	Spare
16-26	Run identification data
27	Date, coordinate system reference data time, and position
28	Day count of year, coordinate system reference data time, and position
29	Apparent sidereal time in radians, coordinate system reference data time, and position
30-40	Used for harmonics
41	Date, epoch
42	Day count of year, epoch
43	Seconds of day, epoch
44	a, semi-major axis (km)
45	e, eccentricity (ratio)
46	I, inclination (deg)
47	Right ascension of ascending node (deg)
48	Rate of change of right ascension of ascending node (deg/day)
49	Argument of perigee (deg)
50	Rate of change of argument of perigee (deg/day)
51	P, period (min)
52	P, rate of change of period (min/day)
53-253	Used for elements, drags
254-300	Spares filled with zeros

DATA RECORDS

Word	Description
0	FORTRAN data record size indicator
1	Type of data item indicator = 1, regular satellite = 2, ascending node crossing = 3, north point = 4, descending node = 5, south point = 6, sunlight entrance = 7, sunlight exit
2	Date of data, time of data item
3	Day count of year, time of data item
4	Seconds of day, time of data item
5	X, satellite position vector (km)
6	Y, satellite position vector (km)
7	Z, satellite position vector (km)
8	X, satellite velocity vector (km/sec)
9	Y, satellite velocity vector (km/sec)
10	Z, satellite velocity vector (km/sec)
11	Longitude (deg), geodetic position
12	Latitude (deg), geodetic position
13	Height above spheriod (km), geodetic position
14	Sx, solar vector (A.U.)
15	Sy, solar vector (A.U.)
16	Sz, solar vector (A.U.)
17	L (earth radii), McIlwain L parameter
18	B (gauss), magnetic field strength
19	Right ascension of B in inertial coordinates (deg)

Word	Description
20	Declination of B in inertial coordinates (deg)
21	Right ascension of spin axis in inertial system (deg)
22	Declination of spin axis in inertial system (deg)
23	Error in right ascension (deg)
24	Error in declination (deg)
25	Angle between spin axis and magnetic field vector
26	Fill (=999999.0)
27	Ascending node crossing number (pass number)
28-297	10 other satellite data items
298	=99 (type of data indicator)
299	Year of data
300	= 999, if no ascending node item occurred = % of orbit in sunlight, if ascending node item occurred in this record

SCADS TELEMENTRY DATA SET

The SCADS Telemetry Data Set is an output data set on tape or disk from the Attitude Determination Subsystem for independent use by the Star Program. Physical specifications are odd-parity, 9-track, and 800 bpi density. The data set consists of a series of files containing two records, the first record being a header record and the second a data record. The data set ends with the double end-of-file. The format of each record type is described below.

HEADER RECORD

Word	Format	Description
1	R*8	Date of pass – YY/MM/DD (BCD)**
2	R*8	Station name – SSSSSSbb (BCD)**
3	R*8	Date of pass – YY/MM/DD (EBCDIC)**
4	R*8	Station name – SSSSSSbb (EBCDIC)
5	I*4	Time of pass – HHMM (EBCDIC)
6	I*4	Data type indicator
7	I*4	Orbit number
8	I*4	Pass record number
9	I*4	Satellite ID – 1011000000000000
10	I*4	Time of pass – HHMM (BCD)**
11	I*4	Total number of SCADS samples
12	I*4	Total number of header-data record pairs created

**Data is left-justified and unspecified bits are zero.

DATA RECORD

Word	Format	Description
1–200	R*8	Ingress time
201–400	R*4	Pulse amplitude
401–600	R*4	Pulse duration
601–800	R*4	Threshold values

C.4

REFERENCES

2-1   S. Valley, ed., Handbook of Geophysics and Space Environ-
ments, McGraw-Hill Book Co., New York, 1965.

2-2   L. G. Jacchia, "New Static Models of the Thermosphere and Exo-
sphere with Empirical Temperature Profiles", Smithsonian Astro-
physical Observatory Special Report 313, May 1970.

2-3   D. K. Weidner, C. L. Hasseltine, and R. E. Smith, "Models of
the Earth's Atmosphere (120 - to 1000 km)", NASA Space Vehicle
Design Criteria, NASA SP-8021, Washington, D.C., May 1969.

2-4   M. Shear, "Small Scientific Satellite-A Sensor Mounting Angle
Study", Computer Sciences Corporation, 5035-10100-01 TM,
Silver Spring, Md., January 1971.

4-1   R. D. Werking, ed., "A Generalized Technique for Using Cones
and Dihedral Angles in Attitude Determination", GSFC Report
X-542-71-222, Goddard Space Flight Center, Greenbelt, Md.,
June 1971.

GENERAL REFERENCES

"Computer Programs for Scanning Celestial Attitude Determina-
tion Systems", Control Data Corporation, Contract No. NAS
5-10495, Minneapolis, Minn., February 1970.

E. J. Pyle and J. Stewart, "Optical Aspect System for the Small
Scientific Satellite", GSFC Report X-711-70-174, Goddard Space
Flight Center, Greenbelt, Md., April 1970.

"Small Scientific Satellite-A Support Instrumentation Require-
ments Document", NASA, Goddard Space Flight Center,
Greenbelt, Md., April 1971.

"Small Scientific Satellite-A Project Development Plan", NASA,
Goddard Space Flight Center, Greenbelt, Md.

"NASA Support Plan for Project SSS-A", Goddard Space Flight Center, Greenbelt, Md., April 1970.

T. Flatley, "S^3-A Attitude Behavior - a Prelaunch Assessment", GSFC Report X-732-70-309, Goddard Space Flight Center, Greenbelt, Md., July 1970.

"Final Report on S^3 Disturbance Torque Analysis", Westinghouse Defense and Space Center, Aerospace Division, Contract No. NAS 5-9753-23, Baltimore, Md., August 1968.

T. W. Flatley, "Magnetic Attitude and Spin Control of the Small Scientific Satellite S^3-A", NASA TND-5572, Washington, D. C., February 1970.

R. W. Fulcher, "System Design of a Unique Magnetic Attitude and Spin Control Subsystem", NASA TN D-6051, Washington, D. C., December 1970.